The Graphical Determination of Operating Conditions for Chromatographic Sequences

A thesis submitted to the University of London
for the degree of
Doctor of Philosophy

by

Rebecca Suzanne Salisbury

Department of Biochemical Engineering
University College London
Torrington Place
London WC1E 7JE

August, 2007

ProQuest LLC
789 East Eisenhower Parkway
P.O. Box 1346
Ann Arbor, MI 48106-1346

I, Rebecca Suzanne Salisbury, confirm that the work presented in this thesis is my own. Where information has been derived from other sources, I confirm that this has been indicated in the thesis.

Signed:...

Abstract

Multiple step chromatography sequences are necessary in biopharmaceutical downstream processing to achieve the desired levels of purity for products such as therapeutic proteins. Traditional methods of process design deal with each step individually, but this can result in a sequence that does not achieve best overall performance. This project proposes a graphical methodology for the identification of operating conditions for a two-step chromatography sequence. The method uses Windows of Operation to incorporate the tradeoffs between yield, purity, and productivity. A tie-line procedure is developed that separates the Window of Operation for the first chromatographic step into two zones. One zone contains those operating conditions that combine to produce a material which can be purified successfully by the second step to produce a product that meets the desired specifications. The second zone consists of operating conditions which will not yield a material that can be adequately purified by a second chromatographic stage to yield a product of the predetermined specifications.

The methodology is valuable in that it helps in achieving the rapid design of a two-step chromatography sequence, and aids in choosing the optimum operating conditions for the first step which are highly dependent upon the operation and specifications of the second chromatographic step.

Simulations carried out using a software package based on the general rate model depict the construction and use of the method applied to a sequence of ion exchange and hydrophobic interaction chromatography separating a three component protein mixture. The methodology is verified successfully using an experimental system that purifies Fab antibody fragments from a three-component system consisting also of Ribonuclease A and Cytochrome C, with a two-stage chromatography sequence, ion exchange followed by hydrophobic interaction chromatography.

Acknowledgements

I am grateful for the guidance and supervision from Nigel Titchener-Hooker throughout my time at UCL. I would also like to thank Dan Bracewell for his input into my project.

Unfortunately, my student years have come to an end, and I have had to get what my friends call a 'proper job'. Thanks to my parents who have supported me through my student years, and have given me the opportunity to achieve all my goals. I have thoroughly enjoyed it all.

And last but not least, thanks to the Prince who, as my parents put it, has put up with me over the past four years!

Table of Contents

List of Figures

List of Tables

List of Symbols

A	cross-sectional area
a_i	constant in Langmuir isotherm for component i ($a_i = b_i C_i^{\infty}$)
b_j	adsorption equilibrium constant for component
Bi_i	Biot number of mass transfer for component i, $k_i R_p / (\varepsilon_p D_{pi})$
C^*	adsorbtion concentration in solution at equilibrium (g L^{-1})
C_{0i}	concentration used for non-dimensionalization, max $\{C_{fi}(t)\}$ (mol L^{-1})
c	concentration of the solute in the mobile phase (mol L^{-1})
c_{bi}	C_{bi}/C_{0i}
c_{pi}	C_{pi}/C_{0i}
C_{bi}	bulk phase concentration of component i (mol L^{-1})
C_{fi}	feed concentration profile of component i (time dependent) (mol L^{-1})
C_i^{∞}	adsorption saturation capacity for component i (mol adsorbate/unit volume of particle skeleton) (mol L^{-1})
C_{pi}, C_{pj}	concentration of component in the stagnant fluid phase inside the particle macropores (mol L^{-1})
C_{pi}^{s}	concentration of component i in the solid phase of the particle (mole adsorbate per unit volume of matrix) (mol L^{-1})
D	diffusivity (m^2 s^{-1})
D_{bi}	dispersion coefficient of component I (m^2 s^{-1})
D_e	intraparticle diffusion (m^2 s^{-1})
D_p	effective diffusivity in particle macropores (m^2 s^{-1})
D_m	intraparticle molecular diffusivity (m^2 s^{-1})
ε_b	bed void volume fraction
ε_p	particle porosity/inclusion porosity
ε_{pi}^{a}	accessible pore volume fraction
F_i^{ex}	size exclusion factor
k_d	dissociation constant (g L^{-1})
k_{eq}	equilibrium constant
k_i	film mass transfer coefficient of component i (m s^{-1})

L	column length (cm)
M_0	Total amount of product in the sample load (g)
$M_{A,i}$	Amount of impurity 1 in fraction i (g)
$M_{B,i}$	Amount of impurity 2 in fraction i (g)
$M_{P,i}$	Amount of product material in fraction i (g)
M_P^1	Amount of purified product at the beginning of collection (g)
M_P^2	Amount of purified product at the end of collection (g)
$M_{T,i}$	Total amount of material in fraction i (g)
M_T^1	Amount of material at the beginning of collection (g)
M_T^2	Amount of material at the end of collection (g)
M_S	Total amount of material in the sample load (g)
N	number of theoretical plates
N_s	number of components
Pe_{Li}	Peclet number for axial dispersion for component i, vL/D_{bi}
q	concentration of component adsorbed to the matrix
Q	volumetric flow rate ($m^3\ s^{-1}$)
Q^*	equilibrium concentration of protein bound to matrix ($g\ L^{-1}$ of resin)
q_{max}	maximum resin capacity ($g\ L^{-1}$ of resin)
r	R/R_p
R	radial coordinate for particle
R_p	particle radius (m)
R_s	chromatographic resolution
t	time (s)
t_0	time of input of sample (s)
t_R	average retention time (s)
V	volume of fluid feed to column (L)
W	Window of Operation area (arbitrary units)
w	peak width at base
w_h	peak width at half-height
w_i	peak width at inflection points
z	Z/L
Z	axial coordinate

ξ_i	dimensionless constant for component i, $3Bi_i\eta_i(1-\varepsilon_b)/\varepsilon_b$
η_i	dimensionless constant, $\varepsilon_p D_{pi} L/R_p^2 \nu$
λ	ratio of the solute molecular diameter to the pore diameter
ρ_s	solvent density (kg m^{-3})
σ	standard deviation
τ	dimensionless time, $\nu t/L$
μ_i	statistical moment
ν	interstitial fluid velocity (m s^{-1})
ν_L	volume of sorbent from the inlet to the point of interest (L)

1. Aims of Research

The production and purification of proteins for use in the pharmaceutical industry is a major area of research in Biochemical Engineering. These novel products are not only helping to save many lives, but are also proving to be quite lucrative for the manufacturers. Annual sales of protein therapeutics are projected to exceed $59 billion (US) by the year 2010, twice the revenue generated in 2001.[1] One of the most important challenges underlying the development of the new generation of human therapeutic products is their successful purification. This is ultimately achieved by lengthy and expensive chromatography stages. New methods are needed to help speed up the design of the stages in order to ensure that the products will become widely available at a timelier rate, and at a lower cost to consumers.

Many Biochemical Engineering steps are often complex, and design solutions often require a compromise based for example on the trade-off between purity and yield.[59] Identifying such a solution can be a lengthy process. Woodley *et al.* describe the graphical method of Windows of Operation, where a Window is defined as 'the operational space determined by the system (chemical, physical, biological) and process engineering constraints and correlations governing the particular process or operation under consideration'.[59] Windows of Operation are predominantly used to define operational spaces for one operation, and have been used successfully for unit operations and processes such as centrifugation (Saite *et al.* [60]) and biotransformation (Collins *et al.* [61]). However, by only examining one unit of operation at a time to determine feasible operating spaces, the impact of

one unit operation on a following unit operation in processing sequences is not taken into account. This can have consequences on successful processing.

Industry regulations specify how pure a product must be before it is introduced for human use. Typically, two or more chromatographic steps are run in sequence in order to achieve the desired purification levels. However, often each chromatographic step is examined individually to find a set of feasible operating conditions. If variations occur in the first stage of operation, the impact on the second stage of processing is often not considered in the determination of a set of operating conditions for that step. Graphical methods examining the affects of changing the chromatography stages' operating conditions could provide industry with rapid, economic and precise means of designing and optimizing chromatography sequences.

It is common practice that chromatograms are the final output in modelling predictions for chromatography stages. However, chromatograms do not easily show the sensitivity of the chromatographic stage's reaction to changes in the operating conditions. To show this sensitivity, Windows of Operation are ultimately produced using the two intermediate steps of fractionation diagrams and purification factor versus yield diagrams. This project sets out to generate a user-friendly, graphical methodology that will allow sequences of chromatographic steps operating at various conditions (i.e. flow rate, sample load) to be examined based on fractionation diagrams, maximum purification factor versus yield diagrams, and Windows of Operation.

A sequence of chromatography steps; ion exchange and hydrophobic interaction chromatography has been chosen as typical of an industrial separation. Data to populate the method is both simulated and experimental, where the

experimental data is based on the purification of Fab' (antibody fragments) from *E.coli* cells. Antibody fragments are important tools used in therapeutic treatments because they are small molecules that can recognize and bind to specific locations in the body. For example, antibody fragments can target and bind to cancer cells, and can be used to specifically deliver anti-tumor drugs to these cells.

The materials to be examined during the course of the project were selected so that the tools developed for the analysis of the chromatography sequences would be generic and hence transferable to the majority of protein separations.

At the beginning of the project, the structure was set out as the following:

The first step was to use simulation in order to examine chromatography sequences. This saves time and the large cost of materials needed in order to run many experimental chromatography sequences. Through simulation, a large data set of chromatograms could be generated for the sequence, containing results for many different combinations of operating conditions (i.e. load volumes and flow rates). The chromatograms would be analyzed ultimately using the technique of Windows of Operation to examine the effects of operating conditions on purity and productivity (Chapter 3). Windows would be examined in order to determine if any patterns or relationships could be found between the Window (i.e. Window area/size) and the sequence operating conditions (Chapter 4). For example, larger Window areas provide a larger range of operating conditions that would produce a product of the desired specifications, whereas smaller Window areas provide less range. Once patterns were detected, using them a methodology could be

generated for the selection of operating conditions for chromatography sequences (Chapter 5).

The above described work would all be based around simulated data. However, it would also be necessary to carry out experiments to verify the simulated results. Using a three-component system and a two-stage chromatography sequence, experiments would be performed in order to verify the methodology generated using the simulated data (Chapter 7). Simulations would be performed using the adsorption isotherm data to verify that the simulated results (i.e. chromatograms) are representative of the experimental results. In order to compare the experimental results to a set of simulated results it would be required to experimentally obtain the adsorption isotherm parameters (Chapter 6). These parameters are input into the simulation package to help generate chromatograms. The simulation package used is described in Section 3.2.2.

This thesis describes the generation and analysis of simulated chromatograms and their resultant Windows of Operation, the generation of the methodology to optimize operating conditions for chromatography sequences, and the experimental verification of the methodology. It also examines the difficulties encountered when determining adsorption isotherms, and provides recommendations for possible future work.

The next section examines techniques and models used for the generation and analysis of data in this project.

2. Introduction

2.1 Overview of Chromatography

Chromatography is a near ubiquitous downstream process used for the separation of entities such as biomolecules (e.g. antibiotics, amino acids), biologics, and fine specialty chemicals.[2] It is defined as a separation based on the differential migration of solutes through a system consisting of two phases, one of which is mobile.[3] In order to produce biological products for therapeutic use, a number of consecutive processes are carried out. For example, in the production of recombinant human leukocyte interferon, [4] the sequence outlined in Figure 2.1 is used.

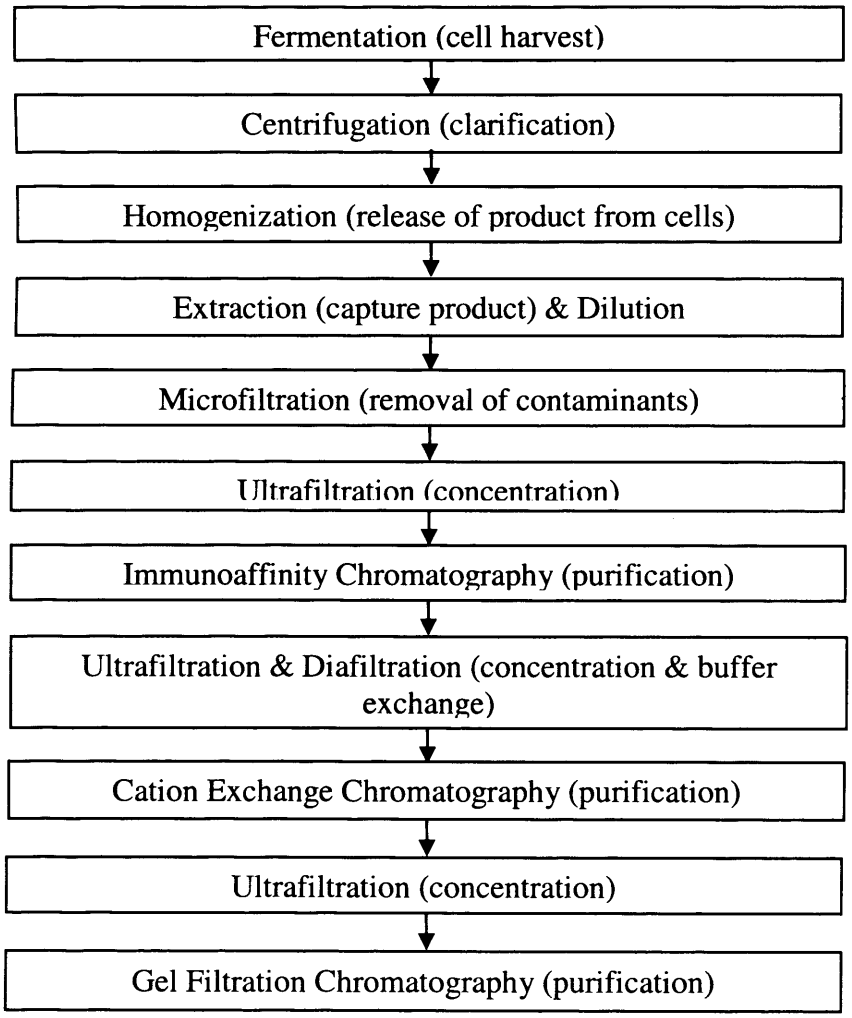

Figure 2.1 Production & Purification of Recombinant Human Leukocyte Interferon [4]

In protein purification, the type of chromatography employed is liquid chromatography, where there is a liquid feed and a solid matrix. Anything that flows through the column (e.g. process feed, buffer solutions, elution solutions) is called the mobile phase. The packing or matrix of the column is termed the stationary phase. A common chromatography setup is seen in Figure 2.2.

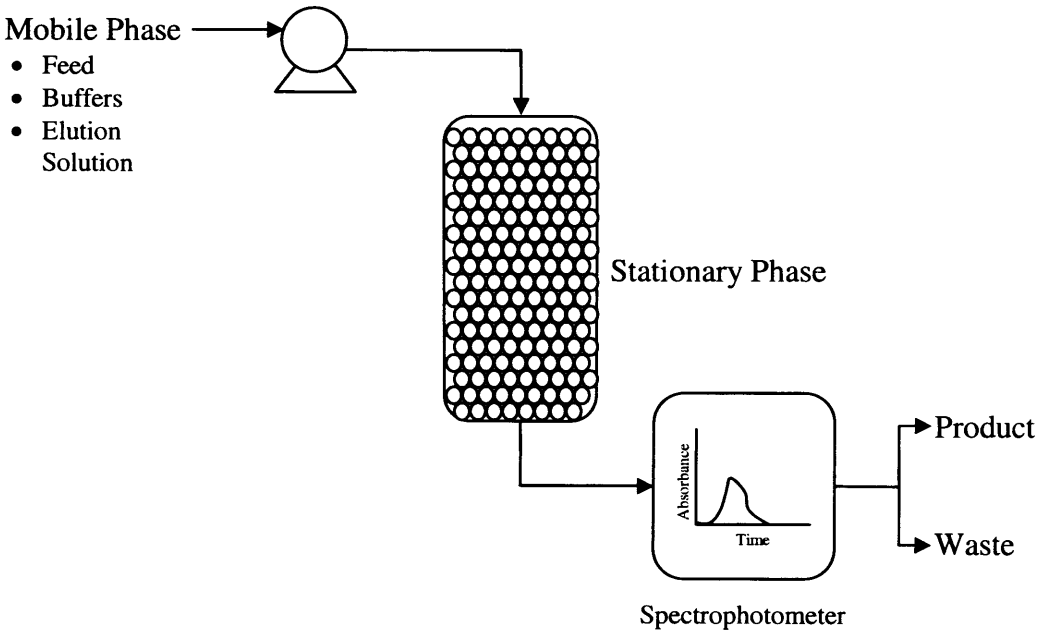

Figure 2.2 Common Chromatography Setup

The goal of chromatography is to achieve high resolution and capacity needed to generate large quantities of high quality, purified product.[5] The resolution is a measure of the extent of separation between two peaks on the chromatogram, representing two components in the chromatographic process.[5] Purity requirements are high for proteins intended for human therapeutic use, and chromatography is used as the final steps for removing protein and non-protein

impurities.[5] These impurities may include growth media components, proteins from the host cell line, and aggregated or chemically modified forms of the product.[5]

There are two mechanisms that can be involved in liquid chromatography, adsorption and size exclusion.[6] Adsorption chromatography involves substances from the feed solution binding to the stationary phase. Ion exchange chromatography, hydrophobic interaction chromatography and affinity chromatography are examples of adsorption chromatography. Size exclusion chromatography is a non-binding method. The separation is based on the rate of migration of the molecules in the process stream, where the rate is dependent on the molecule radius. The above mentioned forms of chromatography will be discussed in more detail in the following sections.

There are two main modes of operating an adsorption chromatography process, frontal chromatography and displacement chromatography.[2] In frontal chromatography, the solute that is being purified does not bind to the column. Instead, the impurities are retained by the stationary phase. For example, when purifying a protein for therapeutic use it is necessary to remove DNA that is present in the process solution. An anion exchanger can be used to adsorb the DNA from the feed stream, thus the product flowing through the chromatography column is the therapeutic protein free of contaminating DNA.[2] During displacement chromatography operations, the solute of interest binds to the column while contaminants flow through. The solute is then eluted by introducing a substance that will absorb more strongly to the matrix, thus displacing the wanted solute.[2]

The chromatographic cycle for adsorption chromatography is composed of four main parts:

1. Loading – The feed solution is introduced to the column. This is usually done in a specific start buffer that is dependent upon the type of chromatography and the proteins of interest.
2. Washing – Once the feed solution has passed through the column, the column is rinsed with the start buffer to remove anything that has not bound to the column.
3. Elution – An elution buffer is introduced to the column and removes proteins that have bound to the stationary phase.
4. Regeneration – Once the material has been eluted from the matrix, solutions are run through the column to prepare the stationary phase for the next purification run.

Elution is an important step in chromatography in order to remove and capture the product from the matrix. There are two main types of elution, isocratic and step/gradient. Isocratic elution occurs when the composition of the mobile phase does not change throughout the separation.[4] In step/gradient elution, the composition of the mobile phase can be changed by introducing a solute with greater affinity for the matrix, thus displacing the solute of interest. Also, the pH of the solution could be changed. This would alter the charges of the bound protein molecules, causing them to unbind. In step elution, the composition of the mobile phase changes stepwise, and during gradient elution, the composition changes at a specified rate. For example, during the loading of the feed solution, the mobile phase may contain no salt. However, the elution

solution may contain 1 M sodium chloride salt. In step elution, the change from the no salt solution to the 1 M salt solution is immediate. In gradient elution, the change from the no salt solution to the 1 M salt solution will occur over a period of time so that the increase in salt concentration is gradual. Gradient elution is often used for the separation of multicomponent protein mixtures.[4, 13] The quality of the chromatography separation is termed its resolution, and is measured in terms of the purity of the component fractions.[4] It is important in protein purification to achieve high resolution, since many of the products are for therapeutic use. Some of the factors that affect resolution include:

1. The nature and composition of the process stream. The concentration, viscosity, buffering properties, pH, and amount of fouling material all affect the resolution obtained by the chromatographic process.[7]
2. The flow velocity. The velocity should be increased to the point at which the upper pressure drop limit is reached, or the resolution deteriorates to an unacceptable level.[7]
3. The temperature. The upper temperature limit is dictated by the stability of the protein. At higher temperatures, the protein may start to degrade, thus affecting the yield and resolution.[7]
4. The particle size of the matrix. Stationary phase particles should have diameters as small as possible to minimize the intraparticle diffusion resistances. However, the size of the matrix particles is dictated by the pressure drop constraints and the ease of packing.[7]
5. The particle shape. Spherical beads are favoured because they give rise to greater permeability in packed beds, and better stability when they are repeatedly used.[7]

6. The porosity. The pores should be large enough so that free diffusion is not hindered significantly. Generally, pores are 10-20 times the diameter of the protein. Thus, for proteins that have a molecular weight of 50,000-100,000 Daltons, it is recommended that pore diameters be 300 Å.[7]

The column, its connections, and its associated auxiliary equipment also have an impact on resolution. Poor configuration of pumps and tubing can cause a decrease in resolution.[4]

The following sections will detail the different types of chromatography that will be used for experimentation and modelling.

2.2 Methods of Chromatography

2.2.1 Affinity Chromatography

Affinity chromatography takes advantage of biological interactions in order to bind specific solutes.[2] It involves the protein of interest binding to immobilized ligands, while the unwanted proteins and other molecules pass through the column. Ligands can be a variety of molecules including monoclonal antibodies, carbohydrates, and cofactors.[8]

In order to recover the product off the column, it is eluted by one of many methods. These include a change in the pH, an increase in the salt concentration, and displacement of the solute with a molecule that has a higher affinity for the ligand.[2] However, there are a couple of problems associated with affinity chromatography elution. Often the product is bound very tightly to the ligand, and harsh conditions are needed to achieve an effective elution.[8] Due to these

harsh conditions (i.e. extreme pH), the protein product may be inactivated. Another problem during elution is that some ligand may be leached off the column.[8, 9] This will contaminate the product stream, and extra purification steps may need to be introduced further downstream in order to remove the leached ligand.

Affinity chromatography offers high selectivity, resolution, and capacity for the proteins of interest.[10] It is an expensive purification method due to the high cost of the ligands.[11] It is preferable to be able to install clean-in-place (CIP) methods so that the column is reusable. However, complications can arise with CIP systems for affinity chromatography rigs. For example, Protein A columns cannot have clean-in-place systems using sodium hydroxide solutions due to the labile nature of the ligand.[9] This excludes the most common and cheapest clean-in-place method.

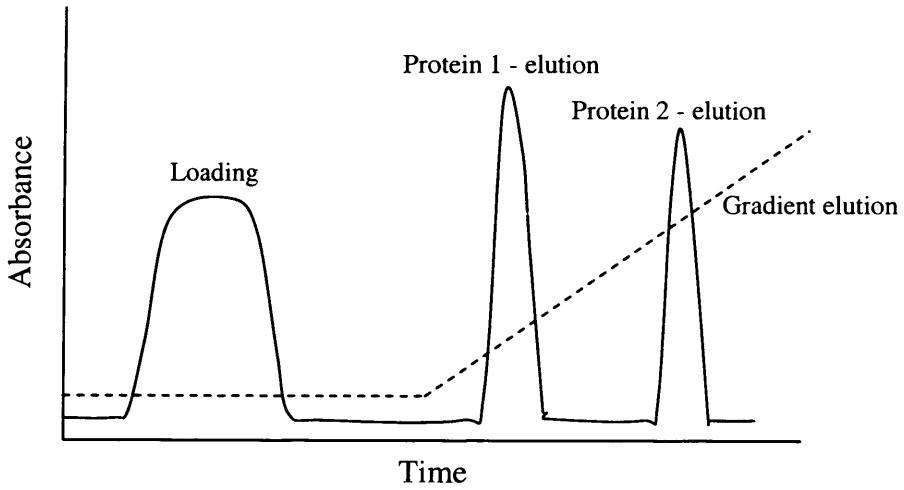

Figure 2.3 Typical Chromatogram for Affinity Chromatography with Gradient Elution[10]

2.2.2 Ion Exchange Chromatography

Ion exchange chromatography is often used in protein purification at both laboratory and manufacturing scale. This is due to its ease of operation, relative cheapness, and its acceptance by regulatory bodies as an effective operation in the production of pharmaceutical proteins.[12]

Ion exchange chromatography involves a separation based on molecular charge. Proteins have an isoelectric point (pI). This is the pH at which there is no charge on the molecule. However, by lowering or raising the pH the protein will obtain a charge. When the pH is above the pI, the protein is negatively charged. When the pH is below the pI, the protein is positively charged.[4]

There are two types of ion exchange columns. Anion exchange columns bind negatively charged molecules. Cation exchange columns bind positively charged molecules.[8] Most protein purifications involve anion exchangers because most proteins are negatively charged at a neutral pH range (pH 6-8).[8]

Ion exchange resins can be silica-based or polymer-based.[2] Uncoated silica-based resins are compatible with water and organic solvents, and have a high affinity for hydrophobic molecules. They are known as rigid molecules, which can be made to have large surface area and small particle size.[2] Silica resin has been used for the purification of many commercial biotech products, but it has been known to denature some proteins and irreversibly bind others.[2] Polymer-based resins are made of cross-linked polymers (i.e. agarose, dextran).[2] They are often larger in size than silica resins, and are less rigid. Agarose is the most commonly used resin in ion exchange chromatography. It is naturally hydrophilic, and is compatible with many proteins and biomaterials. It also can be cross-linked to form a relatively rigid bead.[2]

Ion exchange resins are derivatized with an ionic group (i.e. carboxyl (COO^-), diethylaminoethyl (DEAE, $2C_2H_5N^+HC_2H_5$)). A counter-ion of opposite charge is then linked to the resin by ionic attraction. When the protein is introduced to the column, it is attracted to the resin, and thus displaces the counter-ion so that it is able to bind.[4] Elution of the captured molecules is most often performed by increasing the salt concentration in the elution solution. It can also be done by changing the pH.[8] Displacement of the molecules from the column occurs in the order of relative binding strength.[4] Therefore, this allows the protein of interest to be captured during elution at a separate time from the other proteins if more than one protein has bound to the column.[4]

Unlike affinity chromatography, ion exchange resins will withstand harsh conditions.[4] This will allow good clean-in-place procedures, such as the use of NaOH, to be employed. By reusing columns, the process becomes more economic.

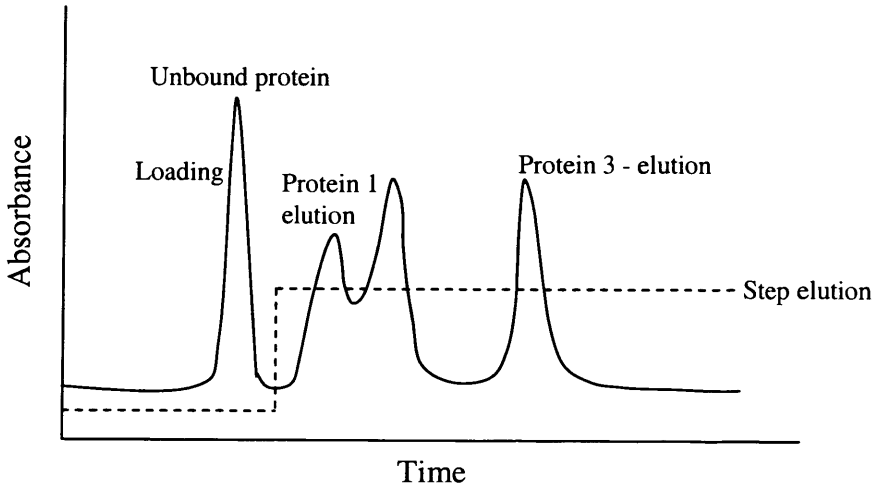

Figure 2.4 Typical Chromatogram for Ion Exchange Chromatography with Step Elution[14]

2.2.3 Hydrophobic Interaction Chromatography (HIC)

Hydrophobic interaction chromatography (HIC) is a separation based on the relative hydrophobicity of proteins.[8, 15] Proteins are composed of hydrophilic and hydrophobic amino acids. Most of the hydrophobic amino acids are located in the core of the protein, but some are located on the surface.[8] Under normal conditions, water molecules surround the protein as hydrophilic groups attract the water. However, when placed in solutions of high salt, the proteins are stripped of their solvation water, and the hydrophobic groups are exposed.[2] An interaction is able to occur between the hydrophobic patches on the protein molecule, and the hydrophobic ligands covalently attached to the chromatography matrix.[16]

The chromatography resin (silica-based or polymer-based as described in section 2.2.2) is coated with hydrophobic ligands, alkyl or aryl groups.[4, 16] Alkyl ligands show purely hydrophobic character, where as aryl ligands can facilitate both hydrophobic and aromatic interactions.[16] Agarose based matrices are the most commonly employed.[16]

HIC is often loaded in high concentrations of ammonium sulphate salt because it favours the stability of many proteins.[4] The column is eluted using decreasing concentrations of salt in the buffer solution, either step-wise or by a gradient.[15] HIC is a good purification step to follow ion exchange chromatography. Since ion exchange uses high salt concentrations to elute the proteins from the column, the product solution can be loaded onto the HIC column with minimal alterations to its composition.[15]

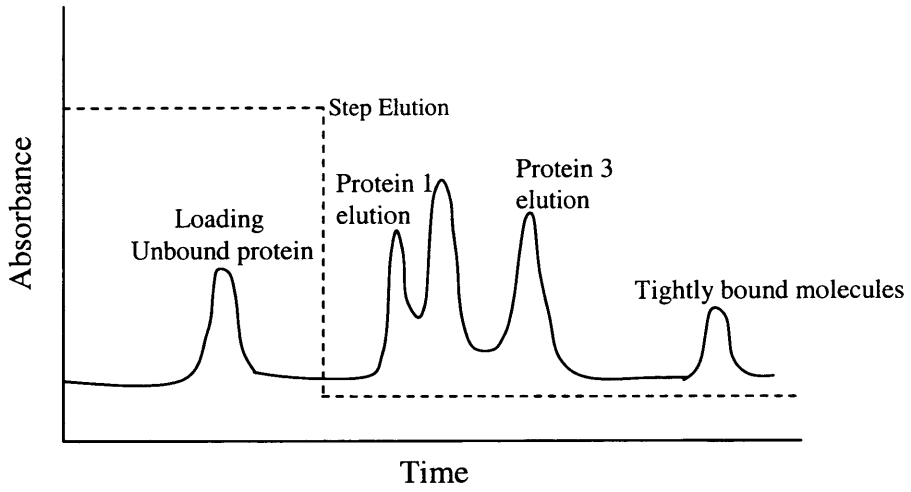

Figure 2.5 Typical Chromatogram for Hydrophobic Interaction Chromatography with Step Elution[14]

2.2.4 Size Exclusion Chromatography

Size exclusion chromatography, also known as gel filtration, is a separation technique based upon the migration rate of molecules of different sizes. Unlike the aforementioned chromatography techniques that involved binding/adsorption, gel filtration is a non-binding method. It is used for the removal and exchange of low molecular weight molecules and salts,[11] and is generally assumed to be a polishing a step in protein purification.

The chromatography matrix is composed of resins of hydrophobic, polymer gels with a broad range of pore sizes.[2] The pore size is dependent on the degree of polymerization of the gel.[2] The product stream enters the matrix, and the solutes diffuse through the beads. Proteins exit the column according to size, with the largest proteins eluting first.[8] Solutes are eluted isocratically (the composition of the buffer remains constant), and the choice of buffer does not

affect the resolution.[15] Therefore, elution usually occurs with a buffer that is needed for the following step or for storage.

Size exclusion chromatography has a low volumetric capacity,[2, 11] and load volumes are usually 0.5-5% of the column volume.[15] Due to the low capacity, gel filtration is an expensive technique.[11] Thus, it is most often used at the end of a purification process.

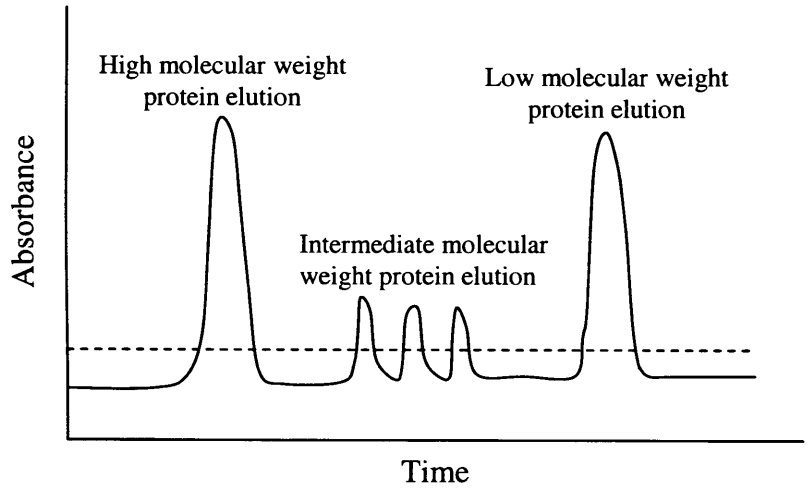

Figure 2.6 Typical Chromatogram for Size Exclusion Chromatography (with Isocratic Elution)[17]

Figure 2.7 summarizes the four discussed methods of chromatography.

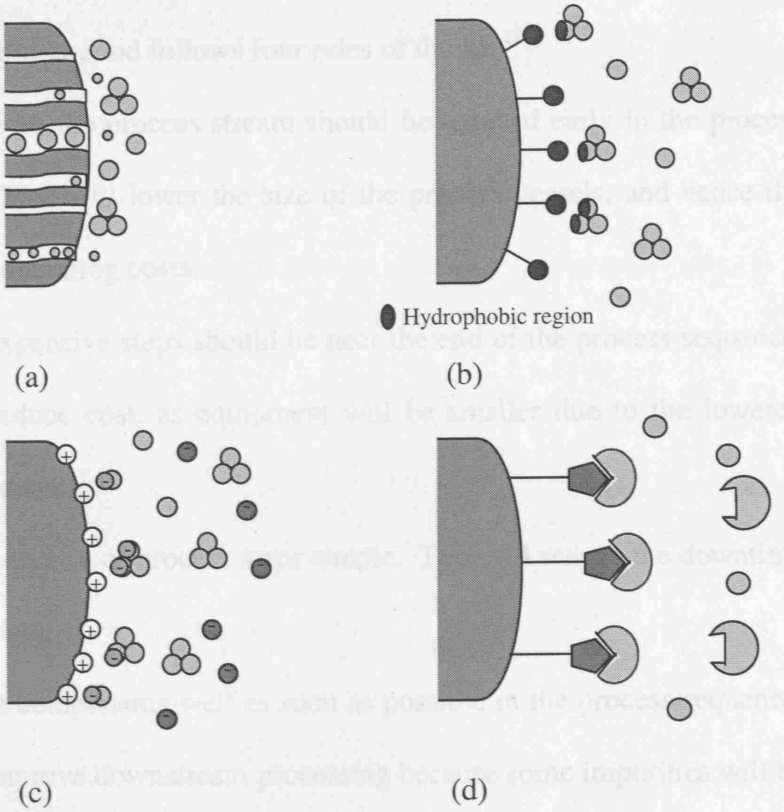

Figure 2.7 Separation Principles of Chromatographic Purification[10]
(a) Gel Filtration, (b) Hydrophobic Interaction, (c) Ion Exchange, (d) Affinity

2.3 Process Interactions

The process sequence, an example of which is shown in Figure 2.1, is designed so that the desired protein purification is achieved. Customers make purchasing decisions based on a product's cost, availability, and quality. Often for the manufacturer to be competitive, it must deliver a high quality product to the market as quickly as possible. The manufacturer is also interested in developing and producing the product at the lowest possible cost.[18] Therefore, it is necessary to find process conditions that give rise to a process that has the best

combination of yield, cost and purity. For many processes the sequence of operations is very similar, and follows four rules of thumb.[18]

1. The volume of the process stream should be reduced early in the process sequence. This will lower the size of the process vessels, and hence the capital and operating costs.
2. The most expensive steps should be near the end of the process sequence. This will reduce cost, as equipment will be smaller due to the lowered process volumes.
3. Keep the sequence of process steps simple. This will reduce the downtime as well as cost.
4. Resolve the components well as soon as possible in the process sequence. This will improve downstream processing because some impurities will be removed early in the process, as well as it will limit product loss due to degradation.

The final purification generally consists of a sequence of chromatography steps.[19] When looking at chromatography sequences, the same four basic rules can be applied. A sequence using ion exchange followed by hydrophobic interaction and ending with gel filtration is a common series of events. Each chromatography operation can be examined in order as a step in a chain of events. The first step is regarded as the capture step. Its purpose is to perform the initial purification of the target protein from a clarified or crude process stream.[14] It should also be rapid, and concentrate the protein while keeping it in a stable environment.[14] Ion exchange is a good option for the first step. It is able to

handle a large volume of the process stream, and concentrates it while operating at a fairly rapid speed and achieving high resolution.[14]

The second step is seen as an intermediate purification step, where there is further removal of bulk contaminants.[14] The objective of the step is to continue to purify and concentrate with a high resolution technique. Hydrophobic interaction chromatography is often the method of choice employed for this step. The process stream eluted from the ion exchange column is of high ionic strength, thus it can be loaded on the HIC column with minimal adjustments. HIC captures, clarifies, and concentrates well, and is able to achieve a high level of resolution especially when operating with gradient elution.[14]

The third step is the polishing step, where the final amounts of trace contaminants are removed.[14] It is also a step in which the pH, salt concentration, and additive concentration can be adjusted in order to prepare the product for storage.[14] Since this step is usually the final (or one of) step in the process, it is necessary that it operates so that an end product of the regulated purity is produced. Gel filtration is often the technique that is employed to carry out the polishing step. As mentioned before, the amount of process stream loaded on a gel filtration column is limited. Therefore, it is logical that this step follows ion exchange and hydrophobic interaction chromatography which are both concentration steps. Also, since gel filtration separates on the basis of molecule size, it facilitates the separation of contaminating molecules from the desired protein.

2.4 Modelling

The following summarizes common models that are used to describe chromatographic systems. The theory behind the different models is explained, and advantages and disadvantages are provided for each. Ultimately, it explains the choice of the General, Multi-Component Rate Model as the model used throughout this thesis due to its ability to deal with complex mixtures representative of protein solutions purified by chromatography. First, adsorption isotherms are described as they are an integral component in the General, Multi-Component Rate Model.

2.4.1 Adsorption Isotherms

Adsorption chromatography (i.e. ion exchange and hydrophobic interaction chromatography) depends on the extent to which material can be adsorbed onto a matrix.[26] This data is summarized by adsorption isotherms which consist of adsorption equilibrium data for a particular component in a sample mixture. Adsorption equilibrium occurs when the distribution of the solute between the solid and liquid phases is at equilibrium and there is no further net adsorption.[27]

One such isotherm is the linear isotherm, characterized by the equation: [2]

$$[q] = k_{eq}[c] \qquad (2.1)$$

where [q] is the concentration of component adsorbed to the matrix, [c] is the concentration of component in the mobile phase, and k_{eq} is the equilibrium constant.

This isotherm is most commonly seen in analytical chromatography, when samples are dilute and small in volume. Due to these properties, in theory all of the solute should be able to bind to the matrix (i.e. the saturation point is never reached), and the concentration of adsorbed solute will increase linearly.[2] However, in preparative chromatography this is not the case due to the higher concentrations and less dilute samples. Therefore, other isotherm relations must be employed.

Freundlich isotherms can be used to describe adsorption equilibria. It is seen in the form of: [2]

$$[q] = k_{eq}[c]^{1/n} \qquad (2.2)$$

The constants k_{eq} and n are dependent upon the characteristics of the adsorption system. When n>1, the adsorption is favourable. However, when n<1, the adsorption is unfavourable.[27] This isotherm can often be used to correlate data on heterogeneous adsorbents over a wide range of concentrations.[57]

Langmuir isotherms have often been used to correlate equilibrium adsorption data for proteins.[2] Adsorption of various components in a complex mixture, like that of a process stream entering the chromatographic stages, is influenced by equilibrium constants that are species specific and the total binding capacity of the resin.[2] Therefore, for each chromatographic system, the Langmuir isotherms will be different. This type of isotherm is often used to correlate data on homogeneous adsorbents.[57]

Langmuir isotherms for multi-component systems are governed by the following equation: [20]

$$C_{pi}^{s} = \frac{a_i C_{pi}}{1 + \sum_{j=1}^{N_s} b_j C_{pj}} \quad ; \text{ where } a_i = b_i C_i^{\infty} \tag{2.3}$$

where C^s_{pi} is the concentration of component i in the solid phase of the particle, C_{pi} and C_{pj} are the concentrations of components i and j in the stagnant fluid phase inside the particle macropores, a_i and b_i are Langmuir isotherm constants, and C_i^{∞} is the adsorption saturation capacity for component i.

This equation will yield a curve similar to that represented by Figure 2.8, and data calculated from it is input into the general, multicomponent rate model.

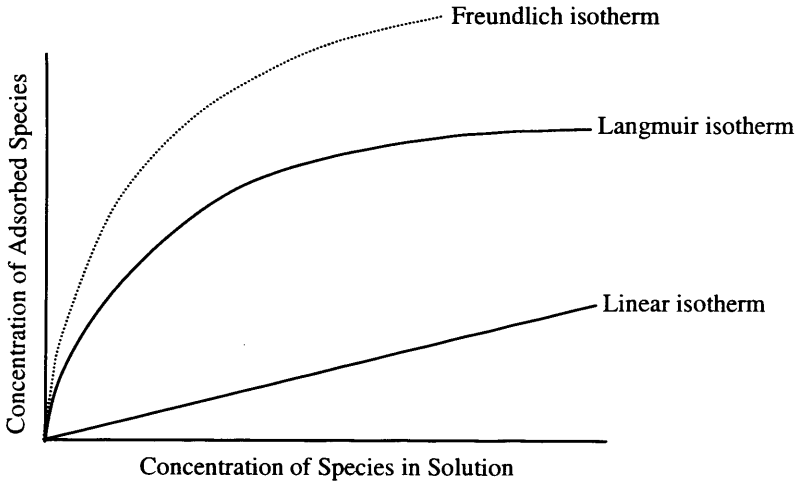

Figure 2.8 Diagram of a representative Langmuir Isotherm, Freundlich Isotherm, and Linear Isotherm

The following describes the four main chromatography models. Adsorption isotherms are required in two of the models, the equilibrium and rate models.

2.4.2 Chromatography Models

There are four main models to describe chromatography. They are the equilibrium model, plate model, statistical model, and rate model. The following sections will describe the different models, and their various assumptions and applications.

2.4.2.1 Equilibrium Model

The equilibrium model describes the equilibrium distribution between the two chromatographic phases, solid and liquid.[4]

The general composition at any point in the chromatography column can be determined by solving the following differential mass balance equation.[4]

$$\frac{DA\varepsilon_b}{Q}\frac{\partial^2 c}{\partial v_L{}^2} = \frac{\partial c}{\partial v_L} + \rho_s \frac{\partial q}{\partial V} + \varepsilon_b \frac{\partial c}{\partial V} \qquad (2.4)$$

The rate at which equilibrium is reached depends on the rate of mass transfer between the solid and liquid phases. The rate expression is given as: [4]

$$\frac{\partial q}{\partial V} = k_i f(c,q) \qquad (2.5)$$

Where, f(c,q) = driving force (equilibrium distribution isotherm).

When the rate of mass transfer is assumed to be infinite, the equilibrium isotherm can be directly substituted into the mass balance. This assumption is the

basis of the chromatography equilibrium model.[4] If the isotherm is linear, the model can be solved analytically. However, when the isotherm is non-linear, the model can only be solved numerically for a small number of components.[4] As most chromatographic systems involve non-linear isotherms and mass transfer effects can be significant, the equilibrium model is not the most valuable tool because the process becomes oversimplified.[4, 20] This will cause problems when predicting changes in operating conditions.

2.4.2.2 Plate Models

Plate models approximate chromatography operations as a series of well-mixed tanks at equilibrium.[2] There are two types of plate models. One model describes the equilibrium of each component in each hypothetical stage of the column.[20] These models can be used for multicomponent systems. However, they use an iterative solving method, thus making them lengthy and hard to solve.[20]

The second model is used in cases of non-ideal flow systems. The assumption is made that in each tank the mixing is complete, thus the solution is homogeneous.[20] This model yields solvable first order differential equations that describe adsorption and interfacial mass transfer processes.[20]

Plate models can also be simplified to explain band broadening observed in chromatography.[2] In 1941, Martin and Synge observed that when the number of tanks used in approximating the process became large and the initial concentration of solute was at a finite concentration in the first tank, the concentration profile through the separation could be described by a Gaussian

Curve.[2] Figure 2.9 shows a Gaussian peak as might be seen when running a chromatography process, as well as the information that can be extracted from the curve.

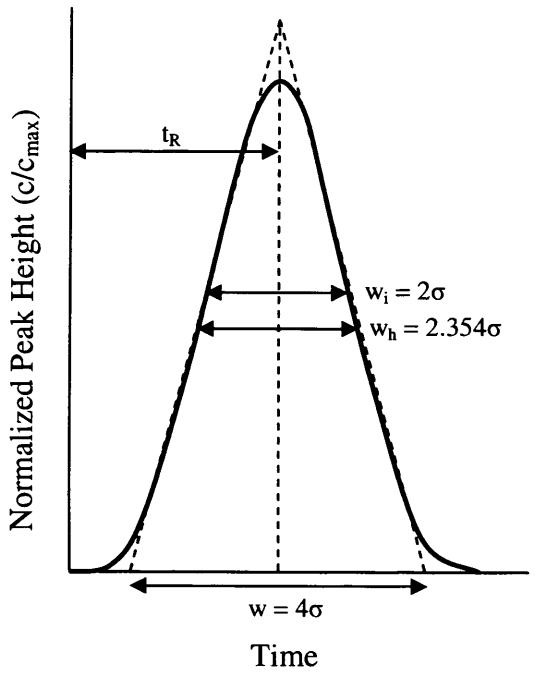

Figure 2.9 Properties of the Gaussian peak,[2] t_R, average retention time; w_i, peak width at inflection points; w_h, peak width at half-height; w, peak width at base; σ, standard deviation

The number of plates, N, can be calculated from the Gaussian peak by the following equation: [2]

$$N = \frac{t_R^2}{\sigma^2} = \frac{t_R^2}{\left(w/4\right)^2} \qquad (2.6)$$

Once the number of plates is known, then the height of the equivalent theoretical plate (HETP) can be calculated. HETP represents the resolving power

of the system, where a smaller value of HETP represents a better chromatographic separation.[2] The variable L is the length of the column.

$$HETP = \frac{L}{N} \tag{2.7}$$

The resolution, the measure of the extent of separation between two peaks in the chromatographic process,[2] can be determined when more than one peak is present on the chromatogram. The equation for resolution, R_s, is given as: [2]

$$R_s = \frac{t_{R,2} - t_{R,1}}{1/2(w_2 + w_1)} \tag{2.8}$$

where the subscripts 1 and 2 represent the two components.

When the value of R_s is larger, the resolution is better. Resolution is increased when the difference between the retention times of the two components is increased, and also when the width of the peaks is decreased.

HETP calculations should be performed at a low concentration of solute, and in the linear binding range.[2] This model is often used to compare the separation of multiple configurations of packing using the same column geometry, resin material, and isocratic elution.[2] However, the model is not widely accepted when using high concentrations of solute and gradient elution.[2]

2.4.2.3 Statistical Model

The statistical model is based on the statistical moments theory proposed by Giddings and Eyring in 1955.[4] They showed that statistical moments characterize a chromatographic elution peak.

The zero-order moment, μ_0, describes the load quantity, of the process stream.[4]

$$\mu_0 = C(L,t)dt \tag{2.9}$$

The first, second, and third order moments have been justified as acceptable to use to characterize chromatographic peaks.[21] The first statistical moment, μ_1, describes the retention time needed for a compound to pass through the column.[22] The results of this moment will be dependent on the equilibrium constants, the coefficient of longitudinal diffusion, and the mobile phase velocity.[22]

$$\mu_1 = \frac{\int_0^\infty C(L,t)t\,dt}{\int_0^\infty C(L,t)dt} = \frac{L}{v}\left[1+\frac{(1-\varepsilon_b)}{\varepsilon_b}\bullet\varepsilon_p\right]+\frac{t_0}{2} \tag{2.10}$$

The second moment, μ_2, describes the chromatography peak width (or variance). This moment is influenced by all the factors characterizing the column, including the column length, the longitudinal and radial diffusion, the equilibrium constants, and the size and shape of the resin particles.[22] The third moment

depends on all these factors as well, and describes the asymmetry of the peak.[22] Higher orders of moments define in more detail the broadening and asymmetry of the peaks, but are not widely accepted methods of characterizing the peak.[21]

$$\mu_2 = \frac{\int_0^\infty C(L,t)(t-\mu_1)^2 dt}{\int_0^\infty C(L,t)dt} \quad [23] \qquad (2.11)$$

$$\mu_2 = \frac{2L}{v}\left[\frac{(1-\varepsilon_b)}{\varepsilon_b} \bullet \frac{R_p^2 \varepsilon_p^2}{15} \bullet \left(\frac{1}{D_e} + \frac{5}{k_i R_p}\right) + \frac{D_{bi}}{v^2}\left(1 + \frac{(1-\varepsilon_b)\varepsilon_p}{\varepsilon_b}\right)^2\right] + \frac{t_0^2}{12} \quad [23] \qquad (2.12)$$

The method of statistical moments has been deemed poor for protein separations. Proteins are too complicated to be represented by simplifying equations since they interact with each other in solution, and there is poor thermodynamic data on protein adsorption.[4] Therefore many simplifying assumptions have to be made in order to apply the method.[4] The use of a lot of simplifying assumptions makes the method a poor predictor of chromatography performance. An example of an application of the method of moments is when it has been used to look at dispersion effects of peripheral elements (i.e. tubing) on chromatographic processes.[21]

2.4.2.4 Rate Model

The rate model is based on the rate equation for mass transfer between the mobile phase and the stationary phase,[20] and assumes the rate of mass transfer to be finite.[4] The general, multicomponent rate model is the most realistic model for all kinds of multicomponent adsorption/desorption chromatography processes.[24] It considers a variety of effects on the chromatography process including axial dispersion, external mass transfer, intraparticle diffusion, and multi-component, nonlinear isotherms.[24] It can be used for any type of adsorption chromatography.[25] The model consists of two sets of differential mass balance equations, one for the bulk fluid phase, and the other for the particle phase.[20] It also assumes that: [20]

1. The process is isothermal, multicomponent, and fixed-bed.
2. The bed is packed with uniform, spherical, porous adsorbents.
3. The concentration gradients in the radial direction are negligible.
4. There is a local equilibrium between the pore surface and the stagnant fluid phase in the macropores for each component.
5. The mass transfer and diffusional coefficients are constant and independent of the mixing effects of the components.

The equation for the bulk fluid phase is the following: [20]

$$-D_{bi}\frac{\partial C_{bi}}{\partial Z^2}+v\frac{\partial C_{bi}}{\partial Z}+\frac{\partial C_{bi}}{\partial t}+\frac{3k_i(1-\varepsilon_b)}{\varepsilon_b R_p}\left(C_{bi}-C_{pi,R=R_p}\right)=0 \qquad (2.13)$$

The equation for the particle phase is the following: [20]

$$(1-\varepsilon_p)\frac{\partial C_{pi}^s}{\partial t}+\varepsilon_p\frac{\partial C_{pi}}{\partial t}-\varepsilon_p D_{pi}\left[\frac{1}{R^2}\frac{\partial}{\partial R}\left(R^2\frac{\partial C_{pi}}{\partial R}\right)\right]=0 \qquad (2.14)$$

In addition, initial and boundary conditions are given in order for the partial differential equation system to be solved.[20]

1. $t=0 \qquad C_{bi}=C_{bi}(0,Z), \quad C_{pi}=C_{pi}(0,R,Z)$ (2.15)

2. $Z=0 \qquad \frac{\partial C_{bi}}{\partial Z}=\frac{v}{D_{bi}}\left(C_{bi}-C_{fi}(t)\right)$ (2.16)

3. $Z=L \qquad \frac{\partial C_{bi}}{\partial Z}=0$ (2.17)

4. $R=0 \qquad \frac{\partial C_{pi}}{\partial R}=0$ (2.18)

5. $R=R_p \qquad \frac{\partial C_{pi}}{\partial R}=\frac{k_i}{\varepsilon_p D_{pi}}\left(C_{bi}-C_{pi,R=R_p}\right)$ (2.19)

The equations can also be in a dimensionless form, as seen below. The dimensionless form of the bulk fluid phase is the following: [20]

$$-\frac{1}{Pe_{Li}}\frac{\partial^2 c_{bi}}{\partial z^2}+\frac{\partial c_{bi}}{\partial z}+\frac{\partial c_{bi}}{\partial \tau}+\xi_i\left(c_{bi}-c_{pi,r=1}\right)=0 \qquad (2.20)$$

The dimensionless form of the particle phase is as follows: [20]

$$\frac{\partial}{\partial \tau}\left[(1-\varepsilon_p)c_{pi}^s+\varepsilon_p c_{pi}\right]-\eta_i\left[\frac{1}{r^2}\frac{\partial}{\partial r}\left(r^2\frac{\partial c_{pi}}{\partial r}\right)\right]=0 \qquad (2.21)$$

The initial conditions for these equations are: [20]

$$\tau = 0, \quad c_{bi} = c_{bi}(0,z), \quad c_{pi} = c_{pi}(0,r,z) \tag{2.22}$$

The boundary equations for the dimensionless equations are: [20]

$$z = 0, \quad \frac{\partial c_{bi}}{\partial z} = Pe_{Li}\left(c_{bi} - {c_{fi}(\tau)}/{c_{0i}}\right) \tag{2.23}$$

For frontal adsorption: $\frac{c_{fi}(\tau)}{c_{0i}} = 1$ (2.24)

For elution mode: $\frac{c_{fi}(\tau)}{c_{0i}} = \begin{cases} 1 & 0 \le \tau \le \tau_{imp} \\ 0 & else \end{cases}$ (2.25)

It is necessary to make modifications to the model in order for it to be used for size exclusion chromatography. A new variable, the accessible pore volume fraction (ε_{pi}^{a}), is introduced to the model to account for the size exclusion effect.[20] When there are very small molecules, there are no size exclusion effects. Thus, $\varepsilon_{pi}^{a} = \varepsilon_p$. For large molecules that are completely excluded, $\varepsilon_{pi}^{a} = 0$. However, for "medium" size particles, $0 < \varepsilon_{pi}^{a} < \varepsilon_p$.[20] For these cases, a size exclusion factor has been introduced so that $\varepsilon_{pi}^{a} = F_i^{ex}\varepsilon_p$. The size exclusion factor is a function of the distribution coefficient of component i, as well as the particle size distribution when the particle sizes are not assumed to be equal.[20] In

order for the general rate model to be modified for size exclusion, the following changes are made to the equation for the particle phase.[20]

$$\cancel{(1-\varepsilon_p)\frac{\partial C_{pi}^{s}}{\partial t}}^{0} + \varepsilon_{pi}^{a}\frac{\partial C_{pi}}{\partial t} - \varepsilon_{pi}^{a} D_{pi}\left[\frac{1}{R^2}\frac{\partial}{\partial R}\left(R^2\frac{\partial C_{pi}}{\partial R}\right)\right] = 0 \qquad (2.26)$$

The first term in the equation is set to zero since component i does not bind to the stationary phase in size exclusion chromatography.[20]

The general, multicomponent rate model can provide a qualitative idea of how changes in parameters (i.e. particle size and pore size) affect the column performance.[4] However, its weakness lies in the complexity of its equations.[4] Since most protein separations involve complex mixtures, the general, multicomponent rate model has been used in the modelling of these separations. Thus, this is the model that has been used throughout this thesis.

2.4.3 Use of Fractionation Diagrams for Chromatographic Optimization

It is common practice that chromatograms are the final output in modelling predictions. However, chromatograms do not easily show the sensitivity of the chromatographic stage's reaction to changes in the operating conditions.[28] A fractionation diagram approach was developed by Richardson and co-workers[48] in the context of protein precipitation that uses fractionation diagrams as well as maximum purification versus yield diagrams to show how process parameters

affect the relationship between product yield, purity, and maximum purification. It was later demonstrated for chromatography by Ngiam *et al.*[28]

Fractionation diagrams plot the mass fraction of eluted product (y-axis) as a function of the mass fraction of the total eluted material (x-axis).[22] The construction of the fractionation diagram is based on the concentration profiles of the different components being separated.[28] The chromatogram is divided into N elements with equal width (time intervals). The example in Figure 2.10 is for a three component separation, where one component is the product and the other components are the impurities. At each interval, i, the total amount of material can be described as:

$$M_{T,i} = M_{P,i} + M_{A,i} + M_{B,i} \tag{2.27}$$

Where M_T is the total mass of material, M_P is the mass of product, M_A is the mass of impurity 1 and M_B is the mass of impurity 2.

As seen in Figure 2.10, the mass fraction of eluted product, Y, is plotted against the mass fraction of eluted material, X, where:

$$X = \frac{\sum_{0}^{i} M_{T,i}}{\sum_{0}^{N} M_{T,i}}, \quad Y = \frac{\sum_{0}^{i} M_{P,i}}{\sum_{0}^{N} M_{P,i}} \quad \text{where } N = \sum_{0}^{\infty} i \tag{2.28}$$

Once the fractionation diagram is constructed, it is possible to calculate further operating performance parameters. This is further discussed in the next section.

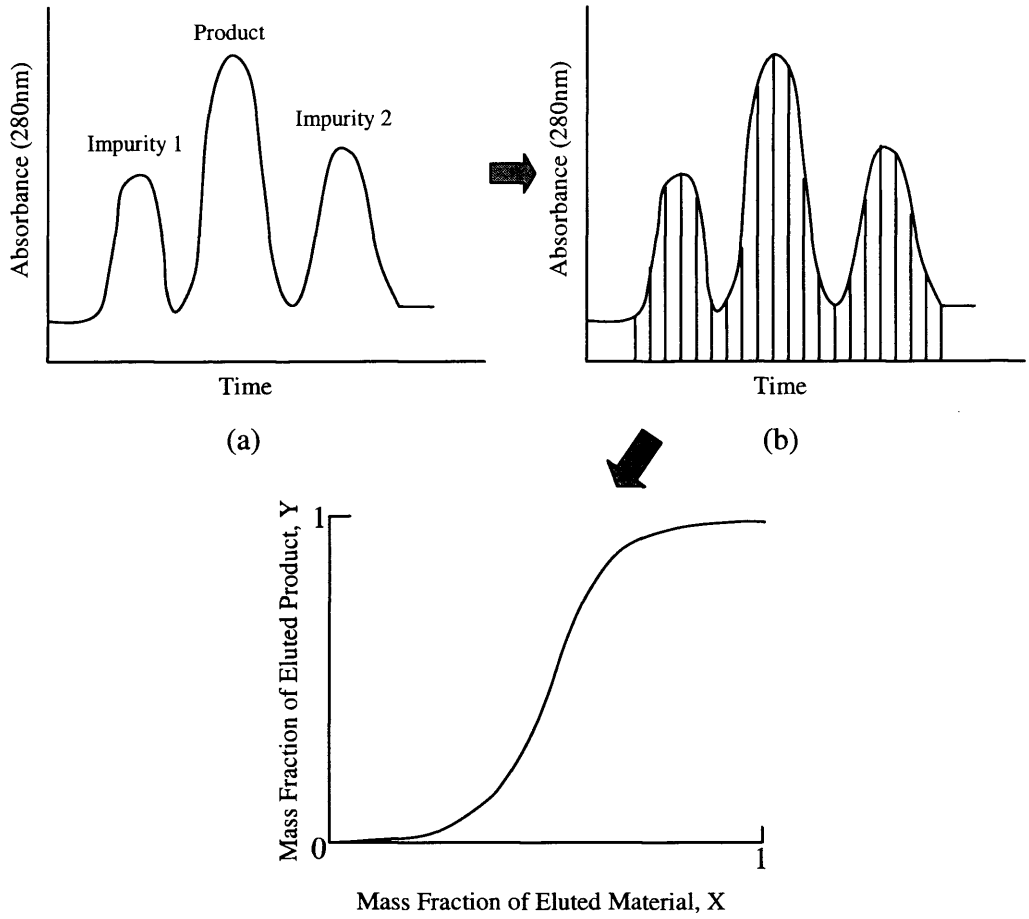

Figure 2.10 Construction of Fractionation Diagram from Chromatogram; (a) Chromatogram for three components, (b) Chromatogram divided into N elements, (c) Fractionation diagram

2.4.4 Purification Factor

Using the fractionation diagram, a purification factor (PF) versus yield diagram can be constructed. This ultimately shows the trade-off between purity and yield. The purification factor, PF, is defined as: [28]

$$PF = \frac{Final\ purity\ of\ product\ after\ purification}{Initial\ purity\ of\ sample\ before\ purification} \tag{2.29}$$

From the fractionation diagram, the purification factor is determined by calculating the gradient between any two points, Y_1 and Y_2, where these two points correspond to the beginning and end of product collection for a particular set of fractions selected from the chromatogram. Mathematically, the purification factor can be calculated as: [28]

$$PF = \left[\frac{M_P^2 - M_P^1}{M_T^2 - M_T^1}\right] \Big/ \left[\frac{M_0}{M_S}\right] \tag{2.30}$$

$$= \left[\frac{M_P^2}{M_0} - \frac{M_P^1}{M_0}\right] \Big/ \left[\frac{M_T^2}{M_S} - \frac{M_T^1}{M_S}\right]$$

Figure 2.11 shows how to arrive at the PF versus yield plot from a fractionation diagram.

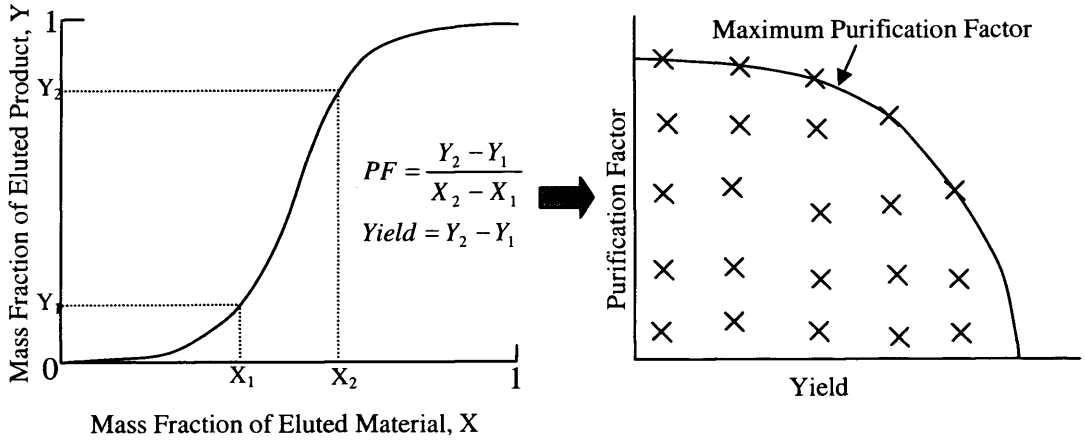

Figure 2.11 Construction of PF vs. Yield Diagram

Since there are an infinite number of possible combinations that can be taken from the fractionation diagram to generate PF values, the PF versus yield

diagram is constructed using a searching-type computer algorithm which seeks all the purification factors corresponding to each yield. Appendix C provides the Purification Factor vs. Yield algorithm. At each yield there exists a maximum purification factor, and from this the maximum purity at the specific yield may be calculated by using equation 2.29. From knowing which yield points (Y_1 and Y_2) give rise to this maximum purification value on the fractionation diagram, the cut points on the original chromatogram may be determined. The cut points show the start and end points of which fractions of the eluant should be collected to give rise to the desired purity and yield. Productivity, the mass of product eluted per chromatographic cycle time per unit volume of matrix, may then be calculated at the desired product yield.

2.4.5 Windows of Operation

Windows of Operation are 2-D diagrams that show how performance criteria are achieved at different combinations of operating conditions. Woodley *et al.* describe a Window of Operation as the 'operational space determined by the system (chemical, physical, biological) and process engineering constraints and correlations governing the particular process or operation under consideration'.[59] They can be used as a tool to help optimize operating conditions in order to meet desired process constraints and product specifications for a range of process units. In the case of chromatography, Windows of Operation can show how performance specifications, such as purity, yield or productivity can be achieved at different combinations of operating conditions, including flow rate and load volume. Figure 2.12 gives an example of how purity and productivity are affected

when linear velocity and breakthrough levels are changed. The darkest shaded region shows the possible combinations of linear velocity and breakthrough level that produce a product that meets both the purity and productivity specifications. This is the Window of Operation. The lighter shaded region above the Window of Operation contains operating conditions that when combined will produce a product meeting only the productivity specification. The lightest shaded region to the left of and below the Window of Operation details operating conditions that when combined will produce a product meeting only the purity requirements. In this work, to produce Windows of Operation, contour plots of the calculated purities and productivities obtained from the simulations and experiments were produced using Matlab 6.5.1 (The Mathworks Inc., Natick, MA, USA).[49] The contour levels were specified by the minimum desired purity and productivity of the chromatographic stage. The overlap between the purity and productivity contours forms the feasible region, or the Window of Operation, which is the process envelope containing all the combinations of operating conditions that will produce a product of the desired specifications. In all figures in this thesis, the Window of Operation is the darkest shaded region.

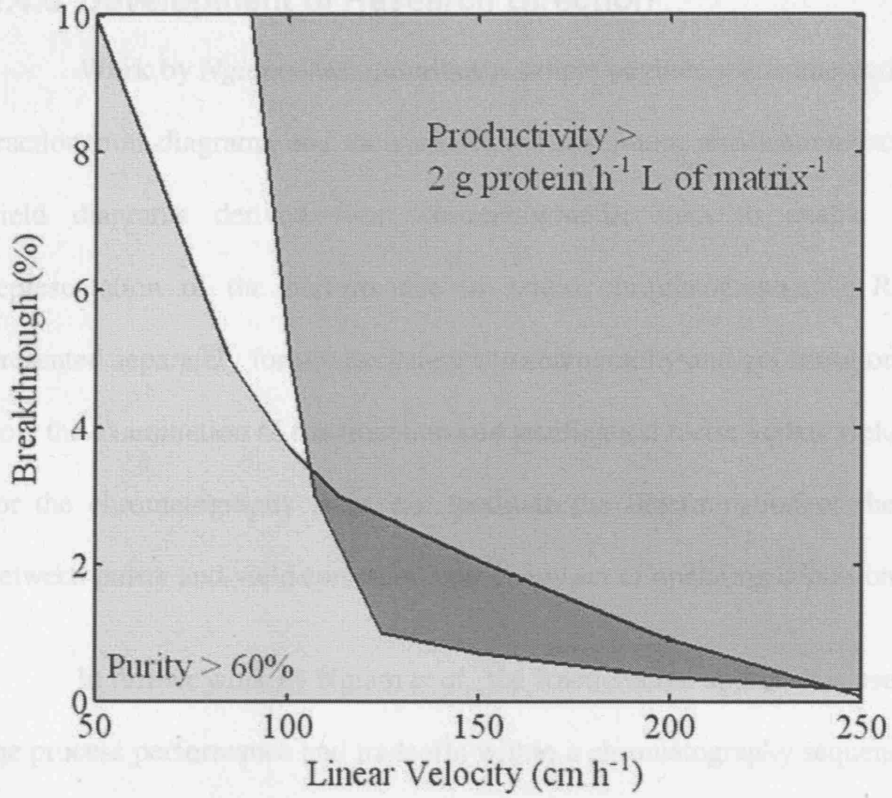

Figure 2.12 Example of a Window of Operation (as produced in Chapter 3)
- Purity > 60%, Productivity < 2 g protein h^{-1} L of $matrix^{-1}$
- Productivity > 2 g protein h^{-1} L of $matrix^{-1}$, Purity < 60%
- Purity > 60% and Productivity > 2 g protein h^{-1} L of $matrix^{-1}$
- Purity < 60% and Productivity < 2 g protein h^{-1} L of $matrix^{-1}$

Windows of Operation have been used to examine the performance of single unit operations. Saite *et al.* examine Windows of Operation for centrifuge selection for the separation of high solid density cell broths [60], and Collins *et al.* examine Windows of Operation for the determination of reactor operation for the microbial hydroxylation of toluene in a two-phase process.[61] Thus far, Windows of Operation have not been used as a tool to examine the performance of sequences of unit operations.

2.4.6 Development of Research Direction

Work by *Ngiam et al.* describes a simple engineering framework that uses fractionation diagrams and their associated maximum purification factor versus yield diagrams derived from chromatographic data to enable the rapid representation of the performance of liquid chromatography.[28] Results are presented separately for ion exchange chromatography and gel filtration, showing how the examination of fractionation and purification factor versus yield diagrams for the chromatography steps can facilitate the determination of the trade-off between purity and yield corresponding to any set of operating conditions.

In further work by Ngiam *et al.*, the fractionation approach is used to study the process performance and tradeoffs within a chromatography sequence.[38] This is done by using a sequence of hydrophobic interaction chromatography followed by size exclusion chromatography. The approach described enables the user to select a set of operating conditions that meets the minimum requirement of product purity without sacrificing yield.

The research presented in this thesis proposes to further expand on the work presented by Ngiam *et al.* A methodology is proposed that uses Windows of Operation to select sets of operating conditions for chromatography sequences, incorporating the trade-off between purity, yield and productivity. This methodology is unique in its use of Windows of Operation to describe feasible operating conditions for unit operation sequences. It is also unique as the results of the determination of feasible operating conditions are presented as operating spaces (incorporating a large set of feasible operating conditions), and not just a

single set of operating conditions as is usually presented in typical optimization solutions and the work presented by Ngiam *et al.*

The next chapter describes in detail how to obtain a Window of Operation from chromatogram data. The methods described in Chapter 3 will be the basis of the development of a methodology to determine operating conditions for chromatography sequences.

3. Production of Windows of Operation

3.1 Introduction

This chapter provides an example of how Windows of Operation are used as a tool to examine chromatogram data in order to determine the effects of operating conditions on process performance. It builds upon the tools presented in the previous chapter, including fractionation diagrams, purification factor vs. yield diagrams, and ultimately Windows of Operation.

3.2 Summary of Materials and Methods

3.2.1 Simulated Process

Simulations were carried out representing the first stage of a chromatography sequence, e.g. ion exchange chromatography. For all the simulations, a hypothetical three component mixture was assumed in order to mimic a multicomponent process stream in industrial separation.[38] The product, first impurity and second impurity had molecular weights of 50 kDa, 150 kDa and 15 kDa respectively. Examples of proteins in the range of 15 kDa include ribonuclease and lysozyme. Ovalbumin and hexokinase have masses around 50 kDa, and IgG has a mass of approximately 150 kDa. The initial concentration of the product was set at 4 g L^{-1} ($8x10^{-5}$ mol L^{-1}), while the first and second impurities had set concentrations of 7.5 g L^{-1} ($5x10^{-5}$ mol L^{-1}) and 0.75 g L^{-1} ($5x10^{-5}$ mol L^{-1}) respectively. As an example, a large scale purification (ion exchange chromatography) of a mammalian expression system producing approximately 100 g per year of product will typically load 2 L of solution on the column, containing a total of 11.3 g of protein of which 2.9 g is product.[37]

Therefore, the simulated system contains materials of the same magnitude as the industrial, large scale purification. The column dimensions and parameters are shown in Table 3.1.

The column was operated at simulated linear velocities of 50, 100, 150, 200, and 250 cm h^{-1}, which relate to flow rates of 3.9, 7.9, 11.8, 15.7, and 19.6 L h^{-1} respectively, and also to achieve 0%, 1%, 3%, 5%, and 10% levels of product breakthrough. Simulations were inclusive of all the possible combinations of flow rate and product breakthrough level.

In initial design considerations, breakthrough is a valuable variable to look at in order to examine the tradeoffs between loading the column so that little product is lost during this initial stage, but sacrifices productivity, and loading the column to the point that a proportion of product is lost during this initial stage, resulting in higher productivity but reduced yields. A theoretical breakthrough curve is shown in Figure 3.1.

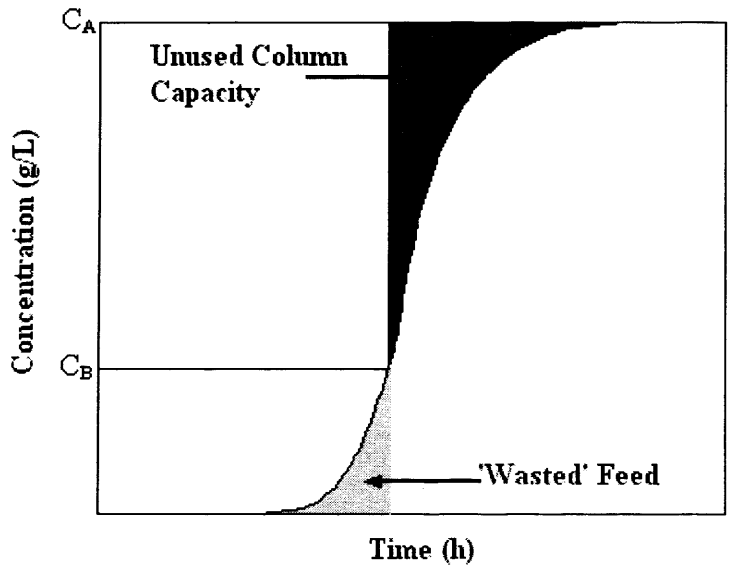

Figure 3.1 Theoretical Breakthrough Curve

If loading continues until the entire bed is saturated (concentration of effluent = C_A), a considerable amount of solute is wasted. To avoid this, loading is usually stopped before the bed is completely saturated. However, if loading is stopped when protein concentration in the effluent is C_B, a portion of the column capacity has not been used.[54] Therefore, it is important in commercial practice to strike a balance in loading the feed material between losing product by saturating the column, and not using the available column capacity, thus costing time (and money).

Table 3.1. Column and Chromatographic Parameters for Simulations of First Chromatographic Stage

Column Parameter	**Chromatographic Step 1 Column**
Diameter (cm)	10
Length (cm)	20
Average Particle Radius, R_p (μm)	45
Bed Void Space, E_b	0.4
Particle Void Space, E_p	0.45
Tortuosity	4
Impurity 1: Langmuir Parameter a	0.01
Impurity 1: Langmuir Parameter b	1
Product: Langmuir Parameter a	3
Product: Langmuir Parameter b	300
Impurity 2: Langmuir Parameter a	14
Impurity 2: Langmuir Parameter b	1400
Displacer: Langmuir Parameter a	0.001
Displacer: Langmuir Parameter b	10000
Desired Product Yield (%)	85

3.2.2 Chromatogram Simulation

Computer simulation is a rapid and economical way of obtaining a variety of chromatography results,[39-45] and greatly facilitates the investigation into chromatography optimization.[46] Data obtained for this analysis were derived from computer simulations carried out using Chromulator version 2.0 (Gu T., Department of Chemical Engineering, Ohio University, Athens, OH, USA).[47] Chromulator is a chromatography simulator package based on the general multicomponent rate model. [4, 20, 24] It is an accepted tool in the development of chromatography steps and is licensed by chemical, pharmaceutical and biotech companies such as Pfizer, Wyeth BioPharma, Schering Plough and Millipore.

There are a number of variables that the user must input in order to use the simulator. Figure 3.2 shows the Chromulator user interface and the inputs that are required.

Simulations are performed using dimensionless time, the definition of which is:

$$Dimensionless\ Time = \frac{Sample\ Volume \times Linear\ Velocity}{Flow\ Rate \times Column\ Length}. \qquad (3.1)$$

All simulations were run using the LC operation option in which the column was loaded and then elution was performed. The different dimensionless times that were required for input were the following:

- t_{imp} – dimensionless time at which the sample is injected
- t_{int} – dimensionless time intervals at which the calculations are performed to make the chromatogram

- t_{max} – dimensionless time describing the total amount of time for which the simulation (breakthrough and elution) is to be run
- t_{shift} – dimensionless time at which the shift between breakthough (loading) and elution occurs

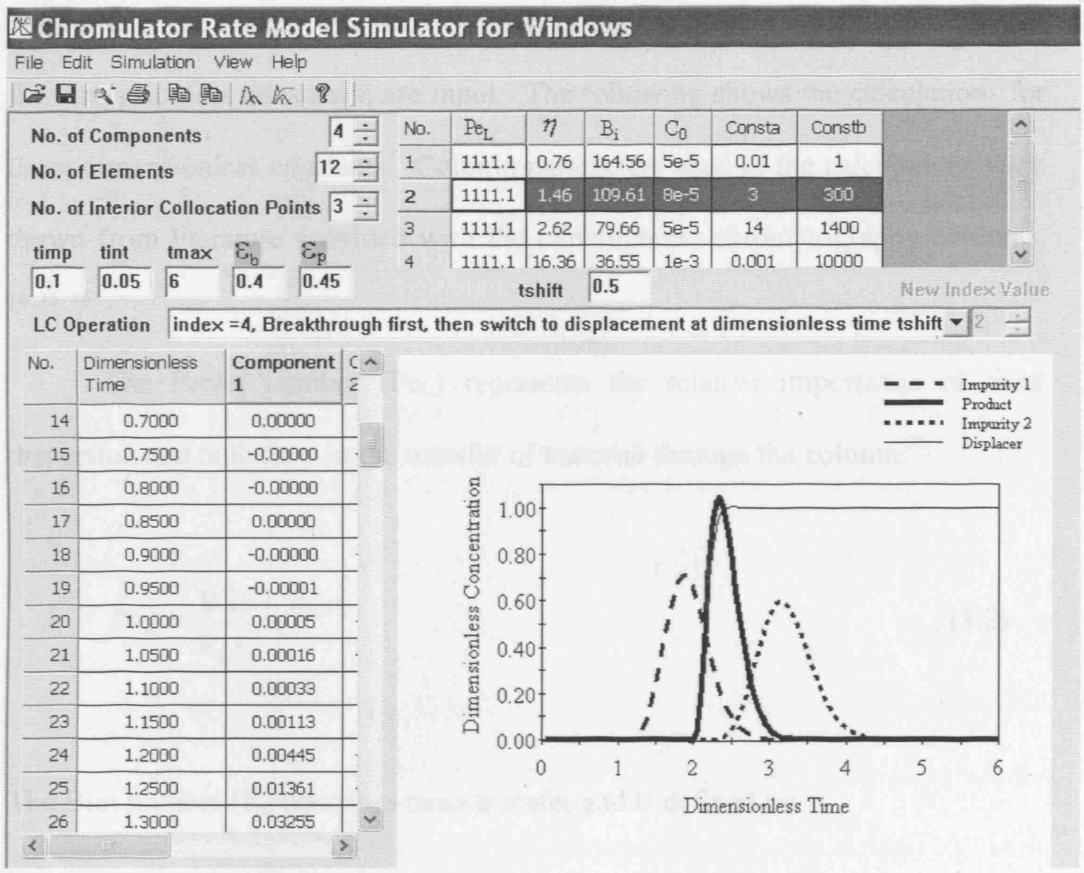

Figure 3.2 Computer Interface for Chromulator Simulation Programme

The column parameters ε_b, bed porosity, and ε_p, particle porosity, are input as well in the same line as the time parameters. In the top, left-hand corner is the number of components, elements and interior collocation points. The number of components is equal to the number of proteins that are being separated in the mixture, plus the component that is used to carry out the elution (i.e. the displacer). The number of elements and collocation points reflects the desired

resolution of the chromatogram. There is better resolution of the simulation when the numbers are higher because more computational iterations are performed. However, this also means that with more iterations, the simulation time will be slower.

Dimensionless constants are entered for each component in the top, right-hand side of the screen. For each component the Peclet number, Biot number and the dimensionless constant η are input. The following shows the calculations for these dimensionless constants. Column parameters used in the calculations were drawn from literature provided with the experimental chromatography columns.[14, 15, 16]

The Peclet number (Pe_L) represents the relative importance of axial dispersion and bulk flow in the transfer of material through the column.[26]

$$Pe_L = \frac{0.1L}{R_p \varepsilon_b} \quad [50,51] \tag{3.2}$$

The Biot number (B_i) describes mass transfer and is defined as:

$$B_i = \frac{Characteristic\ Film\ Transport\ Rate}{Characteristic\ Intraparticle\ Diffusion\ Rate}$$

$$B_i = \frac{KR_p}{\varepsilon_p D_p} \quad [50,51] \tag{3.3}$$

$$\text{where } D_p = D_m + \left(\frac{1 - 2.104\lambda + 2.09\lambda^3 - 0.95\lambda^5}{\tau} \right) \quad [50,51] \tag{3.4}$$

$$\lambda = \frac{Molecular\ Diameter\ of\ Eluite\ d_m}{Pore\ Diameter\ of\ Particles\ d_p} \quad [50,51] \tag{3.5}$$

$$d_m = 1.44 \times (Molecular\ Weight)^{1/3}\ [50,51] \tag{3.6}$$

$$D_m = 2.74 \times 0.00001 \times (Molecular\ Weight)^{-1/3}\ [50,51] \tag{3.7}$$

The dimensionless constant η describes interstitial velocity and is defined as

$$\eta = \frac{\varepsilon_p D_p L}{R_p^2 v}\ [50,51] \tag{3.8}$$

The initial concentrations and Langmuir parameters a and b are also entered for each component. A competitive Langmuir isotherm model[20] was employed to describe the adsorption characteristics. The Langmuir parameters used in the simulations of the chromatographic stage are listed in Table 3.1. The parameter values selected reflect the relative properties only, and are used to define the separation achieved in the chromatographic step.

Once all the variables are entered, the simulation is run and the outputs are a chromatogram (as seen on the right side of Figure 3.2) and a table (seen on the left side of Figure 3.2) detailing the dimensionless concentration of each component at each dimensionless time interval. A typical simulation takes approximately twenty seconds for a computer with a 1.70 GHz processor to complete.

Chromulator is an effective way to rapidly and economically achieve a large amount of chromatography data. However there are a couple of disadvantages associated with the simulation programme. The programme is not able to incorporate a wash step between loading and elution as is commonly

practiced in industry. Also, the simulation programme provides good quality results for protein separations that are Langmuir in their adsorption characteristics. However, the simulation package does not provide an option for the utilization of other adsorption isotherms, nor can the code be accessed in order to make modifications.

3.2.3 Graphical Procedures

Chromatograms do not easily show the sensitivity of the chromatographic stage's reaction to changes in the operating conditions. To show this sensitivity, Windows of Operation are ultimately produced. In order to create Windows of Operation from chromatograms, two intermediate steps are needed. Fractionation diagrams and purification factor (PF) versus yield diagrams must first be constructed.[28, 48] Details of the fractionation diagram, PF versus yield diagram and Windows of Operation techniques are outlined in sections 2.4.3, 2.4.4, and 2.4.5. Figure 3.3 shows a flow sheet detailing the simulation strategy for creating data that will populate the Windows of Operation, and the data treatment in order to produce the Windows. Figure 3.4 provides a summary of how to arrive at a Window of Operation from the chromatogram data.

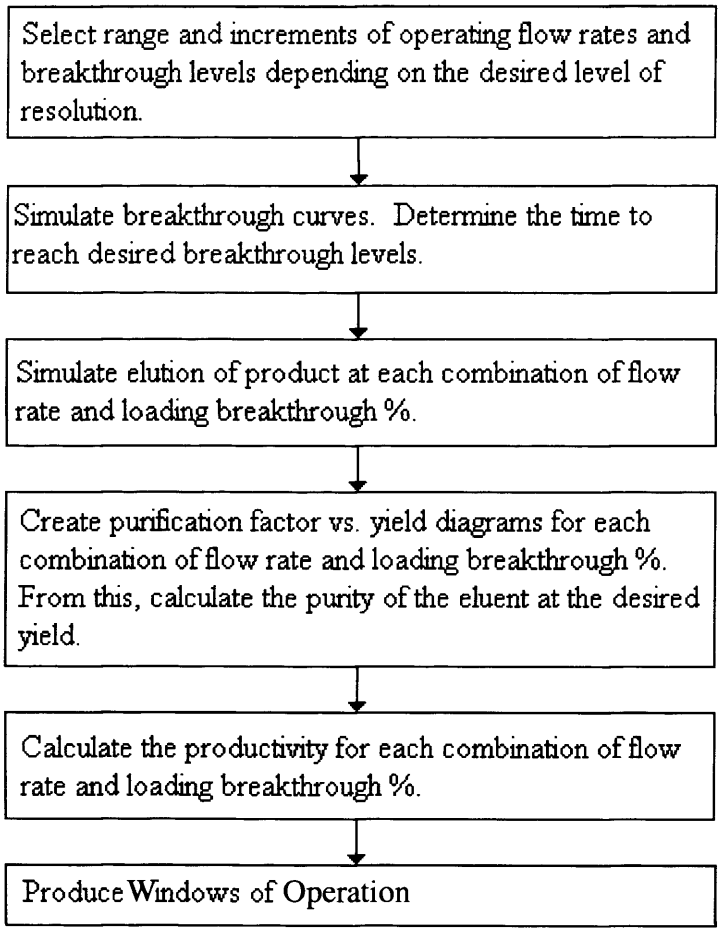

Figure 3.3 Flow sheet for the production of a Window of Operation from multiple chromatograms, fractionation diagrams and purification versus yield diagrams

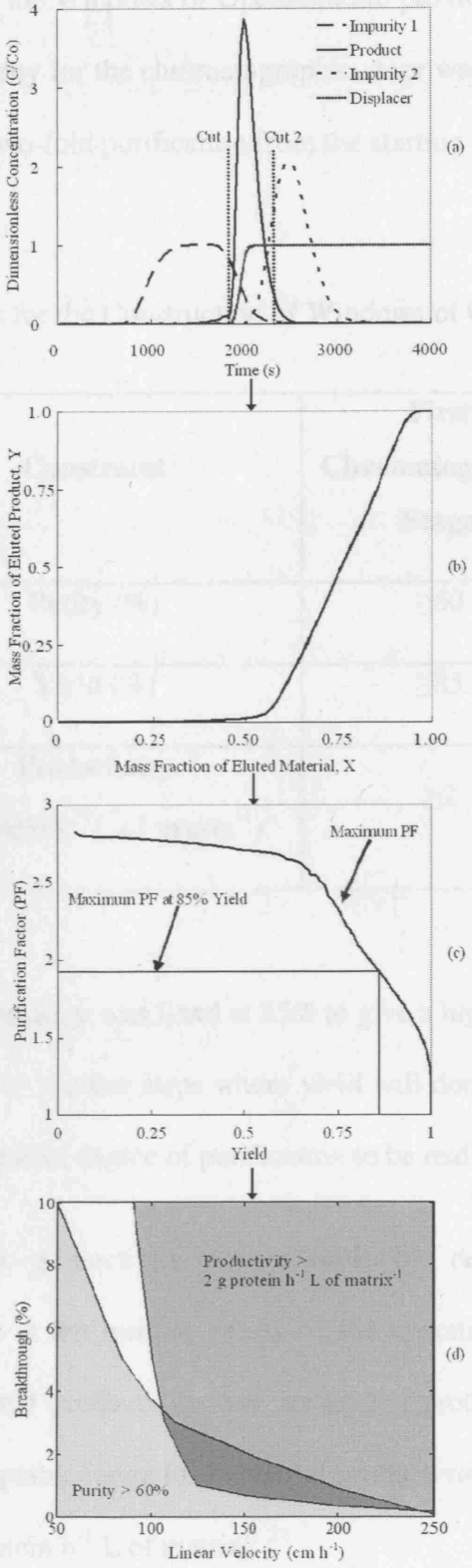

Figure 3.4 Production of a Window of Operation from multiple chromatograms, fractionation diagrams and purification versus yield diagrams. (a) chromatogram for hypothetical, 3 component mixture, (b) fractionation diagram, (c) purification versus yield diagram, (d) Window of Operation

Constraints for the Windows of Operation are provided in Table 3.2. The minimum desirable purity for the chromatographic stage was chosen to be 60% to give approximately a two-fold purification from the starting material.

Table 3.2. Constraints for the Construction of Windows of Operation

Constraint	**First Chromatographic Stage**
Purity (%)	≥60
Yield (%)	≥85
Productivity (g protein h^{-1} L of matrix^{-1})	≥2

The yield for the stage was fixed at 85% to give a high yield representative of early chromatography capture steps where yield will dominate purity, but also to allow for a representative degree of purification to be realized.

The minimum productivity was chosen by determining what the productivity would be at the median values of the operating conditions. From this, a minimum desired productivity was set at 2 g protein h^{-1} L of matrix^{-1}, falling within the acceptable range for industrial productivity for an ion exchange operation of 1-25 g protein h^{-1} L of matrix^{-1}.[37]

3.3 Results

Simulations were run according to the procedure outlined in Figure 3.3 to generate a set of chromatograms, fractionation diagrams, and purification versus yield diagrams with the parameters given in Tables 3.1 and 3.2. The following results are based upon the simulations performed for a breakthrough of 5% and a linear velocity of 150 cm h^{-1} (11.8 L h^{-1}).

A simulation was run to produce a breakthrough curve in order to determine the time to reach the desired breakthrough level. Appendix A provides the data for the breakthrough curve.

The output from the chromatography simulation package includes dimensionless time and dimensionless concentration. The values of time (s), volume (mL) and concentration (g L^{-1}) were added to the spreadsheet by the following calculations:

$$time = \frac{Dimensionless\ Time \times Column\ Length}{Linear\ Velocity} \tag{3.9}$$

$$\begin{aligned} Volume &= \frac{Flow\ Rate \times Time}{60} \\ &= \frac{Linear\ Velocity \times \pi \times (Column\ Radius)^2 \times Time}{60} \end{aligned} \tag{3.10}$$

$$\begin{aligned} Concentration = {} & Dimensionless\ Concentration \times Initial\ Concentration \\ & \times Molecular\ Weight \end{aligned} \tag{3.11}$$

The table provided in Appendix A shows that for 5% product breakthrough, the loading time is needed to be 625 seconds (dimensionless time of 3.25). This is input in the simulation programme in order for it to know when

to switch from loading material to eluting material during the first chromatographic purification stage by a displacement solution.

Figure 3.5 shows the chromatogram obtained with a simulated linear velocity of 150 cm h^{-1} and a product breakthrough of 5%. Appendix B provides the raw output data from the chromatogram simulation

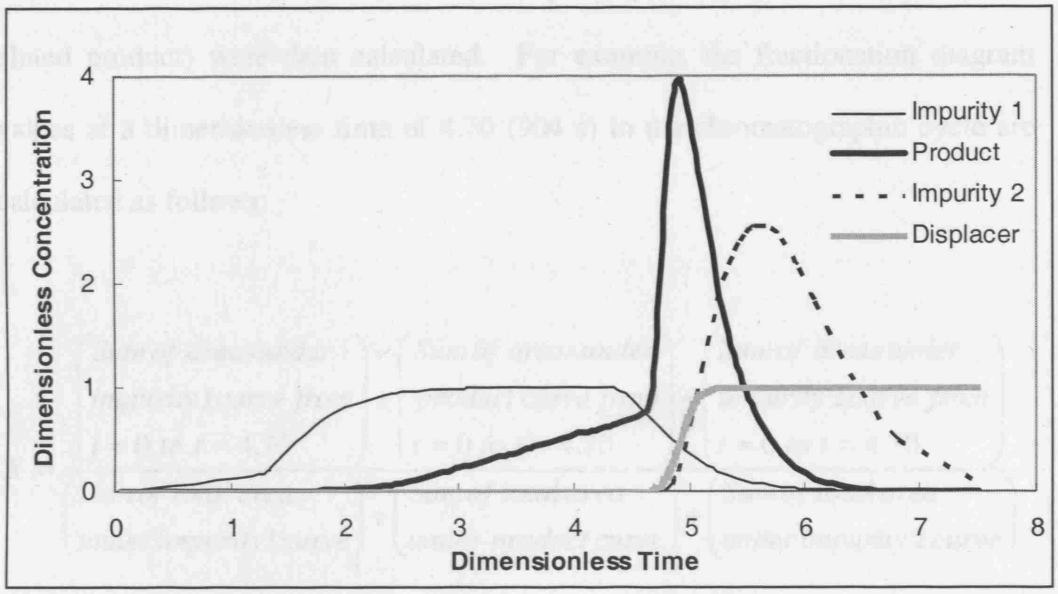

Figure 3.5 Chromatogram – First Chromatographic Stage, Linear Velocity of 150 cm h^{-1} and Loading Breakthrough of 5%

Once the chromatogram data was obtained, the fractionation diagram data was calculated using the concentration data in Appendix B derived from the chromatogram. First, each component's chromatogram curve was divided into a number of segments and the area of each segment under component's curve was calculated using the trapezoidal rule.

$$Area\ Under\ Peak\ Segment = \frac{volume_n - volume_{n-1}}{2} \times (concentration_n + concentration_{n-1}) \tag{3.12}$$

Where n represents each step in the tabulated dimensionless time. In the case of Appendix B, n was representative of a row within the table.

The values of X (mass fraction of eluted material) and Y (mass fraction of eluted product) were then calculated. For example, the fractionation diagram values at a dimensionless time of 4.70 (904 s) in the chromatographic cycle are calculated as follows:

$$X = \frac{\begin{pmatrix} Sum\ of\ areas\ under \\ impurity\ 1\ curve\ from \\ t = 0\ to\ t = 4.70 \end{pmatrix} + \begin{pmatrix} Sum\ of\ areas\ under \\ product\ curve\ from \\ t = 0\ to\ t = 4.70 \end{pmatrix} + \begin{pmatrix} Sum\ of\ areas\ under \\ impurity\ 2\ curve\ from \\ t = 0\ to\ t = 4.70 \end{pmatrix}}{\begin{pmatrix} Sum\ of\ total\ area \\ under\ impurity\ 1\ curve \end{pmatrix} + \begin{pmatrix} Sum\ of\ total\ area \\ under\ product\ curve \end{pmatrix} + \begin{pmatrix} Sum\ of\ total\ area \\ under\ impurity\ 2\ curve \end{pmatrix}} \tag{3.13}$$

$$Y = \frac{Sum\ of\ areas\ under\ product\ curve\ from\ t = 0\ to\ t = 4.70}{Sum\ of\ total\ area\ under\ product\ curve} \tag{3.14}$$

Appendix B shows the calculated values of the segment peak areas under the product, impurity 1 and impurity 2 curves, as well as the fractionation values of X and Y. Figure 3.6 shows the resulting fractionation diagram.

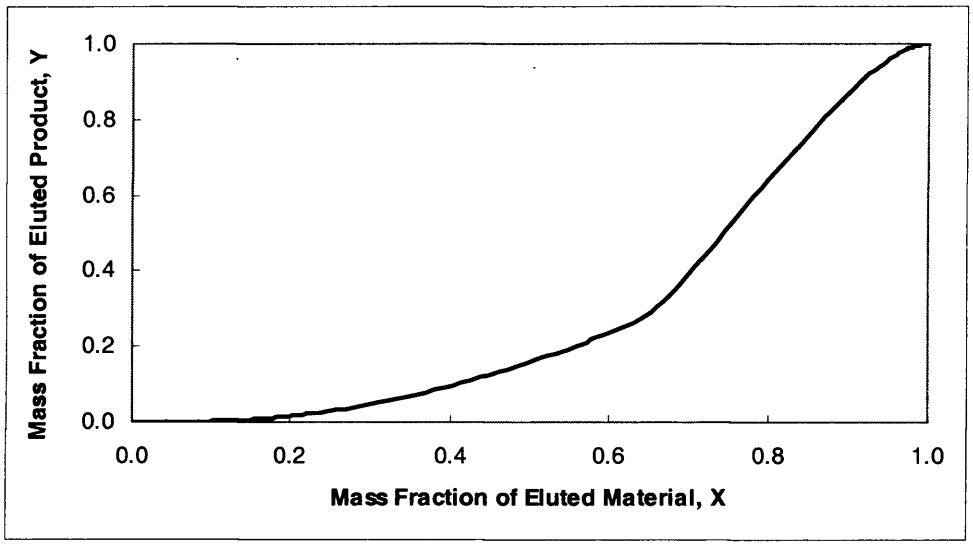

Figure 3.6 Fractionation Diagram – First Chromatographic Stage, Linear Velocity of 150 cm h^{-1} and Loading Breakthough of 5%

Using the Purification versus Yield algorithm provided in Appendix C, the fractionation diagram data was analyzed to produce a maximum purification factor versus yield diagram. The output from the algorithm is provided in Table 3.3 and Figure 3.7.

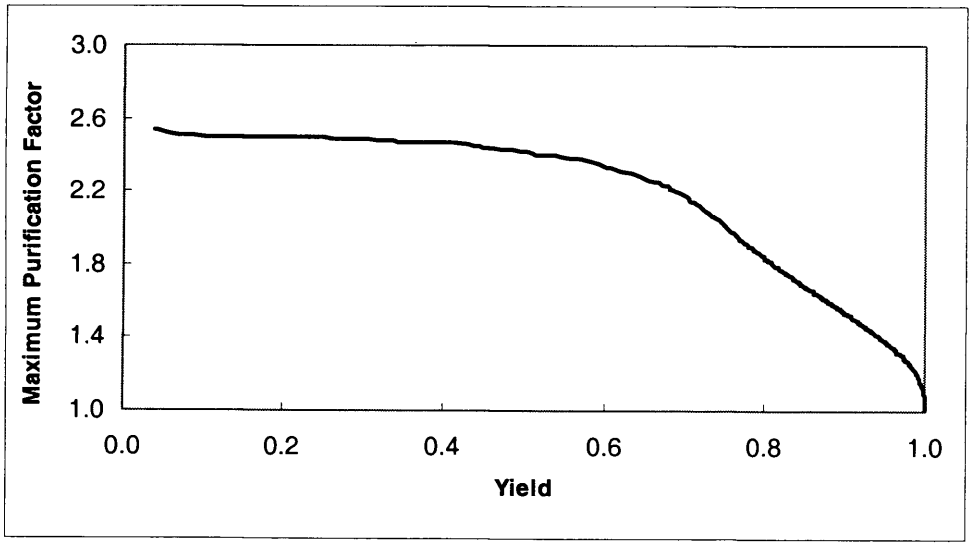

Figure 3.7 Maximum Purification Factor vs. Yield Diagram – First Chromatographic Stage, Linear Velocity of 150 cm h^{-1} and Loading Breakthrough of 5%

Table 3.3 Maximum Purification Factor vs. Yield Algorithm Output Table

Yield	Max PF	Start Yield	% Purity
1.000	1.000	0.000	32.7
0.999	1.092	0.001	35.7
0.996	1.141	0.004	37.3
0.992	1.185	0.008	38.7
0.988	1.214	0.011	39.6
0.980	1.260	0.020	41.1
0.975	1.286	0.025	42.0
0.968	1.313	0.032	42.9
0.962	1.338	0.035	43.7
0.955	1.364	0.043	44.5
0.947	1.391	0.052	45.4
0.940	1.418	0.056	46.3
0.933	1.438	0.061	47.0
0.925	1.464	0.072	47.8
0.917	1.486	0.078	48.5
0.908	1.513	0.090	49.4
0.899	1.539	0.097	50.3
0.893	1.561	0.103	51.0
0.887	1.575	0.110	51.4
0.883	1.588	0.110	51.9
0.876	1.604	0.118	52.4
0.870	1.623	0.125	53.0
0.863	1.644	0.133	53.7
0.856	1.662	0.141	54.3
0.852	1.677	0.141	54.8
0.850	**1.683**	**0.141**	**55.0**
0.848	1.686	0.149	55.1

As stated in Table 3.2, the desired yield is $\geq 85\%$. At a yield of 85%, the maximum purification factor is 1.683. Using the following calculation it was determined that the purity is 55% at a yield of 85%.

$$\%Purity = \frac{Maximum\ Purification\ Factor}{Initial\ Purification\ Factor} \times 100 \qquad (3.15)$$

Finally, the productivity of the chromatography step was calculated. To complete this calculation the time taken for the chromatographic cycle was

required. The Purification versus Yield algorithm also provides the value of the yield at which to start collecting material in order to obtain a product solution that has 55% purity. For an 85% yield, the ideal starting point for product collection was at 14.1% yield. Therefore, the endpoint for material collection is a product yield of 99.1% yield (14.1% + 85%). Referring back to the chromatogram simulation spreadsheet, Appendix B, it is seen that a yield of 99.1% gave a loading and elution time of 1170 s.

The washing and regeneration times must also be factored into the productivity calculation, and are set to be 4 and 5 column volumes respectively. Therefore, the total chromatographic cycle time is calculated to be:

$$\begin{aligned} Chromatographic\ cycle\ time &= Loading\ time + Elution\ time + Washing\ time + Regeneration\ tim \\ &= \frac{1170s}{3600s\,h^{-1}} + \frac{4\times 1.571L}{11.8L\,h^{-1}} + \frac{5\times 1.571L}{11.8L\,h^{-1}} = 1.523h \end{aligned} \tag{3.16}$$

The product mass for an 85% product yield is calculated as:

$$\begin{aligned} Product\ mass &= Molecular\ weight \times Initial\ Concentration \times Load\ Volume \times Yield \\ &= 50000g\,mol^{-1} \times (8\times 10^{-5}\,mol\,L^{-1}) \times 2.04L \times 0.85 = 6.936g \end{aligned} \tag{3.17}$$

Productivity is calculated as:

$$Productivity = \frac{Mass\ of\ Product}{Time\ of\ Chromatographic\ Cycle \times Matrix\ Volume} \tag{3.18}$$

Productivity was determined to be 2.9 g L^{-1} h^{-1}.

Once these steps (producing the chromatograms, fractionation diagrams, Purification Factor versus Yield diagrams, and calculating productivity) are repeated for all the possible combinations of linear velocity and loading breakthrough, a Window of Operation can be produced with the resulting data. Appendix D provides the Matlab code that was used to produce the Window of Operation.

The code allows the user to input the matrix of linear velocity and breakthrough % values that were simulated and the resulting purity and productivity values for each combination of linear velocity and breakthrough %. Matlab uses the input data to create two contours on one diagram based upon the minimum desired purity and productivity. The overlapping contours form the Window of Operation as seen in Figure 3.8.

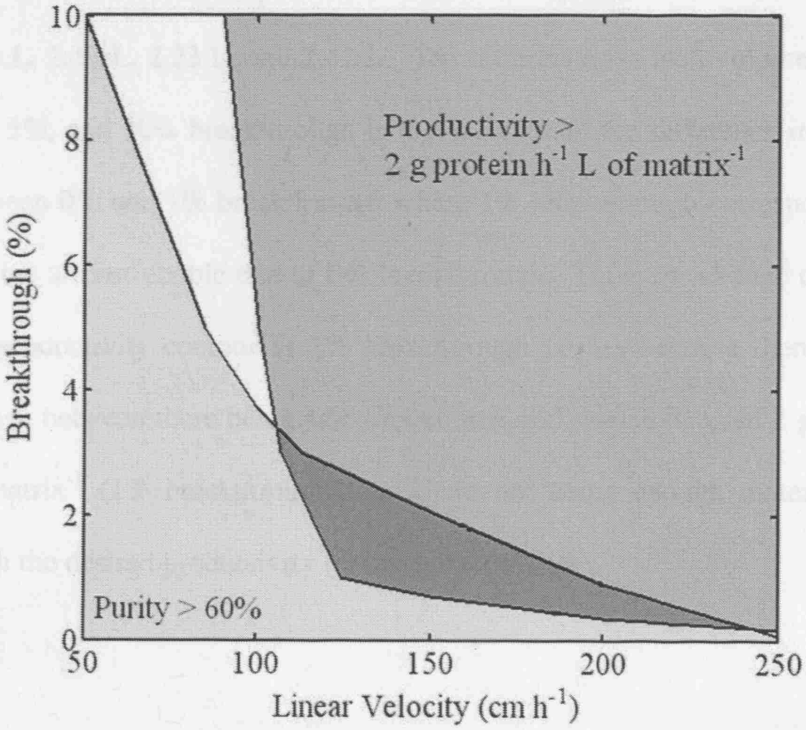

Figure 3.8 First Chromatographic Stage Window of Operation. ■ Region where purity ≥ 60%, and productivity ≥ 2 g protein h^{-1} L of $matrix^{-1}$.

The darkest shaded region in Figure 3.8 is the Window of Operation, and combinations of operating conditions that fall within this region will produce a product of both the desired productivity and purity. Combinations of operating conditions that lie in the shaded region above the Window of Operation only produce a product that meets the productivity criteria, where those which lie in the shaded region below the Window of Operation produce a product that meets only the purity criteria. Operating conditions that lie in the white region will produce a product that meet neither the purity nor productivity criteria.

It is observed that at 1% breakthrough the productivity contour has a sudden change of direction and runs nearly parallel to the x-axis. This can be explained by relating the simulated breakthrough % with its corresponding load volume. For example, at a linear velocity of 50 cm h^{-1} in the first stage operation, 0%, 1%, 3%, 5%, and 10% breakthrough corresponds to load volumes of 1.08 L, 1.94 L, 2.13 L, 2.23 L, and 2.42 L. The differences in load volume between 1%, 3%, 5%, and 10% breakthrough is much less than the difference in load volume between 0% and 1% breakthrough where 1% breakthrough corresponds to a load volume almost double that of 0% breakthrough. Thus, the change of direction of the productivity contour at 1% breakthrough occurs because there is a sudden change between there being just enough material loaded to yield 2 g protein h^{-1} L of $matrix^{-1}$ (1% breakthrough) and there not being enough material loaded to reach the desired productivity (at 0% breakthrough).

3.4 Conclusions

The Window of Operation for the first chromatographic step shows which combinations of operating conditions will yield the desired product for the first chromatography stage. The route to obtain the Window of Operation was protracted, but is greatly facilitated by the use of computer generated spreadsheets and algorithms. Ultimately, the Window of Operation provides a valuable graphical format that displays how key product specifications are affected by changes in operating conditions.

However, the question arises – Would operating conditions in the region determined by the Window of Operation produce a material that could be successfully purified by a second chromatographic stage to meet the required overall product specifications? The next chapter builds upon this and seeks to use Windows of Operation to examine chromatography sequences and the interaction between the first and second chromatographic stages.

4. Chromatography Sequences – Windows of Operation and the Feasible Region Search

4.1 Introduction

The performances of unit operations are rarely independent of each other, since one operation can impact on the performance of successive operations further downstream.[32] Although chromatography stages are run in sequence, optimization usually occurs at a single stage level[33, 34] despite the fact that the outcome of one stage will have a direct impact on the product of the following stage. It is necessary to look at the chromatography sequence as a whole when considering optimal performance, and not just as individual stages.

The primary method of determining the suitability of a chromatographic stage is through the examination of a chromatogram. In practice it proves extremely difficult to examine many chromatograms simultaneously in order to determine what the best combination of operating conditions is for a process, and this problem increases significantly when multiple steps are considered. If all the important conclusions drawn from a number of chromatograms could be captured in a single figure, the choice of operating conditions would be significantly facilitated. This can be done by creating a Window of Operation, a 2-dimensional diagram that shows how performance criteria are achieved as functions of key operating conditions, [35, 36] for example load volume and flow rate for chromatography.

Windows of Operation have been used to describe single unit operations[5,6] and to investigate the interplay between short sequences of operations in primary downstream processing.[36] To achieve robust operation, operating conditions that

lie in the middle of the Window will be selected since these provide for the maximum flexibility in the range of conditions that can be selected. If operating conditions are chosen closer to the boundaries of the Window, and either the properties of the feed stream were to change or operating conditions were to vary, then the chosen conditions may not yield a product that satisfies the pre-set design specifications. Such a solution would not be robust. Figure 4.1 provides an example of this.

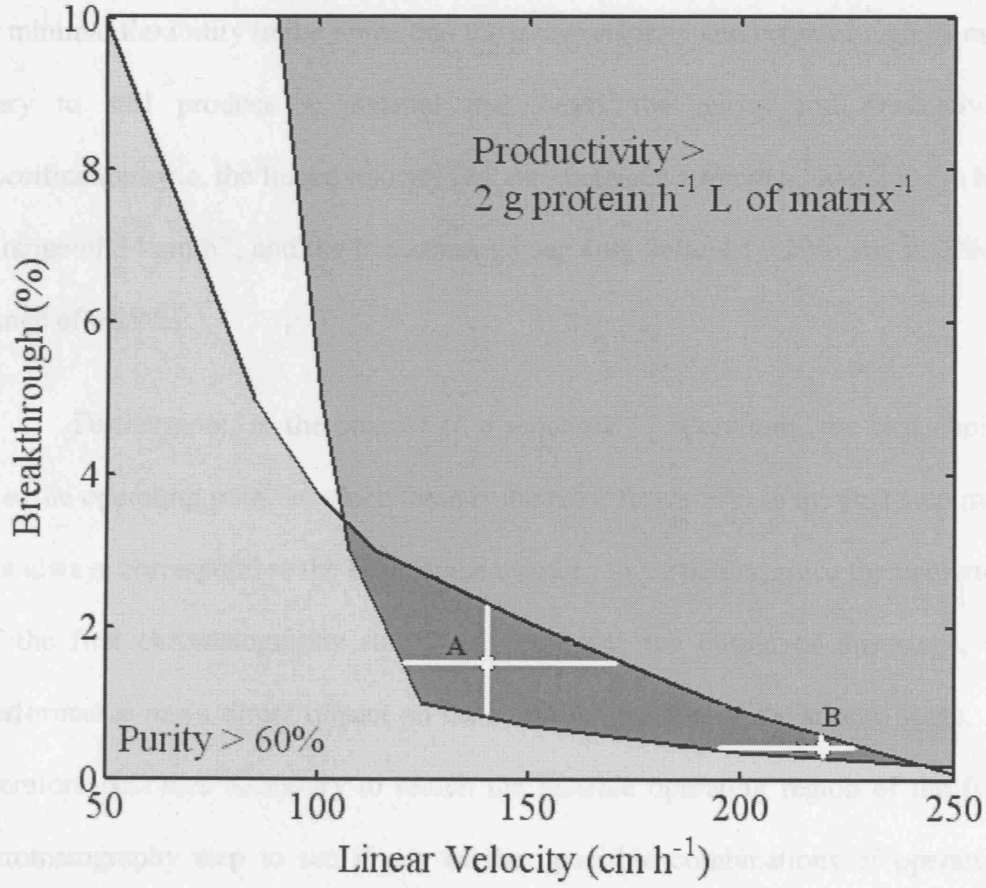

Figure 4.1 Operating Flexibility and Its Relationship to the Choice of Operating Conditions. ■ Desired operating region where purity ≥ 60%, and productivity ≥ 2 g protein h^{-1} L of $matrix^{-1}$.

Point A (linear velocity of 140 cm h^{-1} and breakthrough of 1.5%) is representative of a good choice of operating conditions. If there is variation in the operation, then there is flexibility in both the linear velocity and breakthrough % to still produce a viable material that meets both the productivity and purity specifications (i.e. the linear velocity can vary between 118 cm h^{-1} and 172 cm h^{-1}, a range of 54 cm h^{-1}, and the breakthrough can vary between 0.83% and 2.29%, a range of 1.46%). Point B is representative of a poorer choice of operating conditions (linear velocity of 220 cm h^{-1} and breakthrough of 0.45%) where there is minimal flexibility in the range that the linear velocity and breakthrough % may vary to still produce a material that meets the purity and productivity specifications (i.e. the linear velocity can vary between 196 cm h^{-1} and 230 cm h^{-1}, a range of 34 cm h^{-1}, and the breakthrough can vary between 0.29% and 0.58%, a range of 0.29%).

Furthermore, in the context of a sequence of operations, the best choice (i.e. the operating point at which there is the most flexibility) in the first step may not always correspond to the best choice overall. In particular, since the operation of the first chromatography stage will determine the output of this stage, its performance has a direct impact on the resulting product of the second stage. It therefore becomes necessary to search the feasible operating region of the first chromatography step to see if any of the possible combinations of operating conditions for this step produce a material that can be satisfactorily purified in the second step to meet the preset product quality and quantity constraints. It is the development of a method to enable this which is the subject of the work reported

in this chapter. This chapter details the results of the search of such a feasible operating region using a simulated 2-stage chromatography sequence.

4.2 Summary of Materials and Methods

4.2.1 Simulated Process

The simulated process was based on a two-step chromatographic sequence; ion exchange followed by hydrophobic interaction chromatography. This particular sequence is commonly employed in industry to aid in capturing and concentrating the product.[37]

As in the previous chapter, for all the simulations, a hypothetical three component mixture was assumed in order to mimic a multicomponent process stream undergoing an industrial-scale separation.[38] The product, first impurity and second impurity had molecular weights of 50 kDa, 150 kDa and 15 kDa respectively. Examples of proteins in the range of 15 kDa include ribonuclease and lysozyme. Ovalbumin and hexokinase have masses around 50 kDa, and IgG has a mass of approximately 150 kDa. For the first chromatographic stage the initial concentration of the product was set at 4 g L^{-1} ($8x10^{-5}$ mol L^{-1}), while the first and second impurities had set concentrations of 7.5 g L^{-1} ($5x10^{-5}$ mol L^{-1}) and 0.75 g L^{-1} ($5x10^{-5}$ mol L^{-1}) respectively.

The columns for both the first and second stage operations have bed volumes of 1.5 L. The column dimensions and parameters are shown in Table 4.1.

Table 4.1 Column and Chromatographic Parameters for Simulations of First and Second Chromatography Steps

Column Parameter	**Chromatographic Step 1 Column**	**Chromatographic Step 2 Column**
Diameter (cm)	10	10
Length (cm)	20	20
Average Particle Radius, R_p (μm)	45	34
Bed Void Space, E_b	0.4	0.33
Particle Void Space, E_p	0.45	0.6
Tortuosity	4	4
Impurity 1: Langmuir Parameter a	0.01	25
Impurity 1: Langmuir Parameter b	1	2500
Product: Langmuir Parameter a	3	3
Product: Langmuir Parameter b	300	300
Impurity 2: Langmuir Parameter a	14	0.001
Impurity 2: Langmuir Parameter b	1400	0.1
Displacer: Langmuir Parameter a	0.001	0.001
Displacer: Langmuir Parameter b	10000	10000
Desired Product Yield (%)	85	90

Both columns were run at simulated linear velocities of 50, 100, 150, 200, and 250 cm h^{-1}, which relate to flow rates of 3.9, 7.9, 11.8, 15.7, and 19.6 L h^{-1} respectively, and also to achieve 0%, 1%, 3%, 5%, and 10% levels of product

breakthrough. Simulations were inclusive of all the possible combinations of flow rate and product breakthrough level.

4.2.2 Chromatogram Simulation

Data obtained for this analysis were derived from computer simulations carried out using Chromulator version 2.0 (Gu T., Department of Chemical Engineering, Ohio University, Athens, OH, USA).[47] The simulation mode employed involved loading a specified column for a set amount of time, followed by a displacement step to elute the product, with the final output being a chromatogram.

A competitive Langmuir isotherm model[20] was used to describe the adsorption characteristics. The Langmuir parameters used in the simulations of both chromatographic stages are listed in Table 4.1. The parameter values selected reflect the relative properties only, and are used to define the separation achieved independently in the two chromatographic steps.

4.2.3 Graphical Procedures

Windows of Operation were produced using the graphical methods described in detail in Section 3.3, including the production of chromatograms, fractionation diagrams and purification factor vs. yield diagrams.

Constraints for the Windows of Operation are provided in Table 4.2. Process specifications were chosen for the two chromatographic stages to reflect common process objectives. The minimum desirable purity for the first chromatographic stage (capture) was chosen to be 60% to give approximately a two-fold purification from the starting material. For the second chromatographic

stage (purification), the minimum desirable purity was chosen to be 90%. This figure is the combined purity of the two-step operation and will reflect decisions made in the first step.

Table 4.2 Constraints for the Construction of Windows of Operation

Constraint	First Chromatographic Stage	Second Chromatographic Stage	Combined Sequence Specification
Purity (%)	≥60	≥90	≥90
Yield (%)	≥85	≥90	≥76.5
Productivity (g protein h^{-1} L of $matrix^{-1}$)	≥2	≥2	≥2

The yield values were chosen to allow for an overall sequence yield of at least 75%. The yield for the first operating stage was fixed at 85% to give a high yield representative of early chromatography capture steps where yield will dominate purity, but also to allow for a representative degree of purification to be realized. The yield for the second operating stage was maintained at 90%.

The minimum productivity of the sequence was chosen by determining what the productivity would be at the median values of the operating conditions. From this, a minimum desired productivity was set at 2 g protein h^{-1} L of $matrix^{-1}$, falling within the acceptable range for industrial productivity for an ion exchange operation of 1-25 g protein h^{-1} L of $matrix^{-1}$.[37]

4.2.4 Sequence Examination

Once a Window of Operation was established for the first chromatographic step, different points within the Window were examined to determine if the operating conditions described by the point would yield a material that could be further purified by a second stage to meet the product specifications and yield a second chromatographic stage Window of Operation. Points were tested along contours to see if patterns emerged as operating conditions changed while yield, and either purity or productivity (depending on which contour the tested point was located on) was held constant. Points that lay between the two contours were tested at various locations representing a range of operating conditions within the Window of Operation. Many points were examined within the first stage Window, and the method of comparing the results was by the determination and comparison of the areas of the resulting second stage Windows of Operation.

4.3 Results

Simulations were run according to the procedure outlined in Figure 3.3 to generate a data set of chromatograms, fractionation diagrams, and purification versus yield diagrams with the parameters given in Tables 4.1 and 4.2. These were used as the basis for examining the impact that the outcome of the first chromatographic stage has on the results of the second chromatographic stage. The Window of Operation for the first chromatographic stage, together with the points tested for the second chromatographic stage, is shown in Figure 4.2.

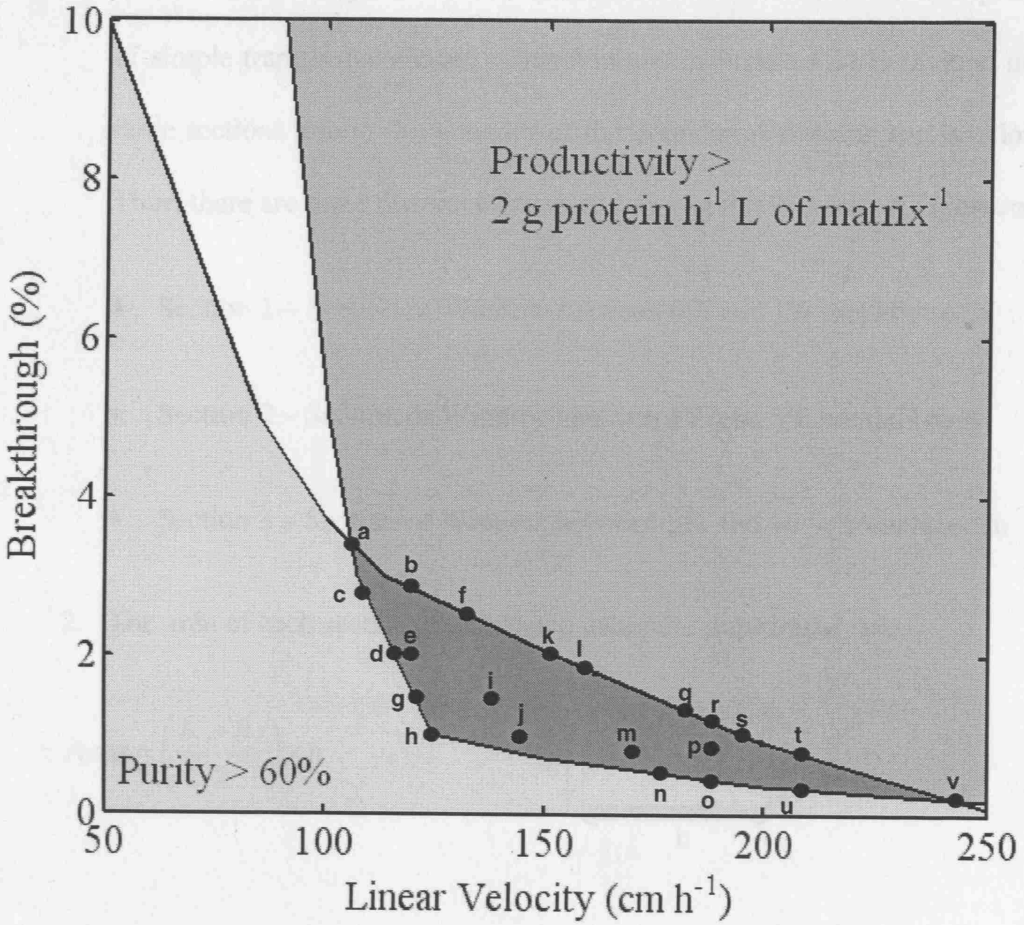

Figure 4.2 First Stage Window of Operation with Tested Points

Table 4.3 describes the first stage operating conditions for the point, the composition of the feed material to the second chromatographic stage, and the resultant Window of Operation area for the second stage. Figure 4.3 a-v shows the resultant second stage Windows of Operation for each tested point.

The following steps were used to calculate the Window of Operation area. The units of the Window area are arbitrary. Figure 4.3a is used as the example Window of Operation.

1. The Window of Operation is divided into a number of sections comprised of simple trapezoidal shapes. The Window in Figure 4.3a is divided into three sections due to the linearity of the boundaries forming the Window. Thus, there are three distinct trapezoids forming the Window of Operation.

   - Section 1 – Section of Window between 0% and 1% breakthrough
   - Section 2 – Section of Window between 1% and 5% breakthrough
   - Section 3 – Section of Window between 5% and 10 % breakthrough

2. The area of each section is calculated using the trapezoidal rule.

$$Area = \left(\frac{b_1 + b_2}{2}\right) \times h$$

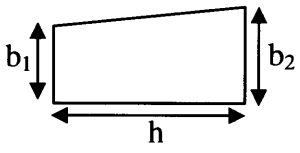

$$Section\ Area = \begin{bmatrix} Area\ of\ trapezoid\ formed \\ between\ the\ left\ edge\ of\ the \\ graph\ and\ the\ right\ edge\ of \\ the\ Window\ of\ Operation \end{bmatrix} - \begin{bmatrix} Area\ of\ trapezoid\ formed \\ between\ the\ left\ edge\ of\ the \\ graph\ and\ the\ left\ edge\ of \\ the\ Window\ of\ Operation \end{bmatrix}$$

$$Section\ 1 = \left[\frac{(105.1 + 144.9)}{2} \times 1\right] - \left[\frac{(62.2 + 107.7)}{2} \times 1\right] = 40$$

$$Section\ 2 = \left[\frac{(91.0 + 105.1)}{2} \times 4\right] - \left[\frac{(55.8 + 62.2)}{2} \times 4\right] = 156$$

$$Section\ 3 = \left[\frac{(98.7 + 91.0)}{2} \times 5\right] - \left[\frac{(52.5 + 55.8)}{2} \times 5\right] = 204$$

$$Total\ Area = 204 + 156 + 40 = 400$$

Table 4.3. Operating Conditions and Window Areas for Tested Points

	1st Stage Operating Conditions		Composition of Feed Material to Second Chromatographic Stage			
Point	**Breakthrough %**	**Linear Velocity (cm h^{-1})**	**Impurity 1 mol L^{-1} x 10^5**	**Product mol L^{-1} x 10^5**	**Impurity 2 mol L^{-1} x 10^5**	**2nd Stage Window Area (Arbitrary Units)**
a	3.50	104	2.29	12.80	5.59	400
b	2.89	119	2.22	12.30	5.46	412
c	2.70	109	2.15	12.70	5.62	459
d	2.00	115	1.86	12.10	5.91	394
e	2.00	119	1.68	11.00	6.18	191
f	2.50	134	1.84	10.60	5.89	119
g	1.50	121	1.56	11.20	6.11	271
h	1.00	125	1.56	11.80	5.88	415
i	1.50	142	1.66	10.70	5.71	206
j	1.00	145	1.42	10.40	5.71	215
k	2.00	152	1.74	10.10	5.65	84
l	1.84	161	1.69	9.70	5.53	36
m	0.70	169	1.35	9.70	5.29	165
n	0.60	179	1.25	9.13	5.16	81
o	0.44	187	1.11	8.50	5.01	6
p	0.85	187	1.04	7.09	4.81	-
q	1.33	183	1.32	8.03	5.17	-
r	1.22	187	1.55	8.98	5.15	-
s	1.00	194	1.48	8.72	5.04	-
t	0.85	209	1.23	7.59	4.79	-
u	0.37	209	1.13	7.99	4.70	-
v	0.32	239	1.05	6.80	4.26	-

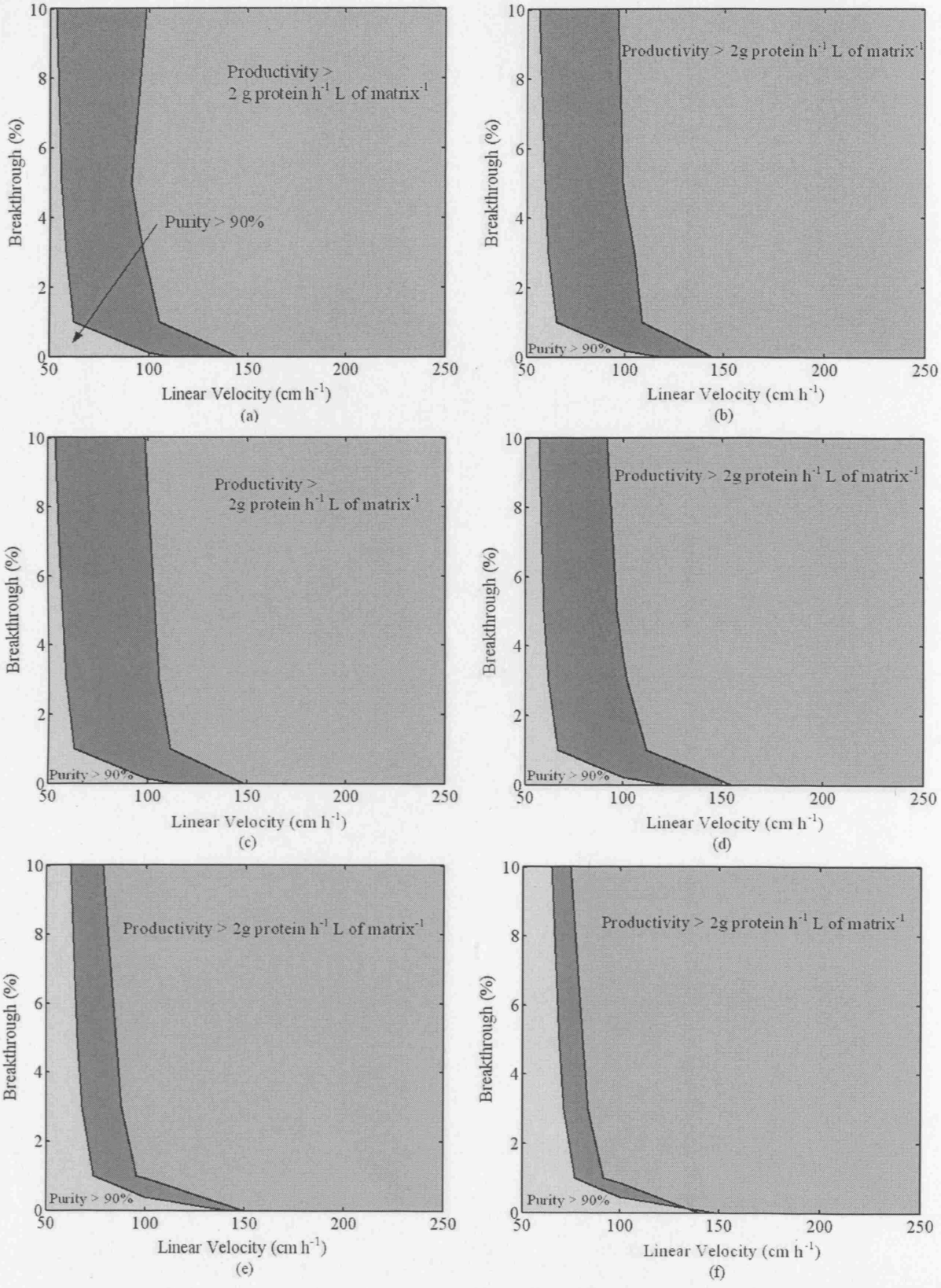
Productivity >
2 g protein h-1 L of matrix-1
Purity > 90%
Breakthrough (%)
Linear Velocity (cm h-1)
(a)
Productivity > 2g protein h-1 L of matrix-1
Purity > 90%
Breakthrough (%)
Linear Velocity (cm h-1)
(b)
Productivity >
2g protein h-1 L of matrix-1
Purity > 90%
Breakthrough (%)
Linear Velocity (cm h-1)
(c)
Productivity > 2g protein h-1 L of matrix-1
Purity > 90%
Breakthrough (%)
Linear Velocity (cm h-1)
(d)
Productivity > 2g protein h-1 L of matrix-1
Purity > 90%
Breakthrough (%)
Linear Velocity (cm h-1)
(e)
Productivity > 2g protein h-1 L of matrix-1
Purity > 90%
Breakthrough (%)
Linear Velocity (cm h-1)
(f)

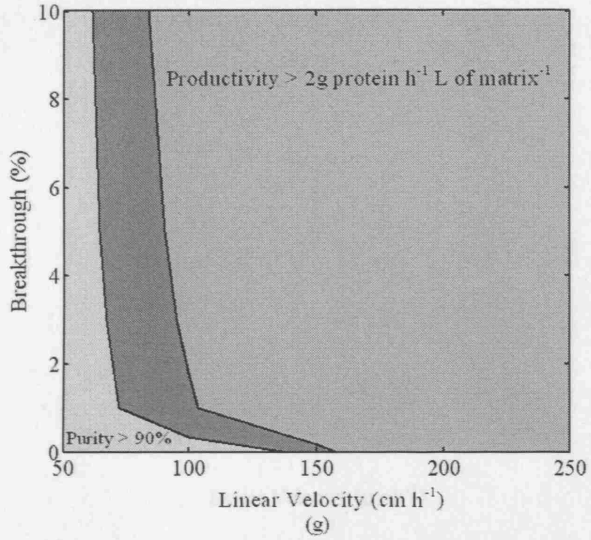
Productivity > 2g protein h-1 L of matrix-1
Purity > 90%
Breakthrough (%)
Linear Velocity (cm h-1)
(g)

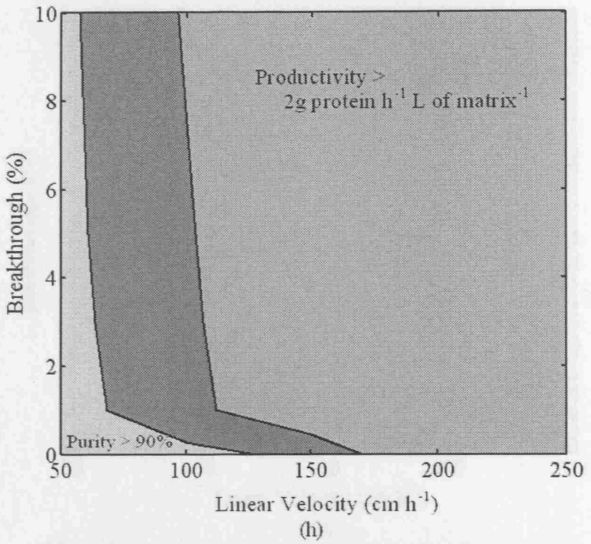
Productivity >
2g protein h-1 L of matrix-1
Purity > 90%
Breakthrough (%)
Linear Velocity (cm h-1)
(h)

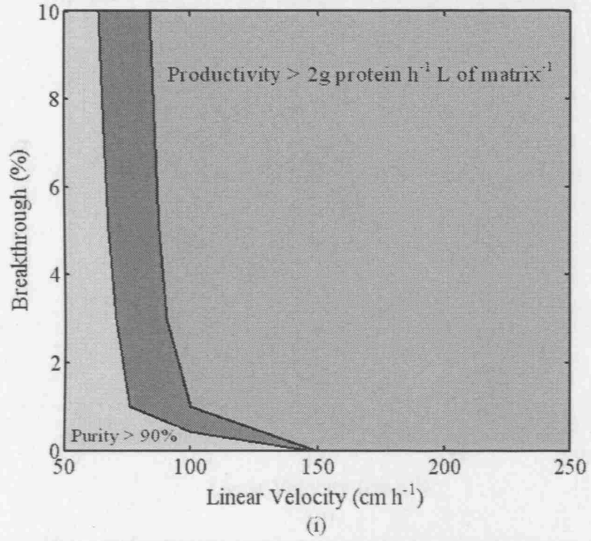
Productivity > 2g protein h-1 L of matrix-1
Purity > 90%
Breakthrough (%)
Linear Velocity (cm h-1)
(i)

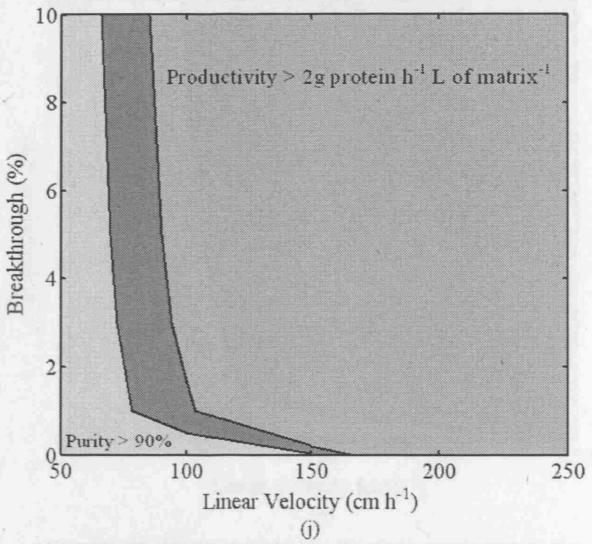
Productivity > 2g protein h-1 L of matrix-1
Purity > 90%
Breakthrough (%)
Linear Velocity (cm h-1)
(j)

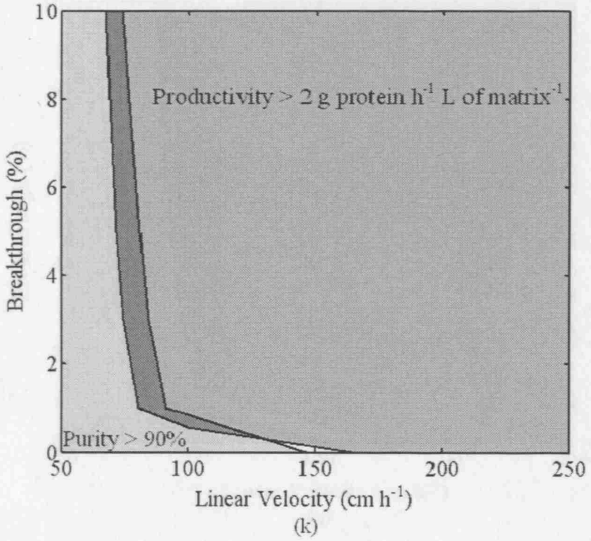
Productivity > 2 g protein h-1 L of matrix-1
Purity > 90%
Breakthrough (%)
Linear Velocity (cm h-1)
(k)

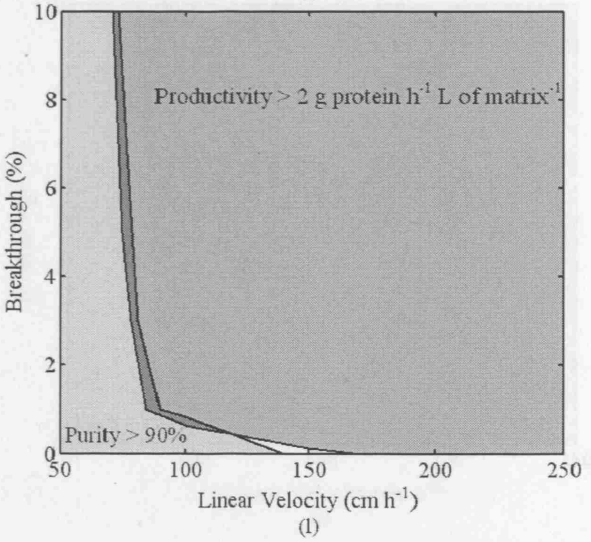
Productivity > 2 g protein h-1 L of matrix-1
Purity > 90%
Breakthrough (%)
Linear Velocity (cm h-1)
(l)

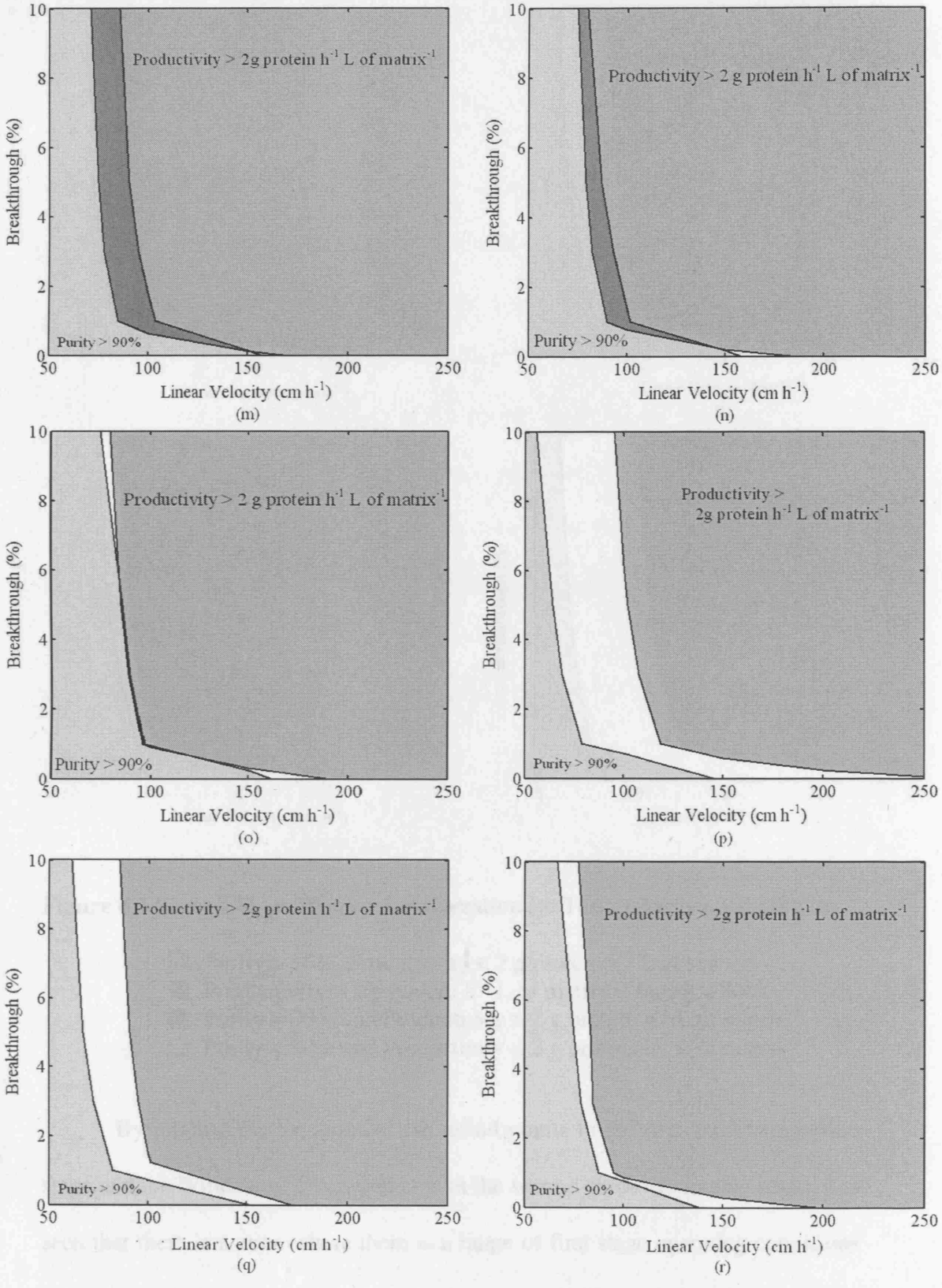
Productivity > 2g protein h-1 L of matrix-1
Purity > 90%
Breakthrough (%)
Linear Velocity (cm h-1)
(m)
Productivity > 2 g protein h-1 L of matrix-1
Purity > 90%
Breakthrough (%)
Linear Velocity (cm h-1)
(n)
Productivity > 2 g protein h-1 L of matrix-1
Purity > 90%
Breakthrough (%)
Linear Velocity (cm h-1)
(o)
Productivity > 2g protein h-1 L of matrix-1
Purity > 90%
Breakthrough (%)
Linear Velocity (cm h-1)
(p)
Productivity > 2g protein h-1 L of matrix-1
Purity > 90%
Breakthrough (%)
Linear Velocity (cm h-1)
(q)
Productivity > 2g protein h-1 L of matrix-1
Purity > 90%
Breakthrough (%)
Linear Velocity (cm h-1)
(r)

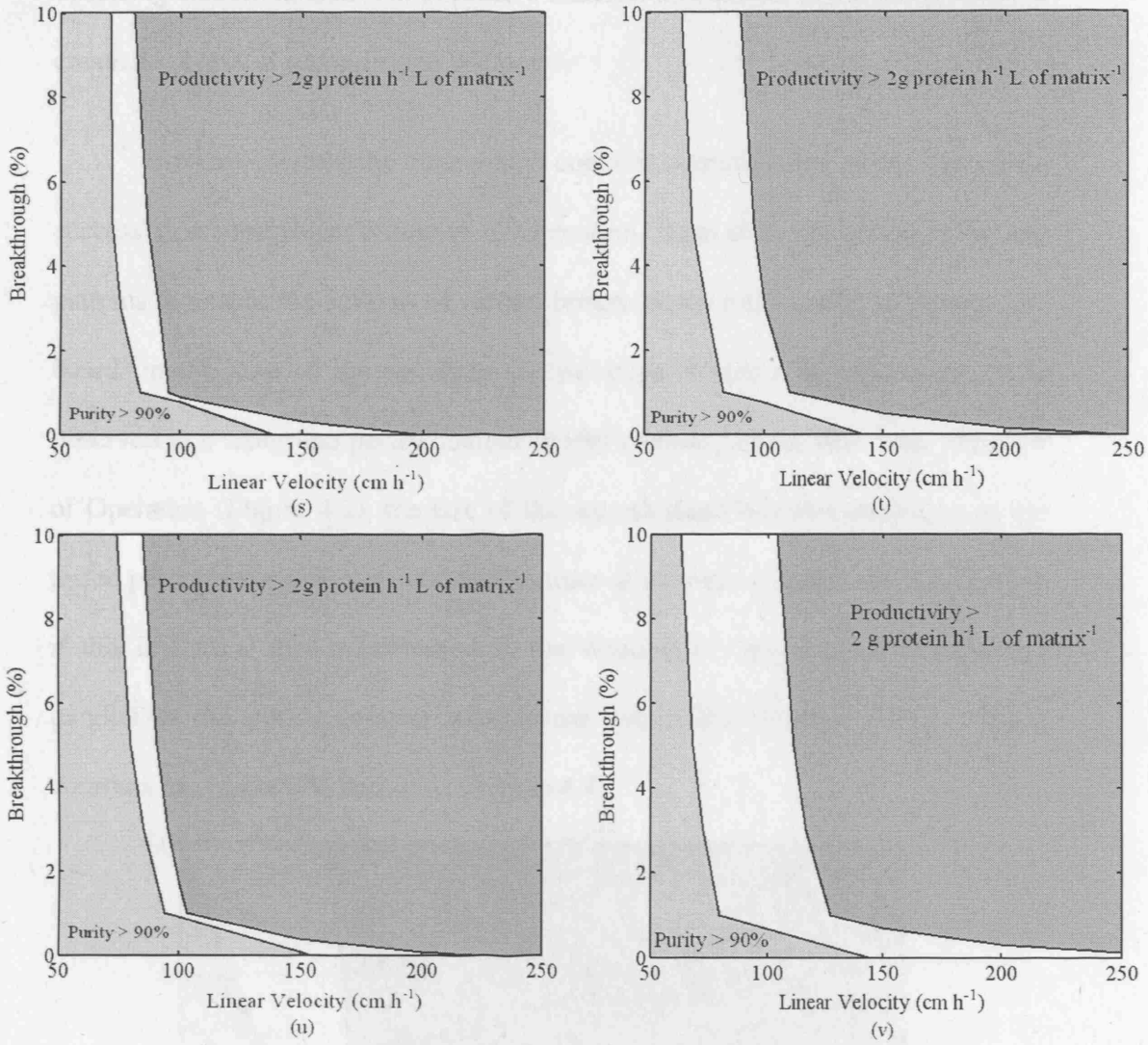

Figure 4.3 Second Stage Windows of Operation for Tested Points a-v on Figure 4.2

- Purity > 90%, Productivity < 2 g protein h^{-1} L of $matrix^{-1}$
- Productivity > 2 g protein h^{-1} L of $matrix^{-1}$, Purity < 90%
- Purity > 90% and Productivity > 2 g protein h^{-1} L of $matrix^{-1}$
- Purity < 90% and Productivity < 2 g protein h^{-1} L of $matrix^{-1}$

By relating the locations of the tested points in the first chromatographic stage and the Window of Operation area in the second chromatographic stage, it is seen that there is a zone where there is a range of first stage operating conditions that will produce a material that can be further purified and successfully create a Window of Operation. There is also a zone in which there is a range of first stage

operating conditions that will produce a material that cannot be further purified to create a successful second stage Window.

However, within the zone which contains operating conditions that create successful second stage Windows of Operation, there does not appear to be any patterns to enable the zone to be further broken down into smaller sub-zones, i.e. based on the size of the resulting second stage Window of Operation. It is observed that along the purity contour (upper contour) of the first stage Window of Operation (Figure 4.2), the size of the second stage Window decreases as the tested points move along the contour in order of ascending linear velocity. To see if this is a trend that is consistent in the Window of Operation, three contours parallel to the purity contour were tested within the Window space. These contours are labeled A, B and C in Figure 4.4.

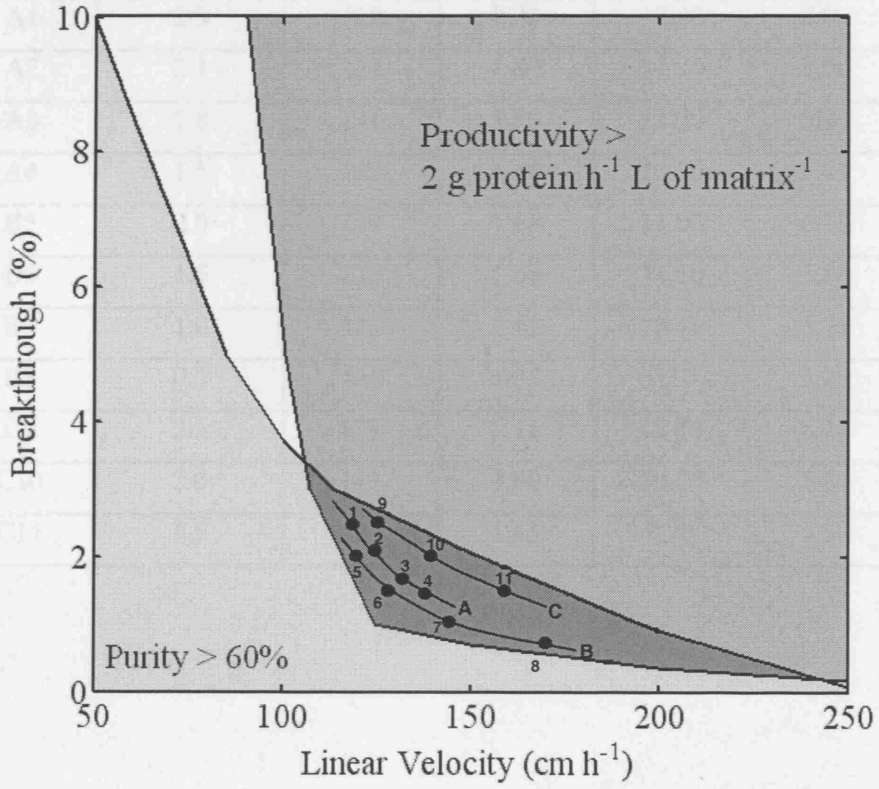

Figure 4.4 First Stage Window of Operation with Tested Contours

Table 4.4 lists the first stage operating conditions for the points along the contours, labeled 1 to 11, the composition of the feed material to the second chromatographic stage and the resultant Window areas for the second stage operation. Figure 4.5 1-11 shows the resultant second stage Windows of Operation for each tested point.

Table 4.4. Operating Conditions and Window Areas for Tested Points along Parallel Contours

	1st Stage Operating Conditions		Composition of Feed Material to Second Chromatographic Stage			
Point	Breakthrough %	Linear Velocity	Impurity 1 mol L^{-1} x 10^5	Product mol L^{-1} x 10^5	Impurity 2 mol L^{-1} x 10^5	2nd Stage Window Area (Arbitrary Units)
A1	2.5	119	2.32	12.80	5.00	543
A2	2.1	127	1.80	11.30	5.90	252
A3	1.8	134	1.73	11.00	5.81	252
A4	1.5	142	1.66	10.70	5.71	207
B5	2.0	119	1.68	11.00	6.18	192
B6	1.5	130	1.66	11.10	5.86	255
B7	1.0	145	1.42	10.40	5.71	216
B8	0.7	169	1.35	9.70	5.29	165
C9	2.5	127	2.11	12.00	5.48	405
C10	2.0	141	1.69	10.20	5.84	69
C11	1.5	159	1.45	9.18	5.59	6

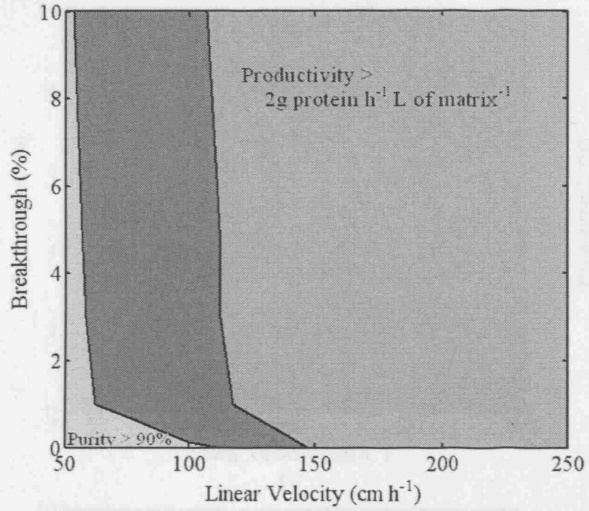
Productivity >
2g protein h-1 L of matrix-1
Purity > 90%
Breakthrough (%)
Linear Velocity (cm h-1)
0
2
4
6
8
10
50
100
150
200
250
(1)

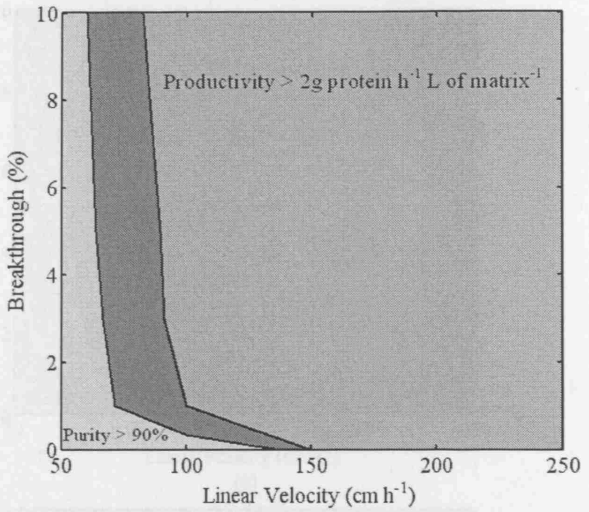
Productivity > 2g protein h-1 L of matrix-1
Purity > 90%
Breakthrough (%)
Linear Velocity (cm h-1)
0
2
4
6
8
10
50
100
150
200
250
(2)

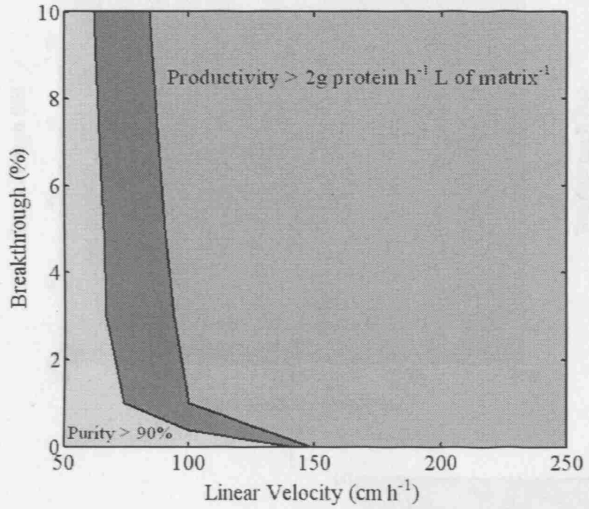
Productivity > 2g protein h-1 L of matrix-1
Purity > 90%
Breakthrough (%)
Linear Velocity (cm h-1)
0
2
4
6
8
10
50
100
150
200
250
(3)

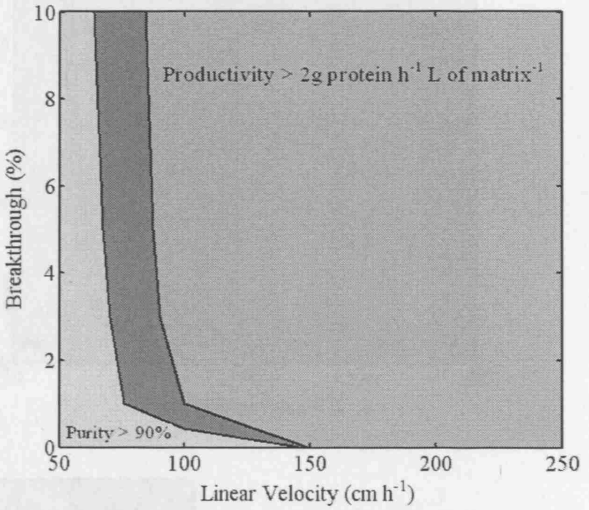
Productivity > 2g protein h-1 L of matrix-1
Purity > 90%
Breakthrough (%)
Linear Velocity (cm h-1)
0
2
4
6
8
10
50
100
150
200
250
(4)

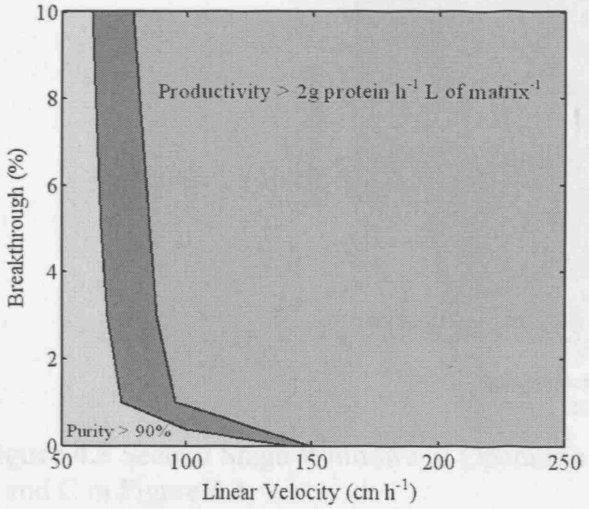
Productivity > 2g protein h-1 L of matrix-1
Purity > 90%
Breakthrough (%)
Linear Velocity (cm h-1)
0
2
4
6
8
10
50
100
150
200
250
(5)

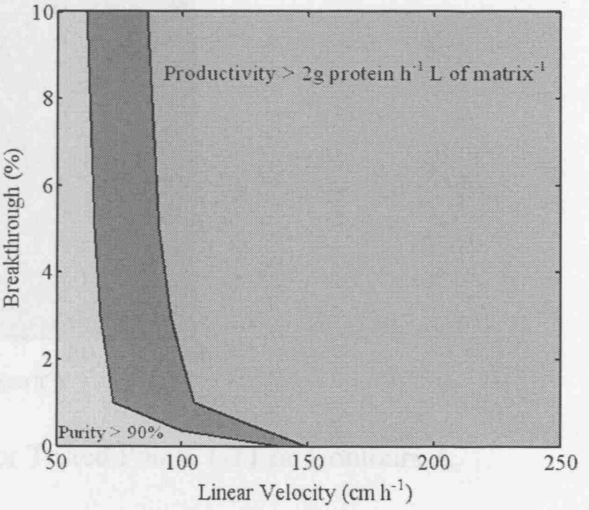
Productivity > 2g protein h-1 L of matrix-1
Purity > 90%
Breakthrough (%)
Linear Velocity (cm h-1)
0
2
4
6
8
10
50
100
150
200
250
(6)

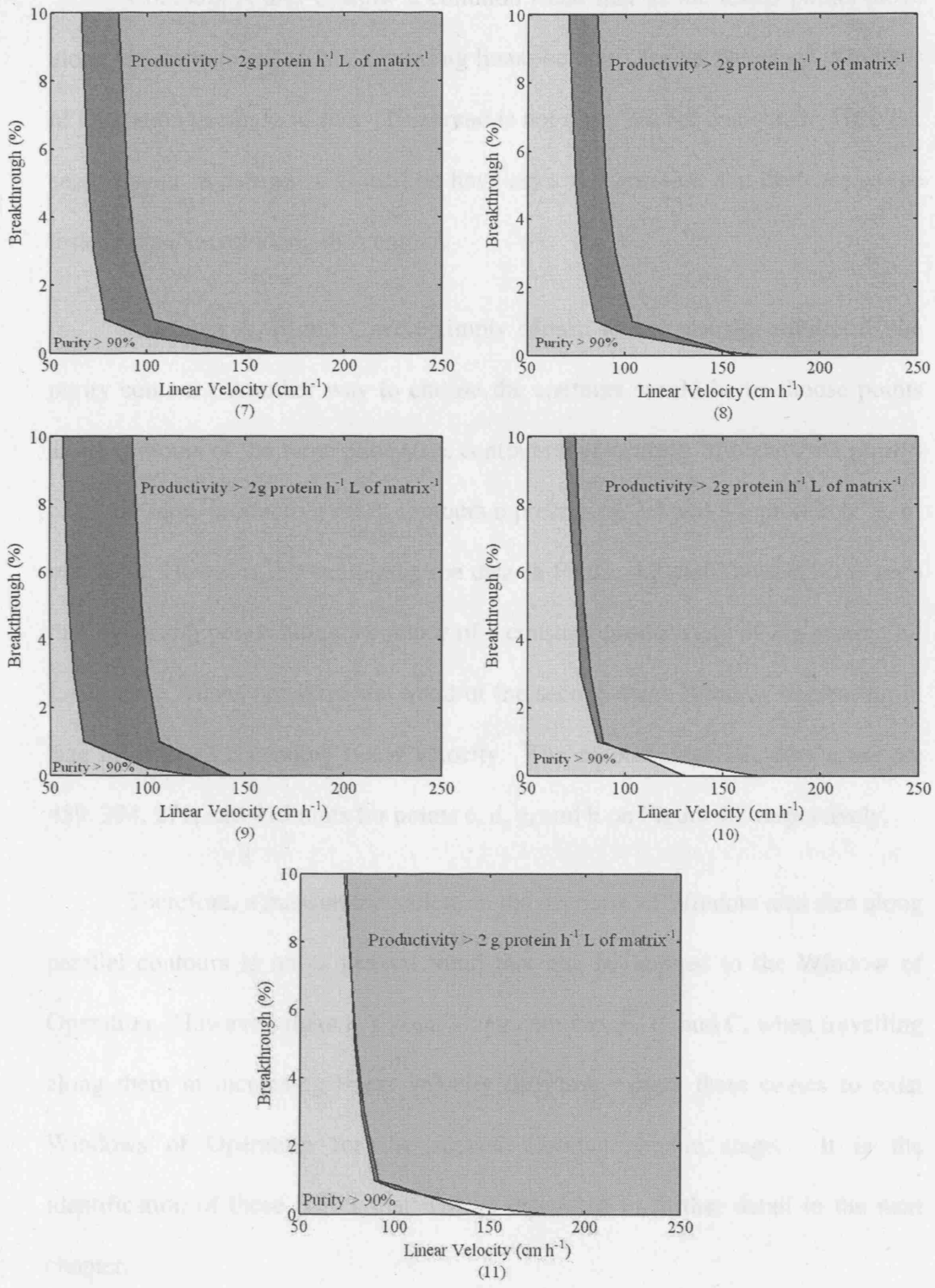

Figure 4.5 Second Stage Windows of Operation for Tested Points 1-11 on Contours A, B and C in Figure 4.4

- Purity > 60%, Productivity < 2 g protein h^{-1} L of $matrix^{-1}$
- Productivity > 2 g protein h^{-1} L of $matrix^{-1}$, Purity < 60%
- Purity > 60% and Productivity > 2 g protein h^{-1} L of $matrix^{-1}$
- Purity < 60% and Productivity < 2 g protein h^{-1} L of $matrix^{-1}$

Contours A and C show a common trend that as the tested points move along the contour in order of ascending linear velocity, the second stage Windows of Operation decrease in size. This trend is not observed for contour B. Here the second stage Windows of Operation have sizes that increase and decrease as the tested points travel along the contour.

Contours A, B and C were simply chosen to run visually parallel to the purity contour. Another way to choose the contours would be to choose points along contours of the same purity (i.e. contours representing 70% and 75% purity) or of the same productivity (i.e. contours representing 2.5 and 3 g protein h^{-1} L of $matrix^{-1}$). However, by examining the data in Figure 4.2 and Table 4.3 it is seen that by testing points along a contour of a constant productivity of 2 g protein h^{-1} L of $matrix^{-1}$ does not show the trend of the second stage Window decreasing in size in order of ascending linear velocity. The second stage Window areas are 459, 394, 271, and 415 units for points c, d, g, and h on Figure 4.2 respectively.

Therefore, a measurable pattern in the decrease of Window area size along parallel contours is not a general trend that can be applied to the Window of Operation. However, there is a point along contours A, B, and C, when travelling along them in increasing linear velocity direction, where there ceases to exist Windows of Operation for the second chromatographic stage. It is the identification of these points that will be discussed in further detail in the next chapter.

4.4 Conclusion

The second chromatographic stage's operation and successful purification is directly impacted by the operation of the first chromatographic stage. If noticeable and reliable trends are found within the first stage Window of Operation showing its impact on the second stage Window, the selection of operating conditions and the operation of the chromatographic stages would be greatly facilitated. Operation is far more robust in a region of the first Window of Operation that yields material that when purified by a second step gives a large second stage Window of Operation than it is in a region of the first stage Window that yields material that is further purified to produce a small second stage Window of Operation. If trends, which effectively correlate the performance of the two stages, could be found, then it would be possible to predict the second stage Window of Operation areas, thus making the selection of operating conditions for chromatography processes more rapid and robust.

The next chapter will detail the methodology developed that enables just such a rapid and effective division of the Window of Operation into two zones, one where first stage operating conditions give rise to a material that can be further purified successfully, and the other where first stage operating conditions do not yield a material that can be further purified successfully.

5. Tie-Line Methodology

5.1 Introduction

This chapter proposes a graphical methodology for the identification of operating conditions for a two-step chromatography sequence. The method is based upon the use of Windows of Operation to incorporate the tradeoffs between yield, purity, and productivity. A tie-line procedure is developed that separates the Window of Operation for the first chromatographic step into two zones. One zone contains those operating conditions that combine to produce a material which can be purified successfully by the second step to produce a product that meets the desired specifications. The second zone consists of operating conditions which will not yield a material that can be adequately purified by a second chromatographic stage to yield a product of the predetermined specifications. The methodology is valuable in that it helps in achieving the rapid design of a two-step chromatography sequence, and aids in choosing the appropriate operating conditions for the first step which are highly dependent upon the operation and specifications of the second chromatographic step. Simulations carried out using a software package based on the general rate model depict the construction and use of the method applied to a sequence of ion exchange and hydrophobic interaction chromatography separating a three component protein mixture.

5.2 Theory – Tie-Line Method

The principle of the tie-line method proposes that it is possible for Windows of Operation for the first stage of the chromatography sequence to be divided into two zones, A and B as shown in Figure 5.1. In both, the target specifications for the first chromatographic stage are met. However, zone A represents conditions that do not give rise to feasible operating Windows for the second chromatographic stage, whilst zone B corresponds to those operating conditions that produce materials that do meet the specifications for the first chromatographic stage, and can be further purified by the second stage to produce a suitable product, i.e. one that complies with the overall product specification set for the process sequence.

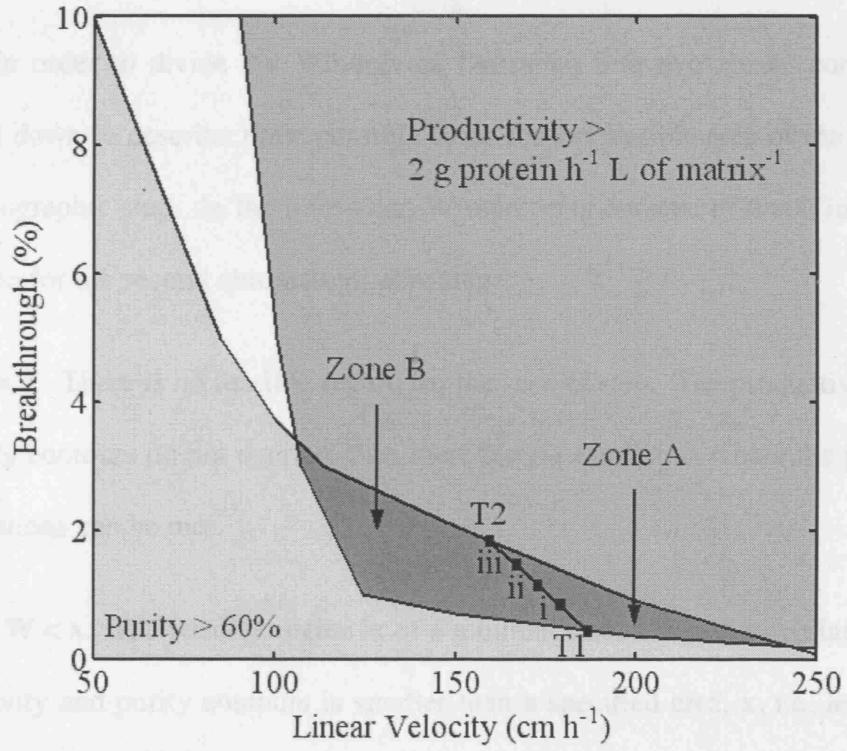

Figure 5.1. Separation of first chromatographic stage Window of Operation into zones A and B by a tie-line

Such a two-zone solution exists because of the following points:

- If breakthrough % gets too low and a smaller amount of material is passed through the column, purity targets may be met, but productivity targets will not be achieved. The opposite may occur if breakthrough % is too high.

- If linear velocity is too low, productivity targets may not be met, but purity targets may be achieved. Conversely, if velocity is too high, desired purity levels will not be reached, but the desired productivity may be achieved.

It is the balance between linear velocity and breakthrough % that allows both the purity and productivity targets to be achieved.

In order to divide the Window of Operation into two zones, conditions were set down to describe three possible cases for the feasible area of the second chromatographic step. In the following, W represents the area of the Window of Operation for the second chromatographic stage.

1. $W = 0$. There is no feasible region for the second step. The productivity and the purity contours do not overlap, thus there are no conditions where the product specifications can be met.

2. $0 < W < x$. The feasible region is of a minimal size, where the overlap of the productivity and purity contours is smaller than a specified area, x, i.e. less than 3% of the available Window area. For example, in Figure 5.1, there is a range of 10 units along the y-axis and a range of 200 units across the x-axis. Therefore, the

maximum available Window space was calculated to be 2000 arbitrary units, thus the minimum Window size was desired to be less than 60 units. Below this size the Window will prove largely inoperable as it is not robust since there is little flexibility within the range of operating conditions contained in the feasible region.

3. $W > x$. The feasible region is larger than the minimum set Window area (i.e. greater than 60 units). Therefore, the sequence is feasible.

The choice of minimum Window size at 3% is illustrated here. In practice the level would be determined based upon detailed knowledge of the system and of the material value.

The division of the first Window of Operation into two zones would be achieved by establishing a tie-line located by points T_1 and T_2, one on the productivity contour and one on the purity contour, that satisfy the second condition $0 < W < x$. This tie-line would be defined such that any material along this line would yield a second stage Window with a minimal size, thus also satisfying the condition $0 < W < x$. This minimal second stage Window of Operation is formed when the two contours just overlap, providing a region in which the transition from 'sequence-infeasible' (Zone A) conditions to 'sequence-feasible' (Zone B) conditions occurs. Hence, the tie-line would separate the 'sequence-feasible' and 'sequence-infeasible' zones.

It is worth noting that in practice, due to the non-linearity of competitive isotherms, the tie-line most likely will be a 2-dimensional region which may display some degree of curvature. In practice though, the purpose of the boundary

is to help determine solutions that result in sequence-feasible operation, and the approximation of a straight line is made as being a reasonable approach for the purposes of initial assessment of sequence feasibility. The assumption of a straight line will also impact the setting of the minimum Window size. If the chromatography is highly non-linear then a greater tolerance may be needed. The procedure for locating T_1 and T_2 is provided in Figure 5.2.

Figure 5.2 assumes that the Window of Operation for the first chromatographic stage has been produced. Points are tested by:

1. Determining the product stream concentrations produced by the operating conditions described by the point on the first stage Window.
2. Creating a new Window of Operation for the second stage operation using the methodology described by Figure 3.3.

The methodology ends when one of the following occurs:

1. All combinations of operating conditions described by the first Window of Operation give rise to a material that can be loaded onto a second chromatographic stage to yield a product that meets the desired specifications.
2. None of the combinations of operating conditions described by the first Window of Operation give rise to a material that can be loaded onto a second chromatographic stage to yield a product that meets the desired specifications.
3. A tie line is produced dividing the first stage Window of Operation into a sequence-feasible zone and a sequence-infeasible zone.

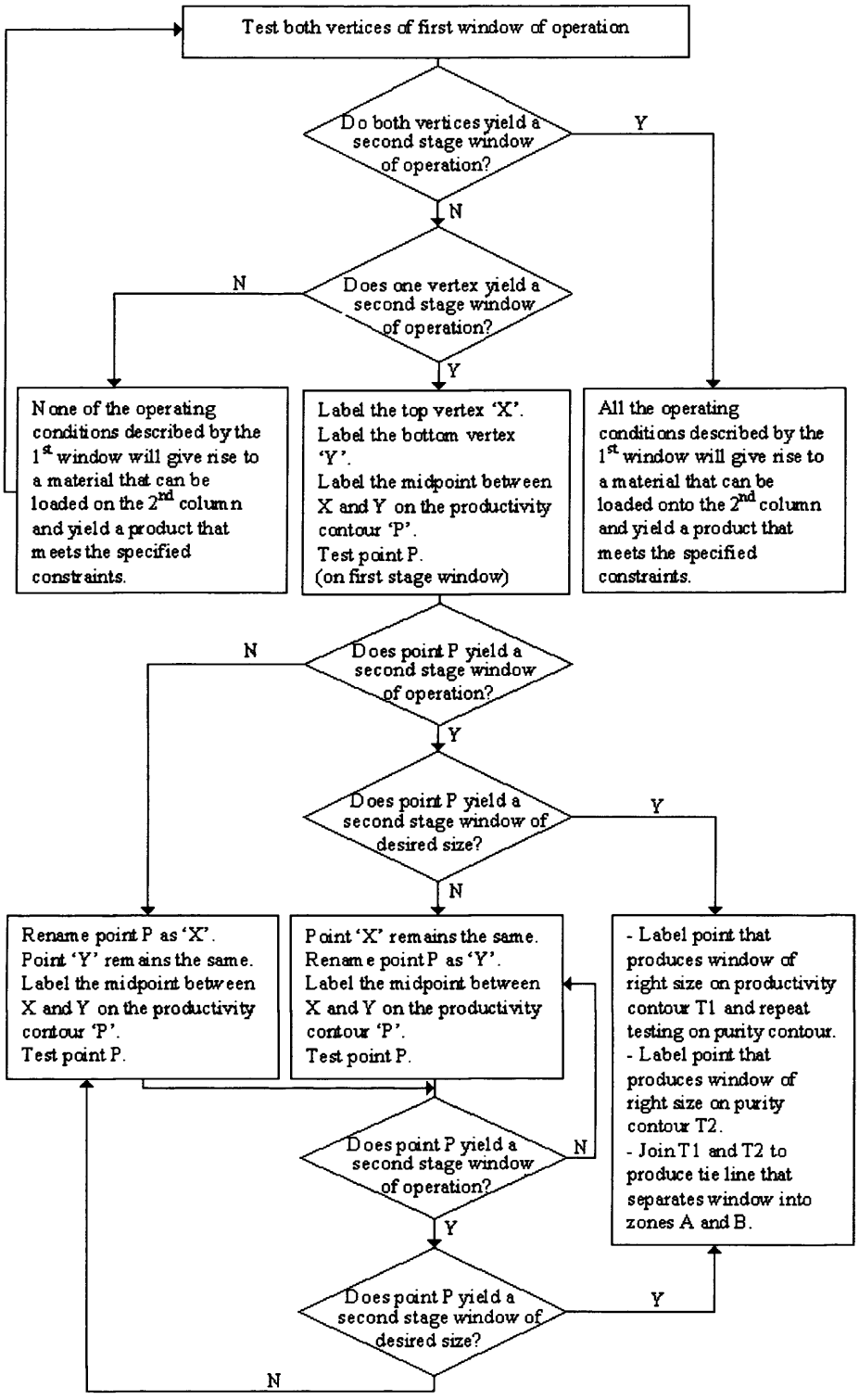

Figure 5.2 Flowchart for the determination of the tie-line for zone A and B separation

5.3 Results

Simulations were run according to the procedure outlined in Figure 3.3 to generate a data set of chromatograms, fractionation diagrams, and purification versus yield diagrams with the parameters given in Tables 4.1 and 4.2. These were used as the basis for testing the sequence methodology developed in this thesis.

The Window of Operation for the first chromatographic stage together with the tie-line defined by T_1 and T_2 is shown in Figure 5.1. In order to determine the placement of the tie-line, the condition for the transition region was set such that $0 < W < 60$. Thus, any second stage Window larger than 60 arbitrary units was determined to be sequence feasible. Points T_1 and T_2 were then determined by following the procedure in Figure 5.2. It was found that conditions defined by the upper vertex of the first stage Window of Operation yielded a material that when further purified produced a second chromatographic stage Window of Operation with an area of 400 units (Figure 4.3a). Conditions defined by the lower vertex of the first stage Window of Operation produced a material that did not yield a second stage Window of Operation (Figure 4.3v). Therefore, the route taken to find T_1 and T_2 in the flowchart seen in Figure 5.2 was for 'one vertex yields a Window of Operation'.

Operating at points T_1 and T_2 in the first chromatographic operation leads to the material properties given in Table 5.1, and these give rise to successful second stage Windows of Operation as seen in Figures 5.3 a and b. Conditions at T_1 yield material that produced a second stage Window of 4.4 arbitrary units in size, while those at T_2 yield a material that produced a second stage Window with

an area of 36.4 arbitrary units. Both feasible regions have areas that satisfy the minimum Window size requirement of $0 < W < 60$ required for the establishment of the tie-line.

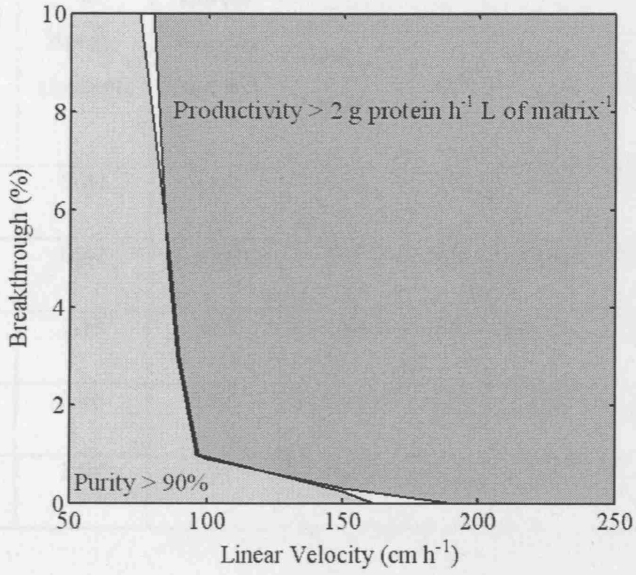

Figure 5.3 Windows of operation for the second chromatographic stage corresponding to material prepared at the first stage by conditions found at either end of the tie-line in Figure 5.1 (T_1-T_2). (a) Second stage Window for T1, (b) Second stage Window for T2

- Purity > 90%, Productivity < 2 g protein h^{-1} L of $matrix^{-1}$
- Productivity > 2 g protein h^{-1} L of $matrix^{-1}$, Purity < 90%
- Purity > 90% and Productivity > 2 g protein h^{-1} L of $matrix^{-1}$
- Purity < 90% and Productivity < 2 g protein h^{-1} L of $matrix^{-1}$

Table 5.1 First Chromatographic Stage Conditions and Results for Material to be Passed to Second Stage Operations for Points on Tie-Line

Stage 1 Simulation Conditions				Composition of Material Produced from Stage 1 Operations						
Point on Tie-Line T_1-T_2 (Fig. 5.1)	Yield (%)	% Break-through	Linear Velocity (cm h^{-1})	Impurity 1		Product		Impurity 2		Purity (%)
				(mol L^{-1}) x10^5	(g)	(mol L^{-1}) x10^5	(g)	(mol L^{-1}) x10^5	(g)	
T1	85	0.44	188	1.11	2.4	8.50	6.0	5.01	1.1	64
i	85	0.82	179	1.30	3.0	8.80	6.8	5.22	1.2	62
ii	85	1.13	173	1.45	3.5	9.21	7.4	5.34	1.3	61
iii	85	1.46	167	1.59	4.0	9.57	8.0	5.43	1.4	60
T2	85	1.84	161	1.69	4.4	9.70	8.5	5.53	1.5	60

Points T_1 and T_2 were joined to form the tie-line. Points along the tie-line were tested to verify that material produced from the first stage conditions they describe could be purified successfully to yield a second stage Window of Operation that satisfies the second condition, $0 < W < 60$. The points that were tested are seen on Figure 5.1 labeled i, ii, and iii, and the resulting second stage Windows are shown in Figures 5.4 a-c. The materials produced in the first chromatographic stage by the conditions described by these points are detailed in Table 5.1. The first stage operating conditions specified by these points produced a material that was purified successfully through a second chromatographic stage to produce Windows of Operation with areas that lay within the transition region. Points i, ii, and iii produced feasible regions for the second stage operation of 0.3, 6.9, and 46.6 units respectively. These results confirm that points along the tie-line represent operating conditions for the first chromatographic stage whose

products can be successfully purified by a second step to provide Windows of Operation of a size that represents the transition between a feasible chromatographic sequence and an infeasible one.

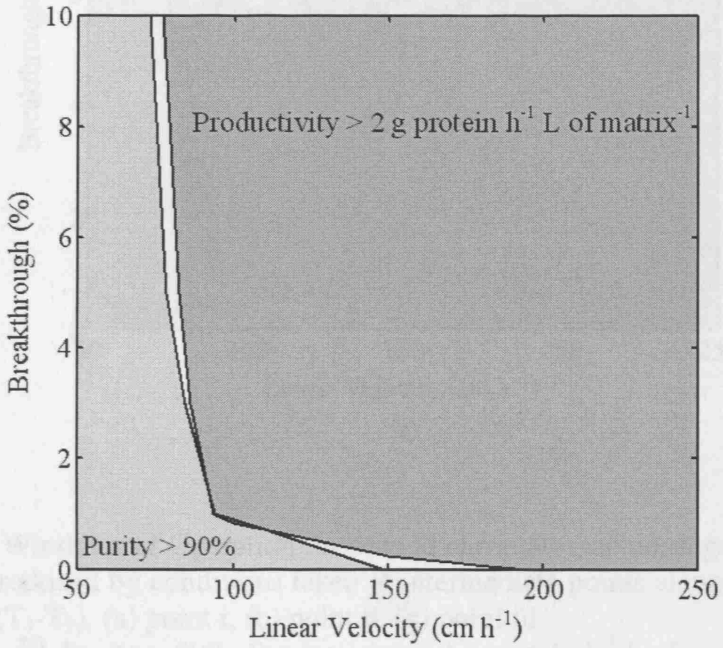

(a)

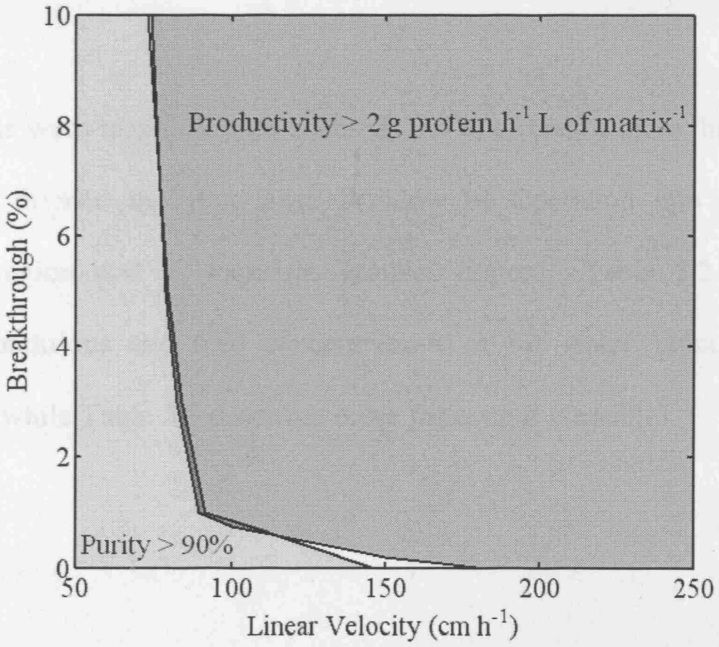

(b)

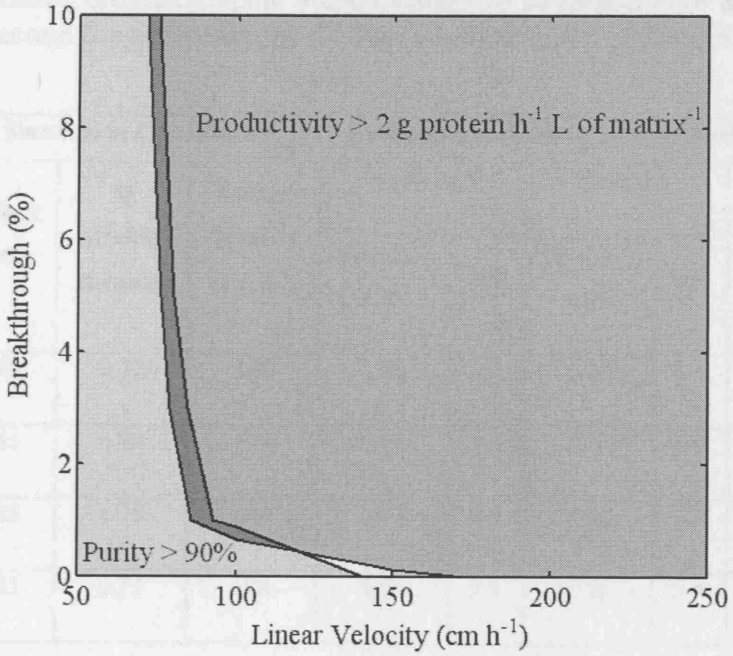

(c)

Figure 5.4 Windows of Operation for second chromatographic stage generated by materials produced by conditions taken at intermediate points along the tie-line in Figure 5.1 (T_1-T_2). (a) point i, (b) point ii, (c) point iii

- ☐ Purity > 90%, Productivity < 2 g protein h^{-1} L of $matrix^{-1}$
- ▒ Productivity > 2 g protein h^{-1} L of $matrix^{-1}$, Purity < 90%
- ■ Purity > 90% and Productivity > 2 g protein h^{-1} L of $matrix^{-1}$
- ☐ Purity < 90% and Productivity < 2 g protein h^{-1} L of $matrix^{-1}$

Points were tested in both zones A and B to demonstrate that the tie-line successfully divided the first stage Window of Operation into a 'sequence-infeasible' region and a 'sequence-feasible' region. Table 5.2 outlines the operating conditions and feed concentrations of the tested points in zone A (infeasible), while Table 5.3 describes those for zone B (feasible).

Table 5.2. First Chromatographic Stage Conditions and Results for Material to be Passed to Second Stage Operations for Points a, b, c, and d of Zone A

Stage 1 Simulation Conditions				Composition of Material Produced from Stage 1 Operations						
Figure	Yield (%)	% Break-through	Linear Velocity (cm h^{-1})	Impurity 1		Product		Impurity 2		Purity (%)
				(mol L^{-1}) x10^5	(g)	(mol L^{-1}) x10^5	(g)	(mol L^{-1}) x10^5	(g)	
5.5a	85	0.32	239	1.05	2.1	6.80	4.5	4.26	0.8	60
5.5b	85	0.44	194	0.91	1.9	7.08	5.0	4.70	1.0	63
5.5c	85	1.78	164	1.54	4.0	9.11	7.9	5.54	1.4	60
5.5d	85	0.73	194	1.03	2.3	7.17	5.4	4.78	1.1	61

Figures 5.5 a-d show examples of the mapping between materials derived from different points in zone A on the first chromatographic stage's Window of Operation and their resultant Windows of Operation for second stage operations. The conditions for points 5.5 a-c were chosen as they represent the extreme corners of zone A. In Figures 5.5 a-c, no Window of Operation was formed for the second stage operation, and the sequence is therefore determined to be infeasible. A point approximately in the middle of zone A was also tested. Figure 5.5 d shows that this point also did not produce a second stage Window of Operation. This analysis confirms that zone A does indeed represent the 'sequence-infeasible' region. (It is theoretically possible that feasible areas might still exist within the infeasible region. The analysis would indicate that should they exist, they would be small and not represent viable and robust conditions for operation.)

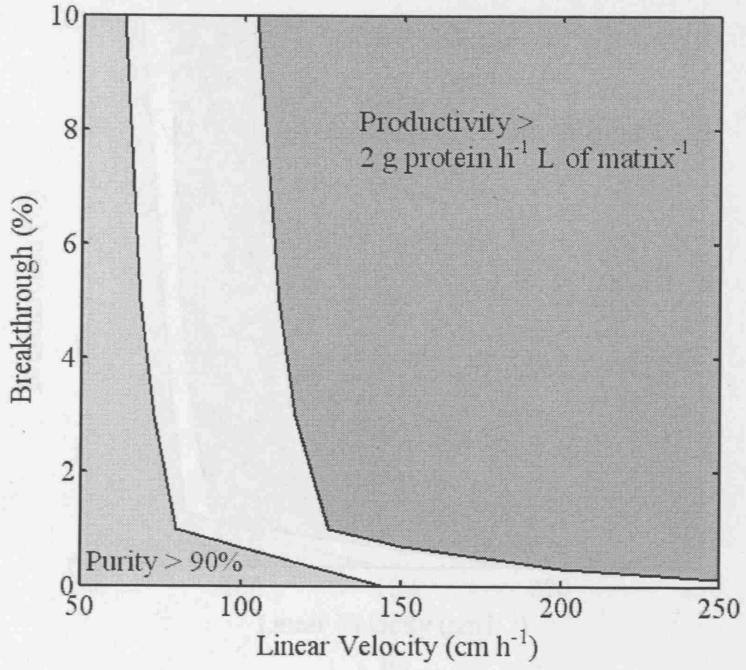
Productivity >
2 g protein h-1 L of matrix-1
Purity > 90%
Breakthrough (%)
Linear Velocity (cm h-1)
0
2
4
6
8
10
50
100
150
200
250

(a)

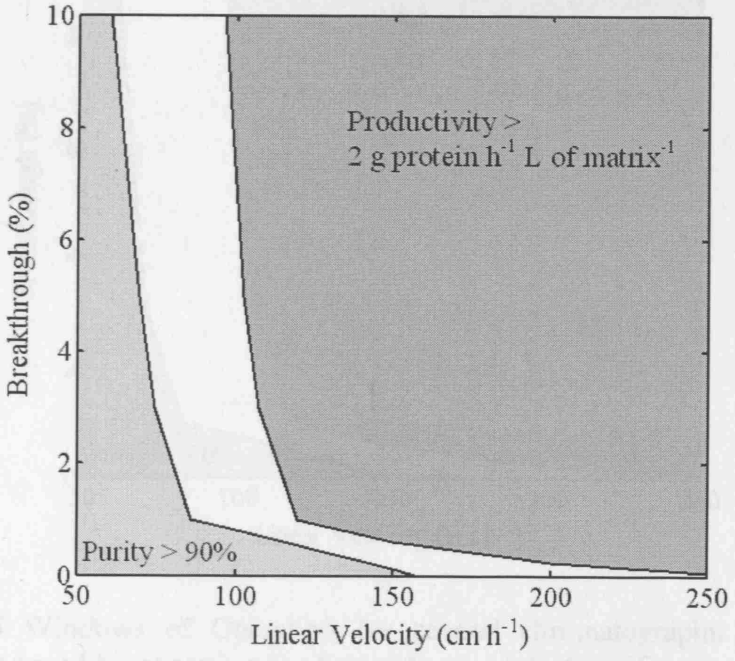
Productivity >
2 g protein h-1 L of matrix-1
Purity > 90%
Breakthrough (%)
Linear Velocity (cm h-1)
0
2
4
6
8
10
50
100
150
200
250

(b)

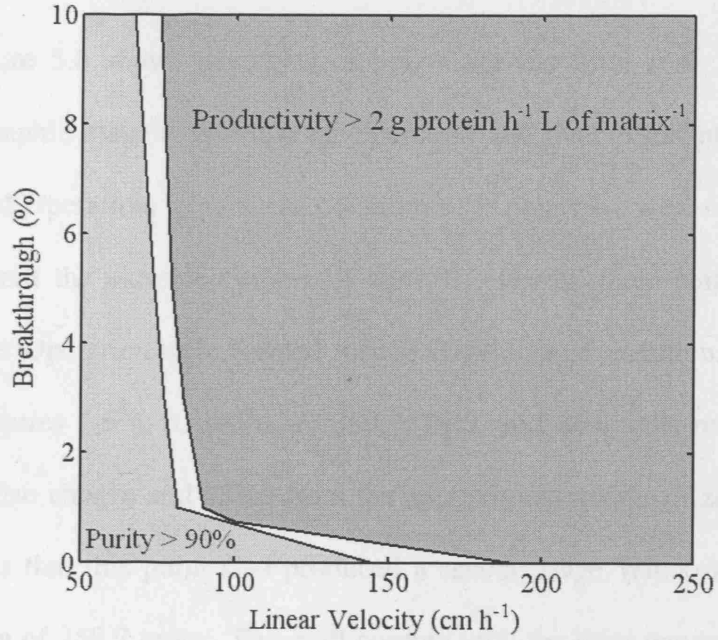

(c)

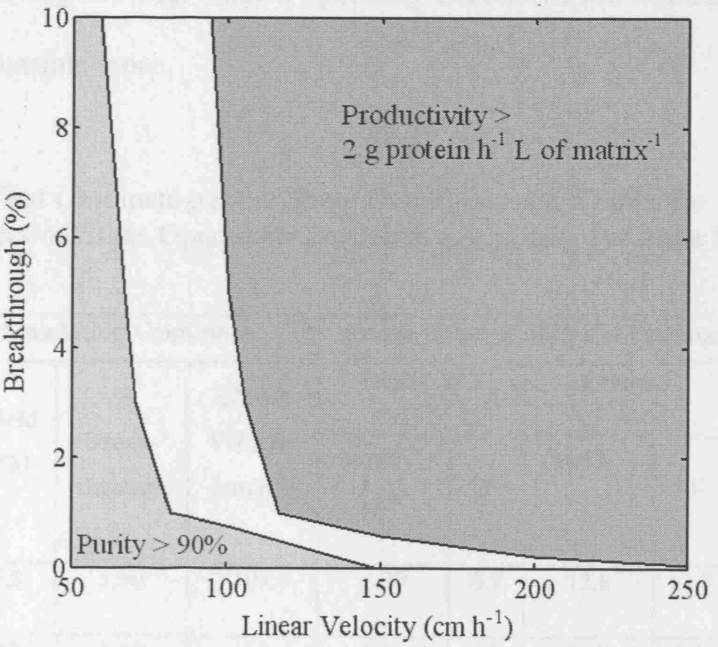

(d)

Figure 5.5 Windows of Operation for second chromatographic stage using material produced by operating conditions from a selection of points in zone A of the first stage Window. (Flow rate, breakthrough % of first stage operation) (a) 239 cm h^{-1}, 0.32%, (b) 194 cm h^{-1}, 0.44%, (c) 164 cm h^{-1}, 1.78%, (d) 194 cm h^{-1}, 0.73%

- Purity > 90%, Productivity < 2 g protein h^{-1} L of matrix^{-1}
- Productivity > 2 g protein h^{-1} L of matrix^{-1}, Purity < 90%
- Purity > 90% and Productivity > 2 g protein h^{-1} L of matrix^{-1}
- Purity < 90% and Productivity < 2 g protein h^{-1} L of matrix^{-1}

Figure 5.6 shows examples of points derived from zone B on the first chromatographic stage's Window of Operation and their resultant second stage Windows of Operation. Again, the conditions for points a-c were chosen because they represent the extreme corners of zone B. For all three points, successful Windows of Operation were formed for the second stage operation. The Window areas of Figures 5.6 a, b, and c are 399.7, 81.3, and 84.8 units respectively. A point was also chosen and tested from the approximate middle of zone B. Figure 5.6 d shows that this point also produced a second stage Window of Operation with an area of 250.7 units. These all comply with the third requirement of W > 60, thus proving the first stage's operating conditions are rightfully within the 'sequence-feasible' zone.

Table 5.3 First Chromatographic Stage Conditions and Results for Material to be Passed to Second Stage Operations for Points a, b, c, and d of Zone B

Stage 1 Simulation Conditions				**Composition of Material Produced from Stage 1 Operations**						
Figure	**Yield (%)**	**% Break-through**	**Linear Velocity (cm h^{-1})**	**Impurity 1**		**Product**		**Impurity 2**		**Purity (%)**
				(mol L^{-1}) x10^5	**(g)**	**(mol L^{-1}) x10^5**	**(g)**	**(mol L^{-1}) x10^5**	**(g)**	
5.6a	85	3.50	104	2.29	6.9	12.8	12.9	5.59	1.7	60
5.6b	85	0.60	179	1.25	2.8	9.13	6.7	5.16	1.1	63
5.6c	85	2.00	152	1.74	4.6	10.1	9.0	5.65	1.5	60
5.6d	85	1.75	134	1.73	4.6	11.0	9.7	5.81	1.5	61

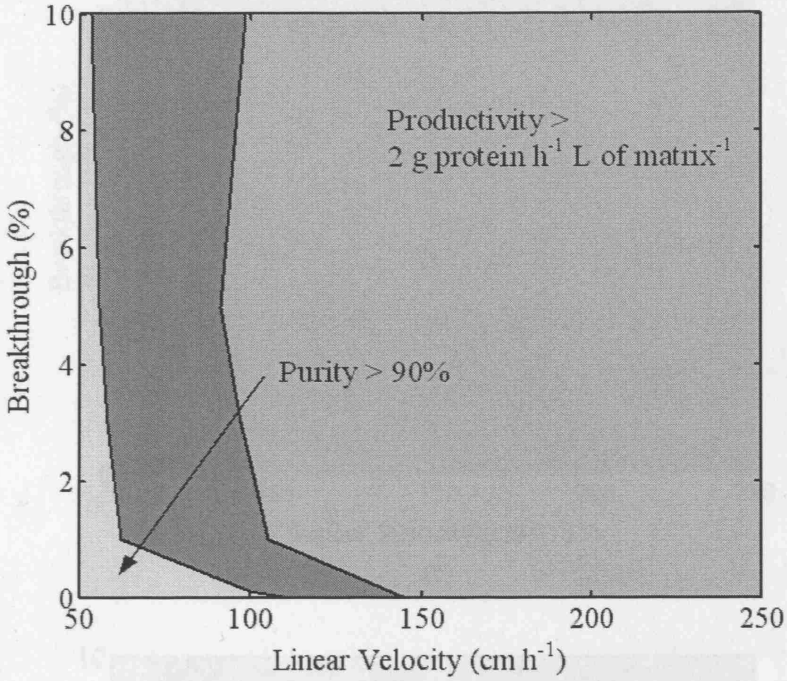
Productivity >
2 g protein h-1 L of matrix-1
Purity > 90%
Breakthrough (%)
Linear Velocity (cm h-1)
0
2
4
6
8
10
50
100
150
200
250

(a)

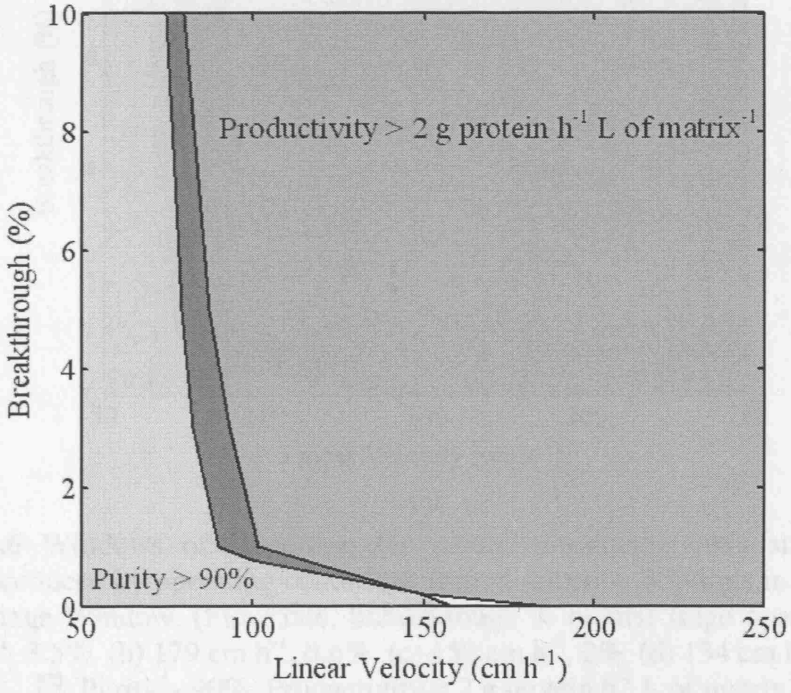
Productivity > 2 g protein h-1 L of matrix-1
Purity > 90%
Breakthrough (%)
Linear Velocity (cm h-1)
0
2
4
6
8
10
50
100
150
200
250

(b)

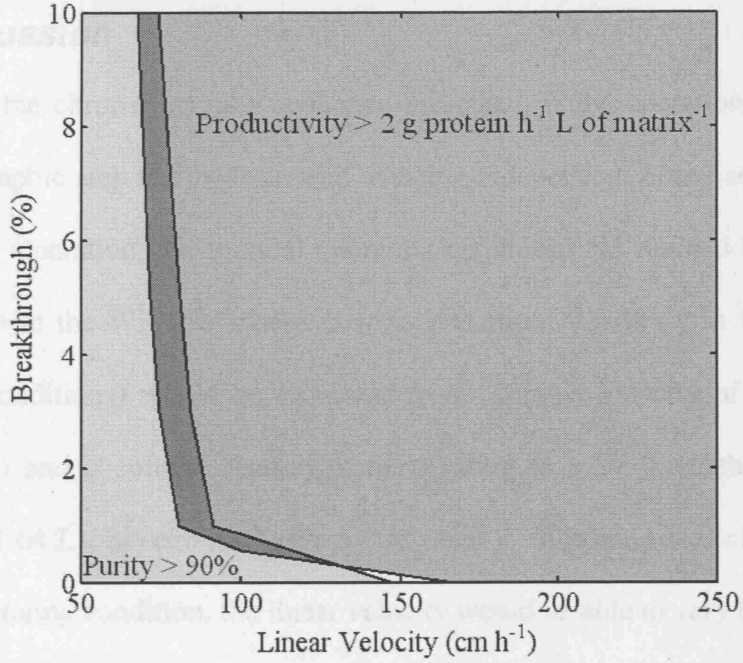

(c)

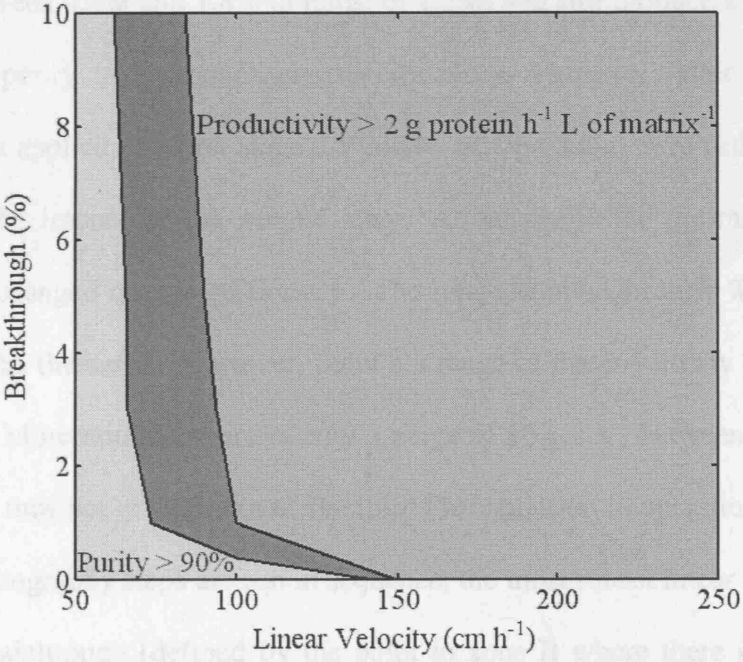

(d)

Figure 5.6 Windows of Operation for second chromatographic stage using material produced by operating conditions from a selection of points in zone B of the first stage Window. (Flow rate, breakthrough % of first stage operation) (a) 104 cm h^{-1}, 3.5%, (b) 179 cm h^{-1}, 0.6%, (c) 152 cm h^{-1}, 2%, (d) 134 cm h^{-1}, 1.75%

- Purity > 90%, Productivity < 2 g protein h^{-1} L of matrix^{-1}
- Productivity > 2 g protein h^{-1} L of matrix^{-1}, Purity < 90%
- Purity > 90% and Productivity > 2 g protein h^{-1} L of matrix^{-1}
- Purity < 90% and Productivity < 2 g protein h^{-1} L of matrix^{-1}

5.4 Discussion

For the chromatography sequence presented, if the operation of the first chromatographic step had been treated as being independent of the second step's Window of Operation, the optimal operating conditions (as defined by the most robust point in the Window where there is maximum flexibility in the range of operating conditions) would be estimated to be a linear velocity of 160 cm h^{-1} (12.6 L h^{-1}) and a column loading corresponding to 1.2% breakthrough (load volume of 1.64 L), as seen in Figure 5.7 as point a. If point a was chosen as the optimal operating condition, the linear velocity would be able to vary between 122 cm h^{-1} and 186 cm h^{-1} (a range of 64 cm h^{-1}) or the breakthrough % would be able to vary between 0.6% and 1.8% (a range of 1.2%) and still produce a product that meets the purity and productivity specifications. However, after the tie-line method was applied, the first stage's Window of Operation narrowed down, thus reflecting the impact of the second stage. Additionally, the optimal operating conditions changed quite significantly. The range in breakthrough % for point a would still be the same. However, point a's range in linear velocity decreases to 50 cm h^{-1}. More notable, there is only a range of 12 cm h^{-1} between point a and the tie-line, thus not giving a lot of flexibility for variation in operation. When the two chromatography steps are run in sequence, the most robust linear velocity and loading breakthrough (defined by the point in zone B where there is maximum flexibility) for the first step are estimated to be 134 cm h^{-1} (10.5 L h^{-1}) and 1.75% (load volume of 1.77 L) respectively. The linear velocity would be able to vary between 118 cm h^{-1} and 163 cm h^{-1} (a range of 45 cm h^{-1}) or the breakthrough %

would be able to vary between 0.8% and 2.4% (a range of 1.6%) and still produce a viable product.

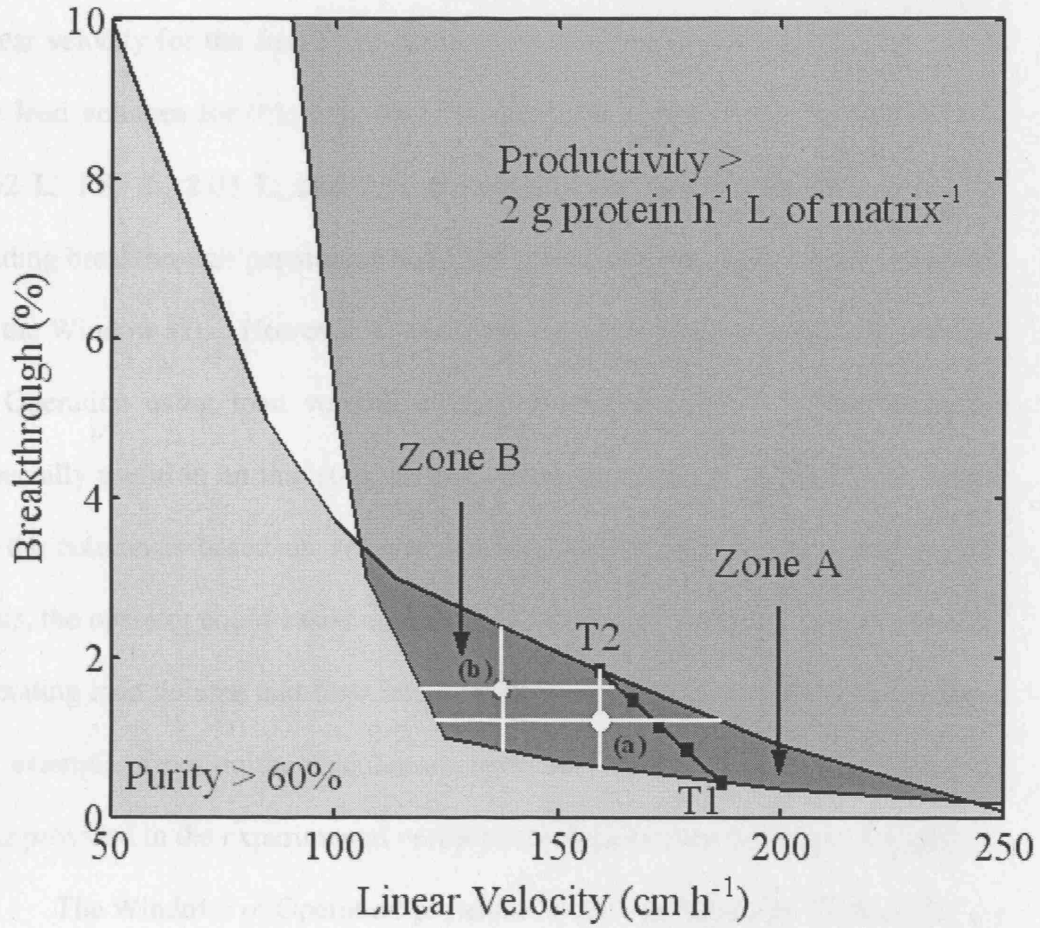

Figure 5.7 Optimal Operating Conditions and the Effect of the Tie-Line (a) Estimated optimal operating condition for first chromatographic stage (160 cm h^{-1}, 1.2% breakthrough) (b) Estimated optimal operating condition for chromatography sequence (134 cm h^{-1}, 1.75% breakthrough)

The results presented investigated the impact of load volume expressed via the level of breakthrough achieved. The load volume corresponding to each breakthrough percentage can also be determined from a breakthrough curve. For example, at a linear velocity of 50 cm h^{-1} (3.9 L h^{-1}) in the first stage operation,

0%, 1%, 3%, 5%, and 10% breakthrough corresponds to load volumes of 1.08 L, 1.94 L, 2.13 L, 2.23 L, and 2.42 L respectively. Breakthrough curves are dependent upon the composition of the material and the flow rate. When the linear velocity for the first stage operation is changed to 150 cm h^{-1} (11.8 L h^{-1}), the load volumes for 0%, 1%, 3%, 5%, and 10% breakthrough become 0.78 L, 1.62 L, 1.87 L, 2.03 L, and 2.31 L respectively. Because of this variability, loading breakthrough percentage and load volume are not readily interchangeable on the Window axis. However, it would also be appropriate to model the Window of Operation using load volume instead of breakthrough %. This would be especially useful in an industrial setting where the range of material to be loaded on the column is based on volume and not breakthrough %. By adopting this basis, the operator could easily consult the Window of Operation to verify that the operating load volume and flow rate lie within the feasible region for the process. An example of basing the calculations upon load volume instead of breakthough % is provided in the experimental verification of the tie-line method in Chapter 7.

The Windows of Operation presented so far were made by fixing yield to a specific value, 85% in the first chromatographic stage and 90% in the second chromatographic stage, and setting minimum purity and productivity values for the contour lines. The alternative would be for the purity to be set to a specific value and minimum productivity and yield values then assigned. For example, the purity for the first chromatographic step could be set at 60%, and the feasible region of the Window would contain conditions that produce a product stream with a minimum of 2 g hr^{-1} L of $matrix^{-1}$ productivity and 85% product yield. The second step could have a set final purity of 90%, while the Window of Operation constraints could be 2 g hr^{-1} L of $matrix^{-1}$ and a minimum yield of 90%. The

resulting first stage Window of Operation inclusive of the tie-line for such a situation is shown in Figure 5.8. The Window of Operation was made by carrying out simulations with the same experimental system as described in the materials and methods section. The second stage Windows of Operation for points T1 and T2 are shown in Figure 5.9. These show that there is minimal overlap between the yield and productivity contours, representative of the transition region between sequence-feasible and sequence-infeasible.

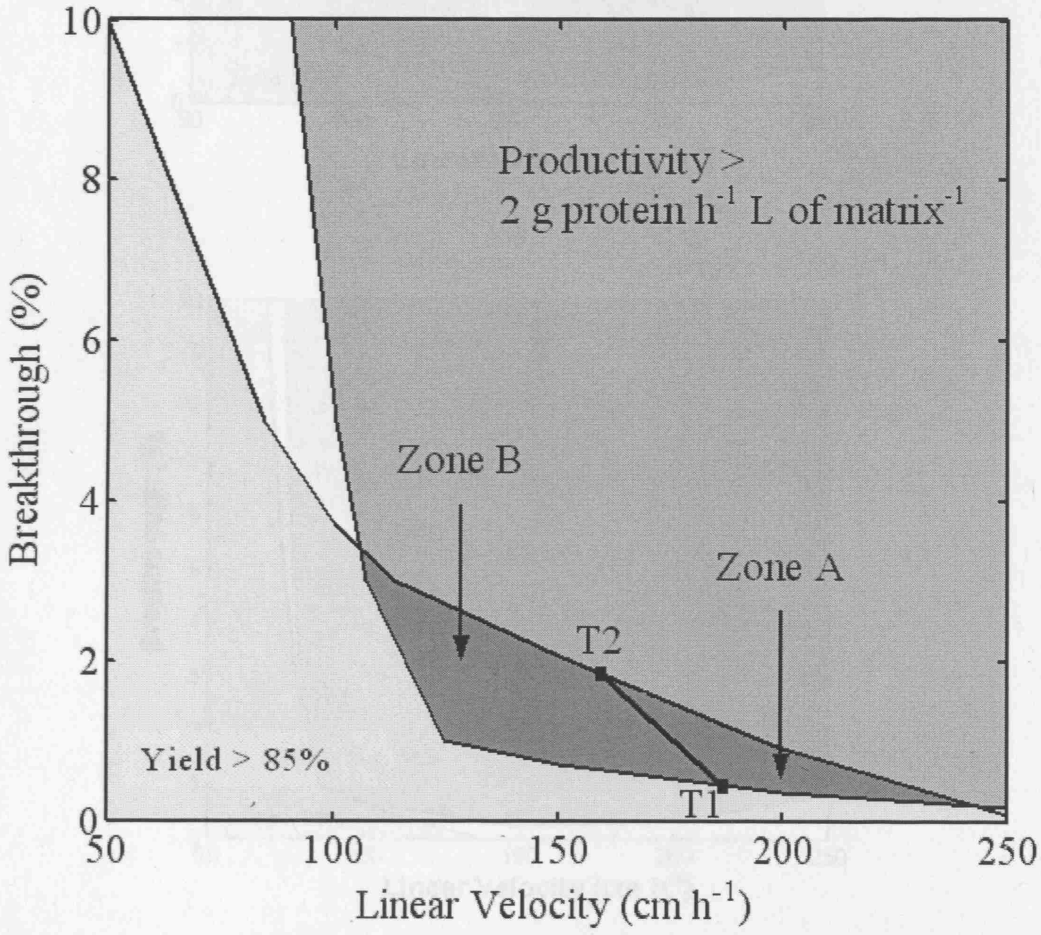

Figure 5.8 Window of Operation for first chromatographic stage, based on 60% purity

- Yield > 85%, Productivity < 2 g protein h^{-1} L of $matrix^{-1}$
- Productivity > 2 g protein h^{-1} L of $matrix^{-1}$, Yield < 85%
- Yield > 85% and Productivity > 2 g protein h^{-1} L of $matrix^{-1}$
- Yield < 85% and Productivity < 2 g protein h^{-1} L of $matrix^{-1}$

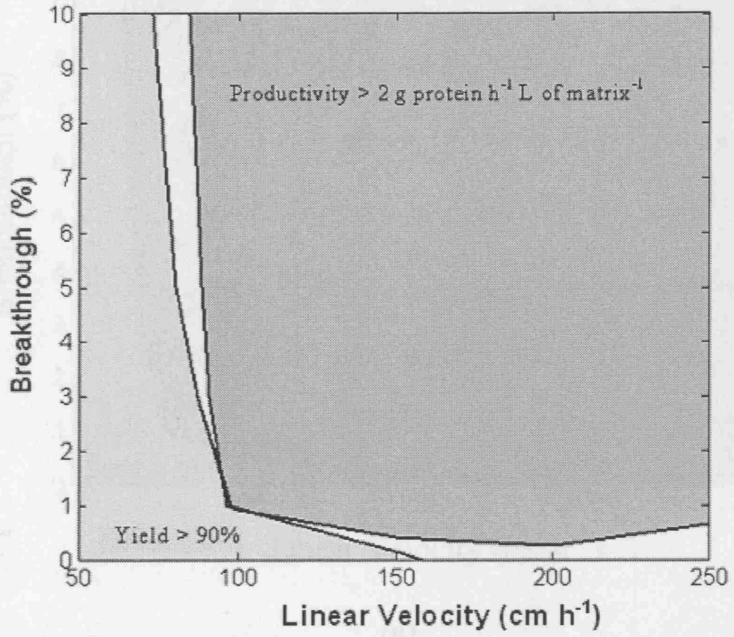

(a)

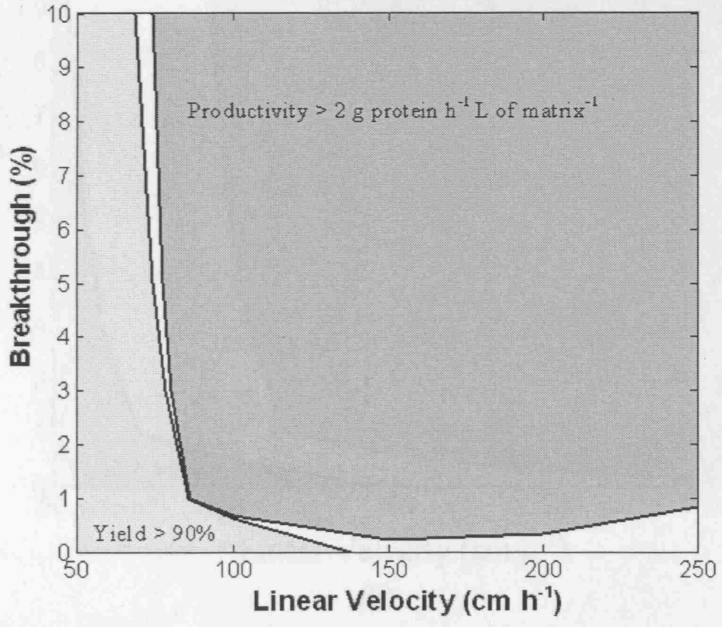

(b)

Figure 5.9 Windows of Operation for second chromatographic stage for points on tie-line in Figure 5.8 (a) Point T1 (b) Point T2

- Yield > 90%, Productivity < 2 g protein h^{-1} L of $matrix^{-1}$
- Productivity > 2 g protein h^{-1} L of $matrix^{-1}$, Yield < 90%
- Yield > 90% and Productivity > 2 g protein h^{-1} L of $matrix^{-1}$
- Yield < 90% and Productivity < 2 g protein h^{-1} L of $matrix^{-1}$

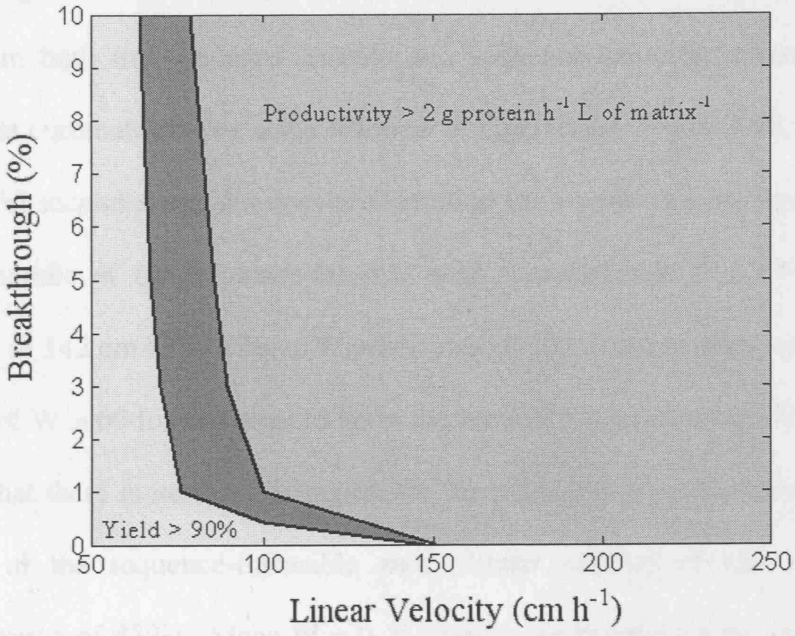

(a)

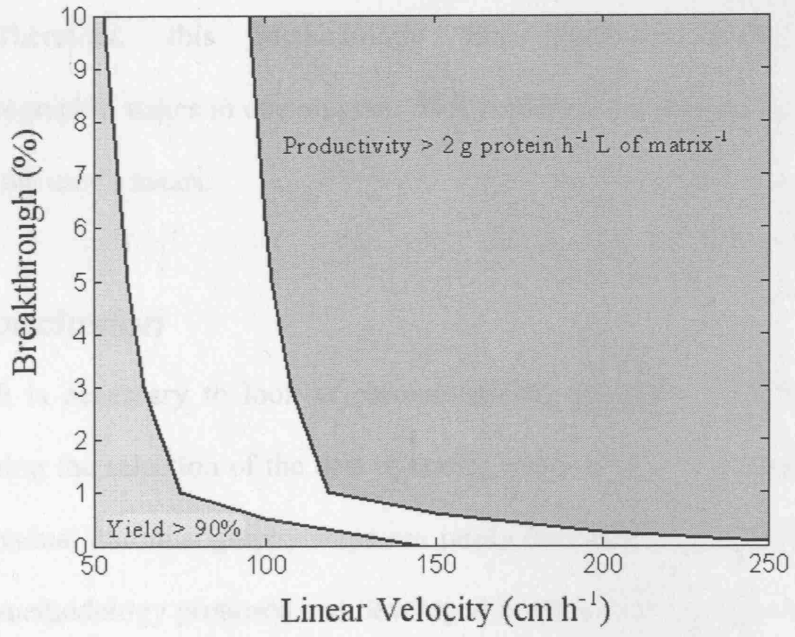

(b)

Figure 5.10 Windows of Operation for second chromatographic stage for points in Figure 5.8 feasible and infeasible zones (a) Point in first chromatographic stage sequence-feasible zone (1.5% breakthrough, 142 cm h^{-1}) (b) Point in first chromatographic stage sequence-infeasible zone (0.85% breakthrough,187 cm h^{-1})

- Yield > 90%, Productivity < 2 g protein h^{-1} L of $matrix^{-1}$
- Productivity > 2 g protein h^{-1} L of $matrix^{-1}$, Yield < 90%
- Yield > 90% and Productivity > 2 g protein h^{-1} L of $matrix^{-1}$
- Yield < 90% and Productivity < 2 g protein h^{-1} L of $matrix^{-1}$

Figure 5.10 shows two second stage Windows of Operation for points that lie within both the sequence-feasible and sequence-infeasible zones of Figure 5.8's first chromatographic stage Window of Operation. Figure 5.10 a shows the successful second stage Window of Operation for a point that lies approximately in the middle of the sequence-feasible zone (breakthrough of 1.5% and linear velocity of 142 cm h^{-1}). It has a Window area of 207 arbitrary units, satisfying the criteria of $W > 60$ for the point to lie in the sequence-feasible zone. Figure 5.10 b shows that there is no feasible region for the point that lies approximately in the middle of the sequence-infeasible zone (linear velocity of 187 cm h^{-1} and breakthrough of 85%). Since $W = 0$, it satisfies the criteria for the point to lie in the sequence-infeasible zone.

Therefore, this methodology for graphically describing two chromatographic stages in one diagram does contain flexibility and can be altered to meet the user's needs.

5.5 Conclusion

It is necessary to look at chromatography sequences as a whole when considering the selection of the best operating conditions, as the performances of the individual chromatography steps are rarely independent of each other. The tie-line methodology proposed and developed in this chapter provides a graphical means for identification of the feasible operating conditions of a two-stage chromatography sequence while incorporating the tradeoffs between yield, purity and productivity. The method separates a first chromatographic stage Window of Operation into two zones, A and B. Zone A consists of operating conditions that produce a material in the first stage operation that cannot be successfully purified

by a second stage to produce a material that meets the desired product specifications. Zone B contains operating conditions that produce a material in the first stage that can be further purified by a second stage to produce a product that meets the required specifications.

Simulated data based on a two-stage chromatographic separation successfully proved the application of the tie-line method. In using the tie-line method, experimental time and cost may be reduced since it limits the number of points that need to be examined in the first stage feasible region.

The next chapters describe an experimental system used to verify the tie-line methodology based upon a two stage chromatographic separation, ion exchange chromatography followed by hydrophobic interaction chromatography, for the purification of Fab' from a three-component feed solution. The purpose of this experimental study will be to bridge between the theoretical development and verification presented so far based upon simulated data, and the real-world application to live biological materials.

6. Isotherm Determination

6.1 Rationale

The tie-line method proposed in this thesis has been established using simulated data. The next step was to verify that the methodology worked for a practical situation. In order to do this, two sets of experiments were planned for a two-stage chromatographic separation of a three-component solution. The first set of experiments was to determine the adsorption characteristics of the proteins making up the three-component system. The vision was then to be able to input these values into the simulation package to:

1. Help demonstrate the similarity between the simulation chromatograms and the experimental chromatograms.
2. Help determine which experiments needed to be carried out, i.e. aid in determining the general area in which the tie-line should be located, thus limiting the number of experiments.

This section describes the experiments carried out to determine the adsorption isotherm values of the three components making up the test solution that was used in the experimental validation of the tie-line method (Chapter 7).

6.2 Materials and Methods

The three components being examined were Fab', Ribonuclease A and Cytochrome C. Ribonuclease A from bovine pancreas (Sigma Chemicals Ltd. Poole, Dorset, UK) and Cytochrome C from bovine heart (Sigma Chemicals Ltd. Poole, Dorset, UK) were used. Their molecular weights are 14kDa and 13kDa for Ribonuclease A and Cytochrome C respectively. These two proteins were selected to represent the impurities of the three-component system that is used for the experimental verification detailed in the following chapter. Fab' is the desired product in the three-component mixture. It has a molecular weight of 50kDa. The next section describes Fab', and the method for obtaining Fab' from an *E. coli* fermentation broth.

6.2.1 Fab Fragments

Fab' is an antigen-binding fragment of the antibody IgG.[27] Antibodies and their fragments are molecules that have high affinity and specificity for their target antigens. They have the potential to provide a novel range of specialized molecules that can be used in the detection or binding of biological entities.[29]

The whole IgG has two identical antigen-binding surfaces which are formed by the pairing of the V_H and V_L chains. The Fab' fragment consists of one light chain and a portion of one heavy chain, thus having one antigen-binding surface.[27]

One of the main uses for antibodies and their fragments is in the treatment of cancerous tumours. An attachment of an effector can allow for drug and radioisotope therapies.[27] However, even though antibodies have high specificity, they are not very useful in treating these tumours. Whole antibody molecules are

unable to penetrate into the tumour and kill the malignant cells.[30] Also, whole antibodies have been known to irradiate bone marrow and lead to toxicity when introduced to the body.[27] Antibody fragments, on the other hand, still retain the specificity of the whole antibody fragment but are able to penetrate tumours more readily.[30] They also are distributed from the blood to the tissues at a more rapid rate, and are cleared from the body more quickly lessening the effects and chance of toxicity.[27]

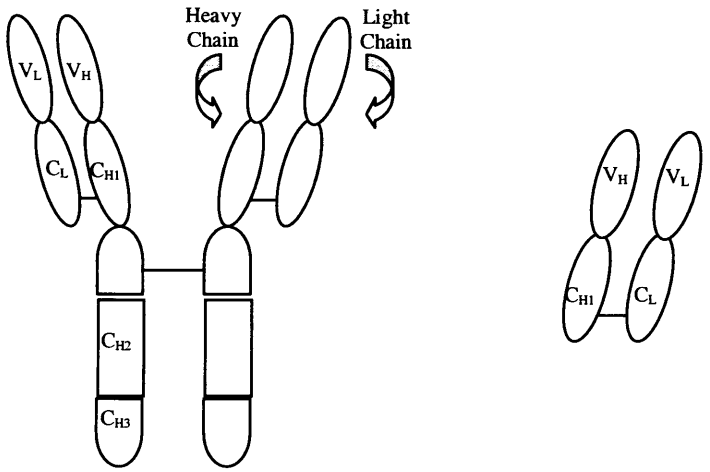

Figure 6.1 Diagram of IgG and Fab; (a) IgG, (b) Fab; V_L = variable light, C_L = constant light, V_H = variable heavy, C_H = constant heavy [27]

Fab' fragments can be prepared recombinantly, providing advantages to the molecules. For example, recombinant Fab' could be made multivalent, thus improving the avidity for the antigen.[27] High-level expression systems have been developed in mammalian cells, but the large amounts of antibody that need to be produced makes this method of production quite expensive.[31] Instead, microbial expression systems (i.e. *E.coli*) are used where large-scale production is much more cost-effective.[31]

6.2.2 Preparation of Clarified Lysate

All reagents were purchased from Sigma Chemicals Ltd. (Poole, Dorset, UK) unless otherwise specified.

The starting material consisted of a fermentation broth of *E.coli* cells (industrial strain, W3110 containing plasmid pTTOD A33 IGS2 producing an antibody Fab' fragment under control of the *lac* promoter) kindly donated by UCB Celltech (Slough, UK). A heat lysis was performed in order to release the components of the cells from the periplasmic space and precipitate contaminants.

316g of *E.coli* cells were suspended in 2.5 L of 100mM Tris buffer (10mM EDTA, pH 7.4) in a 3 L fermenter. For 16 h, the suspension was agitated at 300 rpm, and the temperature was controlled at 60°C. At the end of the process, the lysate was centrifuged in a Beckman J2-M1 centrifuge (Beckman Instruments Ltd., High Wycombe, UK) at 10,000 rpm and 4°C for 1.5 h. The supernatant (clarified lysate) was stored at 4°C.

6.2.3 Affinity Chromatography

Purification of the Fab' from the clarified lysate was performed by packed bed affinity Protein A chromatography using an AKTÄprime™ system (GE Healthcare UK Ltd., Bucks., UK). A XK50 column (GE Healthcare UK Ltd., Bucks., UK) was used, packed with Protein A Sepharose™ 4 Fast Flow (GE Healthcare UK Ltd., Bucks., UK) giving a column diameter of 50 mm and length of 70 mm.

Glycine was added to the clarified lysate to 1 M, and the pH adjusted to 7.5 using 50% (w/v) sodium glycinate. The solution was then filtered using 1.2 μm Millipore filter paper (Millipore Ltd., Watford, UK).

The Protein A column was washed with 10 column volumes of RO water and equilibrated with 10 column volumes of 1 M glycine (pH 8.0) at a linear velocity of 150 cm h^{-1}. After loading the clarified lysate onto the column, the column was washed with 5 column volumes of 1 M glycine buffer. Elution was carried out with 0.1 M sodium citrate buffer (pH 3). Elution fractions were collected when the chromatogram started to peak. 10.5 mL of 1 M Tris buffer (pH 9) was added to every 34.5 mL of Fab' solution collected.

Purified Fab' was buffer exchanged into 5 mM MES buffer, pH 5.5, using an Amicon stirred cell (Millipore Ltd., Watford, UK) with an Ultracel 10 KDa molecular weight cut-off membrane (Millipore Ltd., Watford, UK). The Fab' was determined to be 85% pure using the Agilent Bioanalyzer 2100 and labchip kit (Section 7.2.2).

Once the purified Fab' sample was obtained, batch adsorption experiments were carried out using SP Sepharose FF matrix (GE Healthcare UK Ltd., Bucks., UK). The following details the steps for the preparation of the matrix, the adsorption experiments, and the analysis of the results.

6.2.4 Preparation of Matrix

The matrix, SP Sepharose FF, was provided as slurry in a 20% (v/v) ethanol solution. It was pipetted into a test tube, and allowed to settle. Once the matrix had settled, ethanol was removed using a syringe. 5mM MES buffer at pH

5.5 was added to create 50% (v/v) slurry solution (50% matrix, 50% buffer). The slurry was shaken gently and allowed to settle. Liquid was removed from on top of the settled matrix particles, MES buffer was again added to make a 50% (v/v) slurry solution, and the matrix was left to equilibrate overnight.

6.2.5 Adsorption Experiments

The matrix slurry was gently shaken to make a homogeneous mixture, and was added to 2 mL Eppendorf tubes in the quantities of 10, 20, 50, 100, 200, 400 and 1000 μL. The matrix was allowed to settle, and the remaining liquid was removed leaving quantities of 5, 10, 25, 50, 100, 200 and 500 μL of matrix in each tube.

1 mL of 2.35 mg mL^{-1} Fab' in 5 mM MES buffer at pH 5.5 was added to each tube. The tubes were left to mix on a shaker overnight. This was repeated for Ribonuclease A (2.36 mg mL^{-1}) and Cytochrome C (2.68 mg mL^{-1}), and all experiments were performed in triplicate.

The pI values for Fab', Ribonuclease A and Cytochrome C are 9, 9.5 and 10 respectively. SP Sepharose is a matrix used for cation exchange. Therefore, in order for proteins to bind, the pH of the chromatography system should be below the pI of the protein. At pH 5.5, all three proteins should bind to the column.

6.2.6 Experimental Analysis

The mixer was turned off, and the matrix was allowed to settle to the bottom of the tubes. Liquid was pipetted out of the tubes, and measurements were made to determine the amount of protein remaining in solution (not bound to the matrix). The concentration of Fab' was determined with a Protein G assay. The concentrations of Ribonuclease A and Cytochrome C were both measured

spectrophotometrically at 280 nm and 550 nm respectively. The following sections describe each assay in more detail.

6.2.6.1 Protein G Assay

HPLC analysis was performed using an Agilent 1100LC with autosampler (Agilent Technologies, UK). A HiTrap Protein G HP column (GE Healthcare UK Ltd., Bucks., UK) was used for determining Fab' concentration. 100 mL of sample was injected onto the column with loading buffer (20 mM sodium phosphate, pH 7.4) at a flow rate of 3 mL min^{-1}. After 1.5 min, bound Fab' was eluted from the column by introducing an elution buffer (20 mM sodium phosphate, pH 2.5). Detection was carried out at 220 nm. Quantitation was carried out by comparing the elution peak area to a standard curve (Appendix E). All samples were measured in triplicate with a typical variation of ± 1%.

6.2.6.2 A280 and A550 Assays

The concentration of Cytochrome C was determined by measuring the absorbance of the solution at 550 nm. For the A550 assay, each sample was put in Sarstedt (Sarstedt AG and Co., Nümbrecht, Germany) polystyrene cuvettes. The spectrophotometer was blanked using 5 mM MES buffer. The measured absorbances at 550 nm were compared to a standard curve (as seen in Appendix E) to determine the concentration of Cytochrome C.

Ribonuclease A concentration was determined by measuring the absorbance of the solution at 280 nm. For the A280 assay, samples were put in a quartz cuvette. The Genesys 6 spectrophotometer (Thermospectronics, Rochester, NY, USA) was blanked using 5 mM MES buffer. The measured absorbance

values at 280 nm were compared to a standard curve to determine the Ribonuclease A concentration. Results performed in triplicate were reproducible varying by ±5%.

6.2.6.3 Calculations

The amounts of C*, the equilibrium concentration of protein in the fluid phase, and Q*, the equilibrium concentration of protein bound to the matrix, were determined. The Langmuir isotherm equation of

$$Q^* = \frac{q_{max} C^*}{k_d + C^*} \tag{6.1}$$

can be arranged to

$$\frac{1}{Q^*} = \frac{1}{C^*} \cdot \frac{k_d}{q_{max}} + \frac{1}{q_{max}} \tag{6.2}$$

By plotting 1/Q* versus 1/C*, the values of k_d and q_{max} were determined from the slope and the intercept of the plot. These values were then used in the following equations to determine the Langmuir parameters, a and b.

$$b = \frac{1}{k_d} \quad \text{and} \tag{6.3}$$

$$a = q_{max} \cdot b \tag{6.4}$$

The Langmuir parameters, a and b, were substituted back into the simulation programme (Chromulator – Section 3.2.2) to verify that they produce chromatograms similar to those obtained during ion exchange chromatography.

6.3 Results

The adsorption isotherms for Fab', Cytochrome C and Ribonuclease A are shown in Figure 6.2.

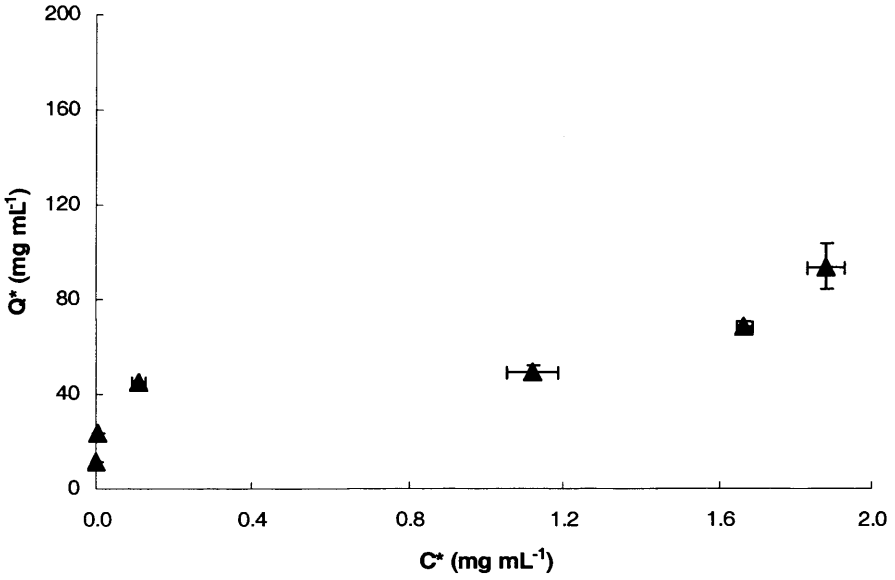

(a)

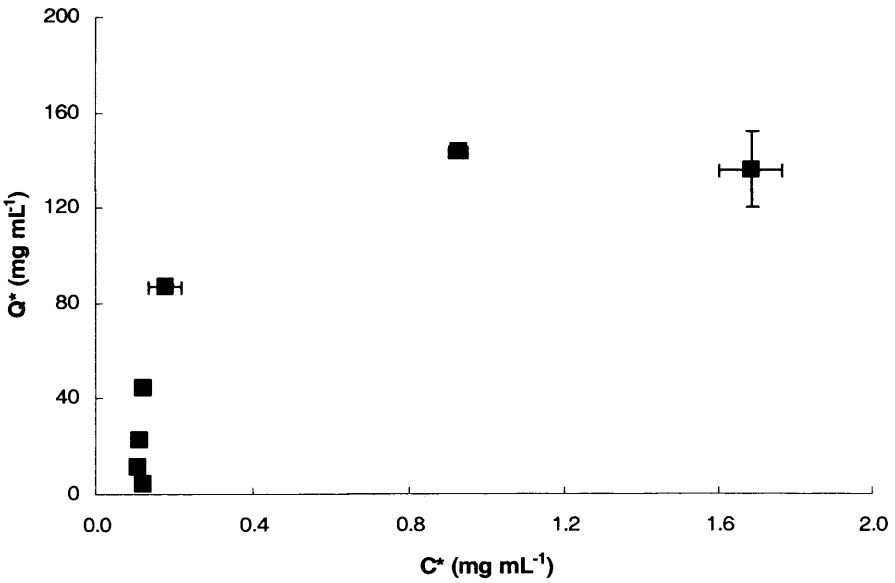

(b)

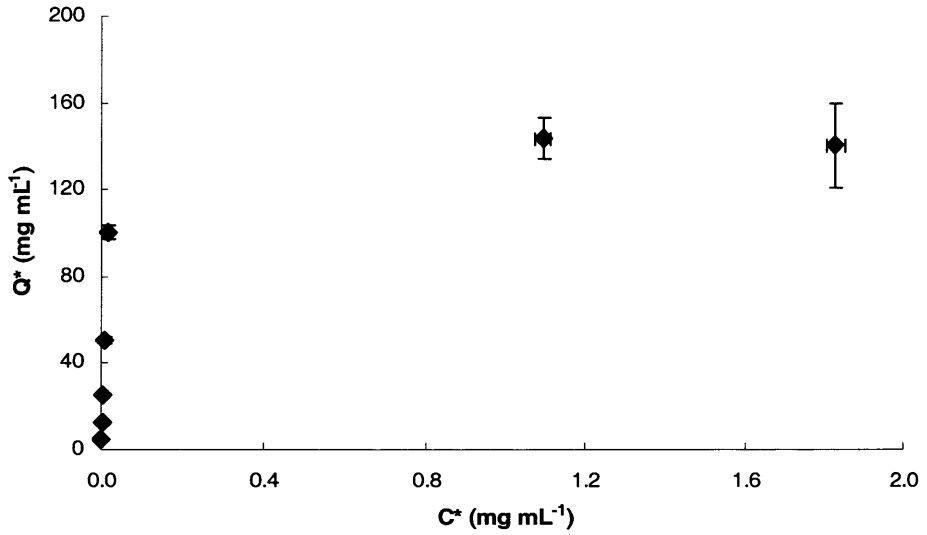

(c)

Figure 6.2 Adsorption Isotherms: (a) Fab', (b)Ribonuclease A and (c) Cytochrome C. Figures include error bars based on standard deviation.

The shapes of the Ribonuclease A and Cytochrome C isotherms are Langmuirian. However, the Fab' isotherm, does not resemble the shape attributed to Langmuir. When 1/Q* is plotted against 1/C*, the outcome would be a straight line if the isotherm was Langmuir. However, Figure 6.3 a-c shows that this is not the case.

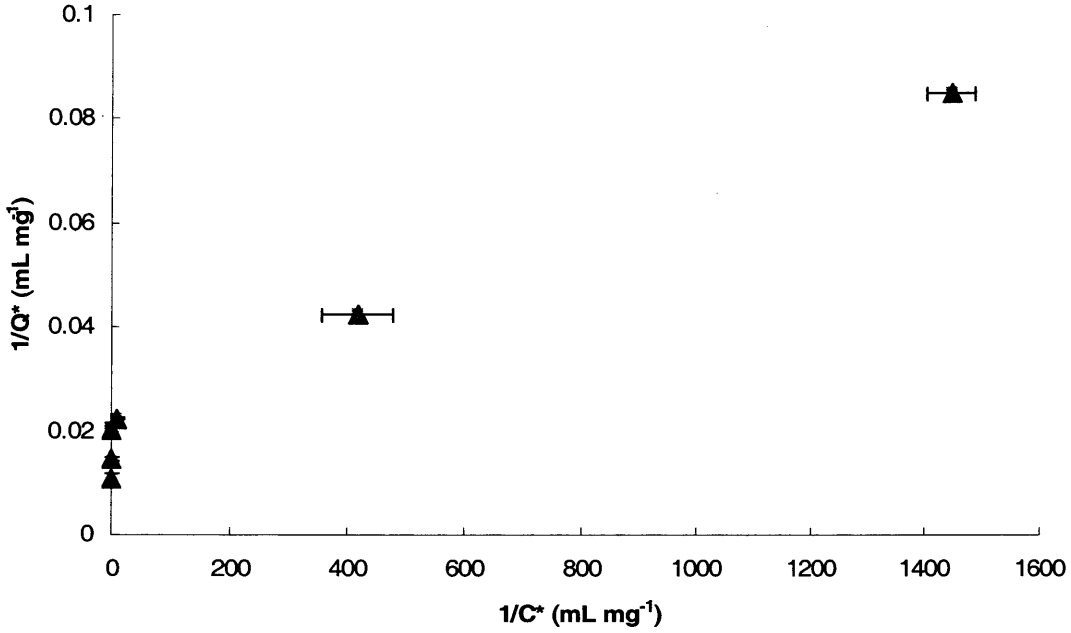
0.1
0.08
0.06
0.04
0.02
0
1/Q* (mL mg-1)
0
200
400
600
800
1000
1200
1400
1600
1/C* (mL mg-1)

(a)

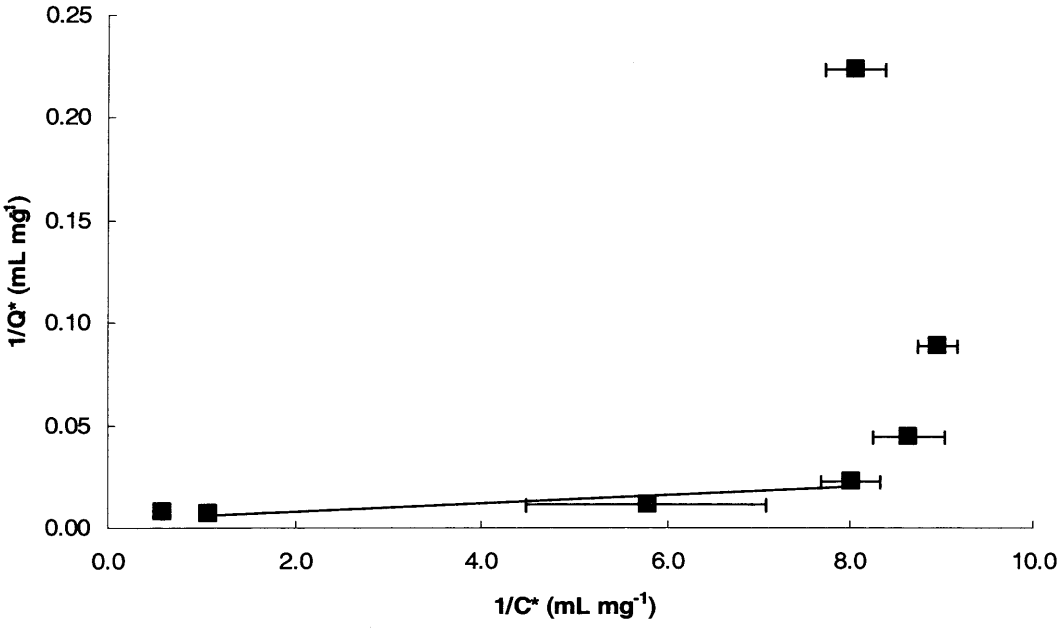
0.25
0.20
0.15
0.10
0.05
0.00
1/Q* (mL mg-1)
0.0
2.0
4.0
6.0
8.0
10.0
1/C* (mL mg-1)

(b)

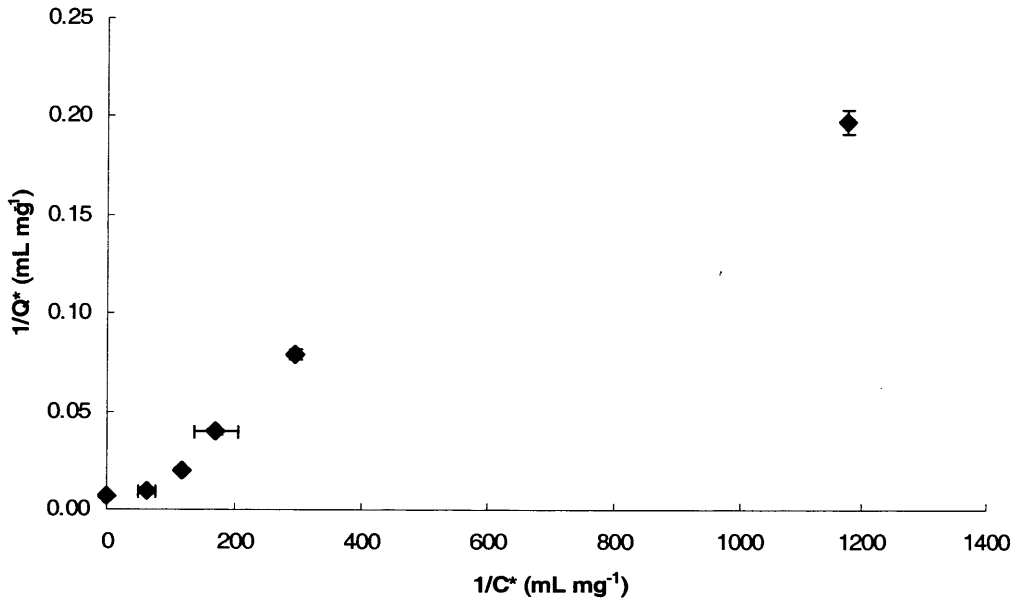

(c)

Figure 6.3 Linearized Langmuir Isotherm Data. (a) Fab' (b) Ribonuclease A (c) Cytochrome C. Figures include error bars based on standard deviation.

The region of the figure in which the chromatography process would be operated at, i.e. C* between 0-1 mg mL^{-1} was examined to see if any Langmuir-type trends could be extracted. Figures 6.4 a-c show the data examined.

Although they are still not linear, a line of best fit was approximated and Langmuir parameters were estimated. Table 6.1 summarizes the results of the Langmuir parameter calculations together with the correlation coefficient R^2 which relates to the goodness of the fit of the line.

Table 6.1 Derived Langmuir Parameters

			Langmuir Parameter		
Protein	**q_{max} (g L of resin^{-1})**	**k_d (g L^{-1})**	**a**	**b**	**R^2**
Fab'	45.1	2.25	20000	444	0.9988
Ribonuclease A	285.7	0.57	500	2	0.8351
Cytochrome C	192.3	0.02	10000	52	0.9030

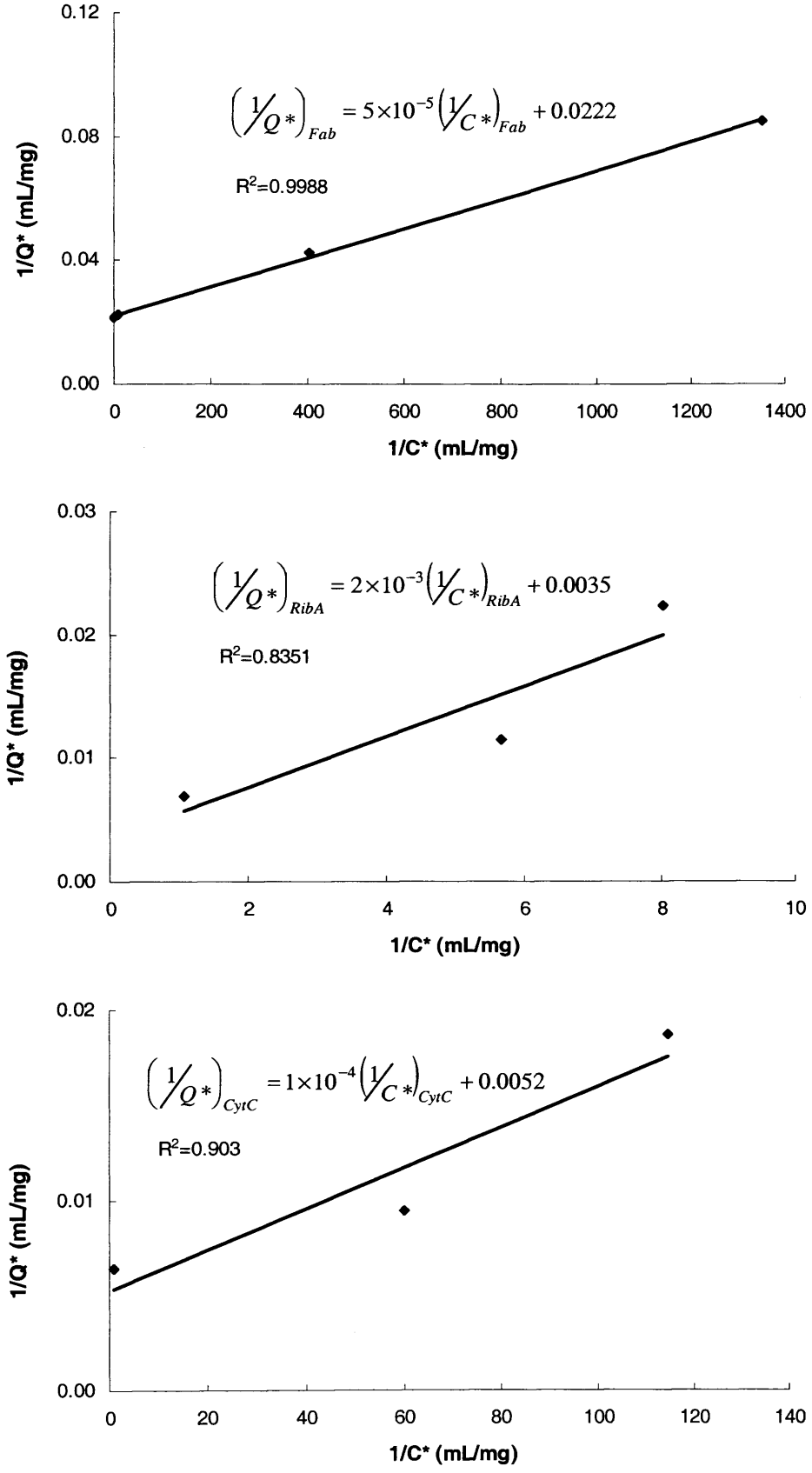

Figure 6.4 Linearized Langmuir Isotherm Data in Feasible Operating Range of 0 mg mL^{-1} < C* < 1 mg mL^{-1} (a) Fab' (b) Ribonuclease A (c) Cytochrome C

The values of the Fab' parameters are somewhat lower than expected. Table 6.2 summarizes published data for Fab' binding on a SP Sepharose column at pH 5.

Table 6.2 Least Squares Estimates of Fab' Parameters in the Langmuir Isotherm Model [55]

Conductivity (mS cm^{-1})	**q_{max} (g L of $resin^{-1}$)**
1.3	242 ± 11
5	119 ± 4
10	52 ± 18

An explanation for this reduction in q_{max} may relate to the conductivity of the Fab' solution used in the adsorption experiments, 0.36 mS cm^{-1}. Under these conditions, it would be expected that the value of q_{max} for the experimental system should be greater than 242 g L of $resin^{-1}$. Conversely, q_{max} for Cytochrome C was larger than expected. For ion exchange chromatography, q_{max} for Cytochrome C would be expected to be in the range of 34 g L^{-1}[56]. Therefore, the experimental data obtained was not consistent with the relative values of q_{max} between Fab' and Cytochrome C presented in the literature. This will have an impact on the shape and positioning of chromatograms produced by simulation.

The next step was to input these values into the Chromulator simulation programme to see if the simulated data was similar to that obtained by the experimental chromatograms. Ion exchange chromatography was carried out on a SP Sepharose FF HiTrap column (GE Healthcare UK Ltd., Bucks., UK), which has a column volume of 1 mL. The experiment was carried out at a flow rate of 1

mL min^{-1} and a load volume of 2 mL containing a mixture of Fab', Ribonuclease A and Cytochrome C, each with a concentration of 0.5 mg mL^{-1}.

Table 6.4 summarizes the parameters input into the Chromulator model in order to simulate the above described chromatography run, where sodium chloride was used for elution. The Peclet number, Biot number and the dimensionless constant were calculated using equations 3.2 to 3.8 and the column parameters listed in Table 6.3. For simulation purposes, the values of Langmuir parameters, a and b, for sodium chloride were assigned as 0.001 and 10000 respectively. This was to provide a solution that had a higher binding affinity to the matrix than the proteins adsorbed during column loading, thus allowing for elution.

Table 6.3 Column Parameters Required to Determine Peclet Number, Biot Number and Dimensionless Constant, η

Column Parameter	**Value**
Column Length	2.5 cm
Column Diameter	0.7 cm
Bed Porosity, ε_b	0.35
Particle Porosity, ε_p	0.88
Particle Radius, R_p	0.0035 cm
Pore Diameter, d_p	275 Å
Particle Tortuosity, τ	4

Table 6.4 Parameters Required for Chromulator Simulations

Protein	Initial Concentration (mol L^{-1}) x 10^5	Peclet Number (Pe_L)	Biot Number (B_i)	Dimensionless Constant - η
Fab'	1.00	210	21.0	0.7
Ribonuclease A	3.65	210	15.2	1.3
Cytochrome C	3.85	210	15.0	1.3
Sodium Chloride	100000	210	6.4	10.4

When run as a three component system, the simulation programme crashed when elution began. This was determined to be caused by the Langmuir parameters for Ribonuclease A. Subsequently, the simulation was run for a two component system consisting of Fab' and Cytochrome C. This yielded chromatograms, but very dislike those produced by experimentation. Figure 6.5 a and b show this comparison.

Comparisons between Figure 6.5a and b should be made based on the relative positions and shapes of the chromatographic peaks. They should not be drawn upon when the first peak started to elute as experimental data was taken when material started passing through the column, not when the elution buffer was first introduced as is presented by the simulated data. Simulated data shows the Cytochrome C peak starting to elute slightly in advance of the Fab' peak. However, experimental data shows that the Fab' peak elutes well before the Cytochrome C peak. In this cation exchange system at pH 5.5, the expected order of elution determined by the pI values of the proteins would be Fab' (pI value of 9) followed by Cytochrome C (pI value of 10) as seen in the experimental data.

A difference was also noted in the broadness of the Cytochrome C peaks, where the experimental peak was much broader than that of the simulated peak. The Chromulator input parameters for Cytochrome C were altered in order to determine which parameters would have an effect on the shape and the location of the curve. No significant changes were noticed by altering the Peclet number between 1 and 500, or by altering the Biot number between 1 and 150. Altering the dimensionless constant, η, had an effect on peak shape. When the number was increased, the peak became narrower. However, since its value was calculated as 1.3, decreasing η towards zero did not have a significant impact upon the peak shape. By increasing the Langmuir parameter, a, there was a direct impact on peak shape and its position in the chromatogram. Figure 6.6 shows the effect of increasing the value of Langmuir parameter, a, to 100,000 (much larger than the calculated value of 10,000). The peak starts to elute after Fab' and with a broader shape. Although this resembles the experimental results more (as seen in Figure 6.5b), it is still not an exact match. Finally, altering Langmuir parameter, b, between 1 and 500 did not have an effect on the Cytochrome C peak.

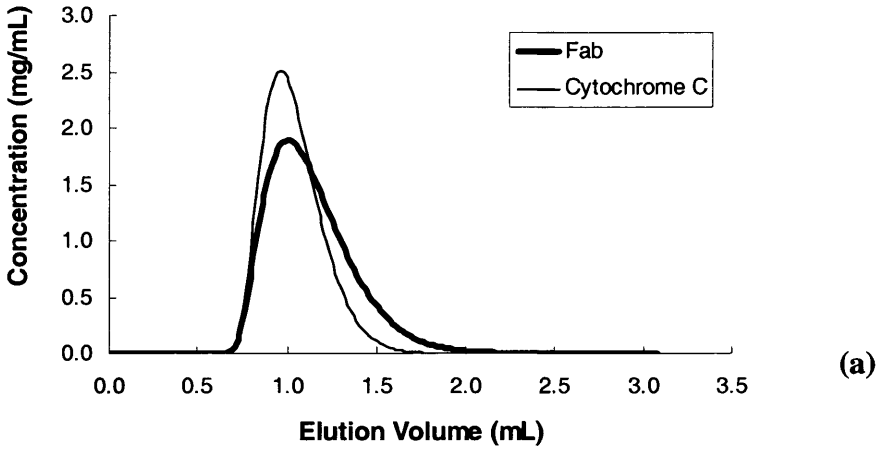

(a)

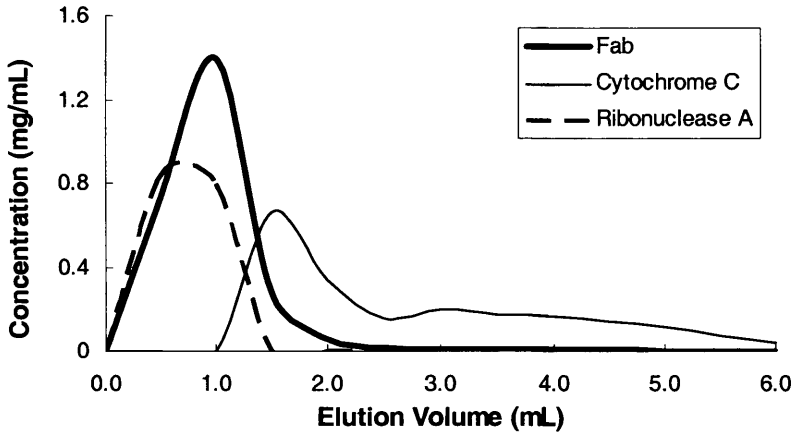

(b)

Figure 6.5 Comparison of Simulated and Experimental Data (a) Simulated Chromatogram (b) Experimental Chromatogram. Simulated parameters from Tables 6.3 and 6.4.

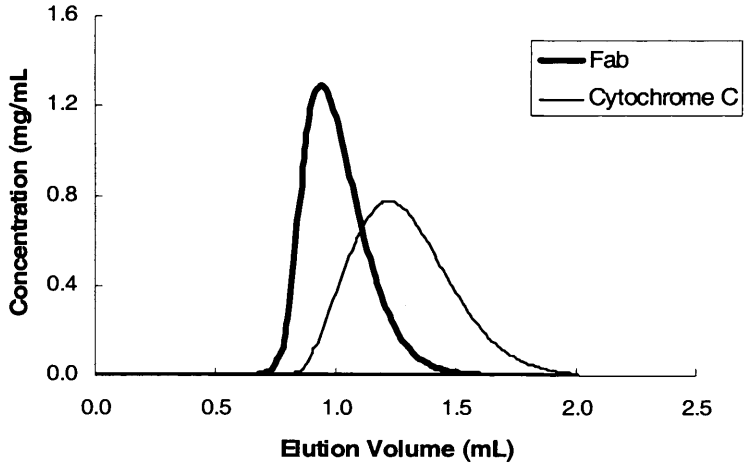

Figure 6.6 Simulated Chromatogram – Simulation parameters from Tables 6.3 and 6.4. Langmuir Parameter, a, for Cytochrome C increased to 100,000.

6.4 Conclusions and Recommendations for Future Work

The purpose of these experiments was to determine the isotherm parameters for the three experimental proteins; Fab', Ribonuclease A and Cytochrome C. The value in running the experiments would be to simplify the overall selection process by helping to determine which operating parameter combinations need to be examined experimentally. For example, if a first stage Window of Operation is produced experimentally, simulations could then be carried out to narrow the range of points required to be tested experimentally in order to determine the position of the tie-line. However, since adsorption of the three proteins did not appear to be Langmuirian, nor could the data be satisfactorily approximated to be Langmuir, the simulation model could not be used to verify or to predict the experimental results.

The Chromulator simulation package is based upon the competitive Langmuir isotherm and does not provide the flexibility to model with other isotherm types. In order for modelling to be considered as part of the overall selection scheme, it would be necessary to incorporate different isotherm models (i.e. Freundlich Isotherm). The user could select the specific isotherm relating to a particular protein, and hence the simulated data would be much more process-specific and accurate.

Although the isotherm data could not be used to run valid computer simulations, it was decided to pursue experiments using Ribonuclease A, Fab' and Cytochrome C as the three-component experimental system. This was because these three proteins provided a separation in both ion exchange chromatography and hydrophobic interaction chromatography that produced Windows of Operation that were valuable to examine in the verification of the tie-line theory.

The resolution between the three components' peaks in both ion exchange and hydrophobic interaction chromatography were noticeably different with changes in load volume and flow rate (as demonstrated in the next chapter), thus making it a valuable experimental mixture.

The next section describes the results of the experimental verification of the tie-line methodology.

7. Experimental Verification of Tie-Line Method

7.1 Introduction

Throughout this thesis, a tie-line method has been developed that allows a first stage Window of Operation to be divided into two zones. One zone contains operating conditions that produce a material in the first chromatographic stage that cannot be successfully purified by a second stage to produce a product that meets the desired yield, purity and productivity requirements. The other zone contains operating conditions that produce a material that is successfully purified by a second chromatographic stage to produce a product that meets the desired specifications. So far, all the evidence proving the methodology has been based on simulated data. This chapter describes the use of a model experimental system to verify the tie-line method described in the previous chapters.

This chapter presents results that show the application of the tie-line method to a two-stage chromatographic separation of a three-component protein mixture. This chapter contains the following:

- The production of the first stage Window of Operation
- The search for the tie-line using the methodology described in Figure 5.2
- The verification of the tie-line by testing points along it to show that they produce Windows of Operation that lie within the before mentioned transition region
- The verification of zones A and B by testing points in both regions to show that their Window of Operation areas lie within the acceptable limits.

7.2 Materials and Methods

7.2.1 Experimental Setup

The tie-line methodology was verified using a two stage chromatography system consisting of ion exchange chromatography (IEC) followed by hydrophobic interaction chromatography (HIC), a typical separation used in industry. An example of the use of the sequence is the purification of recombinant HIV reverse transcriptase. In this process, *E.coli* lysate undergoes ammonium sulphate precipitation, ion exchange is used to capture the transcriptase, and hydrophobic interaction chromatography is used to concentrate and further purify the product.[58]

Both chromatography stages were run on an ÄKTAprime™ system (GE Healthcare UK Ltd., Bucks., UK). A three component mixture containing Ribonuclease A, Cytochrome C, and Fab' was loaded onto each column with the desired purified product being Fab' and Ribonuclease A and Cytochrome C being impurities. These proteins were chosen as they have properties such that there is a separation that can be used to make Windows of Operation. This is because there is still overlap between the protein concentration profiles when the proteins are eluted from the column. If resolution was very good and there was a perfect separation, there would be no requirement for Windows of Operation. Fab', as the product, is of particular interest in the biotech industry in the treatment of illness such as cancerous tumours because of its high specificity and its ability to penetrate solid tumours, and the ability of the body to clear them rapidly from the blood, thus reducing toxicity.

A SP Sepharose FF HiTrap column (GE Healthcare UK Ltd., Bucks., UK) with a column volume of 1 mL was used for IEC. All three components had an

initial concentration of 0.5 mg mL^{-1} for IEC. A Butyl HP HiTrap column (GE Healthcare UK Ltd., Bucks., UK), as recommended by UCB Celltech, with a column volume of 1 mL was used for HIC, the second stage operation. Initial concentrations varied according to the operation of the first chromatographic step, and ranged from 0.094 mg mL^{-1} to 0.391 mg mL^{-1} for Ribonuclease A, 0.138 mg mL^{-1} to 0.442 mg mL^{-1} for Fab', and 0.061 mg mL^{-1} to 0.274 mg mL^{-1} for Cytochrome C. Both stages were operated at flow rates of 0.6 mL min^{-1} (100 cm h^{-1}), 1 mL min^{-1} (150 cm h^{-1}) and 1.6 mL min^{-1} (250 cm h^{-1}) which was in accordance with the recommended flow rates/linear velocities provided with the columns, and load volumes of 2 mL, 10 mL and 20 mL. Experiments were inclusive of all the possible combinations of flow rate and load volume, giving nine runs per experimental set.

IEC was run using a loading and washing buffer of 5 mM MES (all reagents were from Sigma Chemicals Ltd. Poole, Dorset, UK unless otherwise specified) at pH 5.5, and an elution buffer of 5 mM MES, 1 M NaCl at pH 5.5. HIC was operated using a loading and washing buffer of 0.1M phosphate, 2M ammonium sulphate at pH 7, and an elution buffer of 0.1M phosphate at pH 7. The following outlines the volume attributed to the chromatographic cycle:

- Loading: Dependant upon experimental load volume
- Washing: 5 CV with loading buffer
- Elution: 8 CV with elution buffer
- Regeneration: 5 CV with RO water, 5 (CV) with loading buffer

Experiments were run, and chromatograms were generated. Fractions were taken in uniform intervals. For IEC, fractions were collected every 0.3 mL. Fractions were collected every 0.4 mL for the HIC stage since it had better resolution. When the resolution was better, there was less overlap between the peaks on the chromatogram. Thus, there was a lot less time during elution when more than one component was eluted from the column at the same time. Because of this, fractions could be collected at longer intervals because not as many fractions were required to examine the elution profiles of the three components.

The collected fractions were analyzed in three ways:

1. A Protein G assay was used to determine the concentration of Fab' present in the sample (section 6.2.6.1).
2. The absorbance measurement at a wavelength of 550 nm was used to determine the Cytochrome C concentration (section 6.2.6.2).
3. The Bioanalyzer assay was used to determine the Ribonuclease A concentration.

7.2.2 Agilent 2100 Bioanalyzer and Protein 200/230 Labchip® Kit

The Agilent 2100 Bioanalyzer (Agilent Technologies, UK) provides information of the sizes and relative concentrations of the proteins in a sample. It works using electrophoresis, sizing proteins by driving them through microchannels.

The Protein 200/230 Labchip® Kit (Agilent Technologies, UK) contains a denaturing solution, a gel solution, and a ladder (used as a standard solution that

provides markers for sample comparisons). 4 μL of sample and 2 μL of denaturing solution were added into 0.5 mL microcentrifuge tubes, and centrifuged for 15 s. 6 μL of ladder was added to a microcentrifuge tube. All the samples (and ladder) were placed on a UBD heating block (Grant Instruments Ltd., Cambridge, UK) set at 100°C for 5 min, and then were centrifuged for 15 s. 84 μL of deionized water was added to each tube, and vortexed. 12 μL gel solution was added into the protein chip, and 6 μL of each sample (which was prepared according to manufacturer instructions) was pipetted into the appropriate wells in the chip. The chip was inserted into the 2100 Bioanalyzer and the automated cycle started with the output being an electopherogram. The quantitation reproducibility is ± 10% (Agilent Technologies, UK). Results were compared to a standard curve (Appendix E) to determine the Ribonuclease A concentration.

When there was Fab' present in the sample, the peak area of the Ribonuclease A curve could be compared to the peak area of the Fab' curve to verify the Ribonuclease A concentration since the amount of Fab' present had already been determined by the Protein G assay. Samples were initially assayed twice with the Bioanalyzer assay. After 50 samples were analyzed, it was determined that there was not a significant amount of variability between the repeat analyses. Since the Bioanalyzer assay was very expensive (£300 for a kit that analyzes 300 samples) and time consuming (approximately 40 minutes to prepare and analyze 10 samples), it was decided to only run one assay per sample since in total there were approximately 1500 samples to analyze.

In the HIC samples, there was more resolution in the separation, and many fractions only contained Ribonuclease A. Instead of using the Bioanalzyer assay

which is expensive and time consuming, in fractions containing only Ribonuclease A, A_{280} measurements were performed to quantitate Ribonuclease A concentration. The Bioanalyzer assay was only used for fractions containing both Fab' and Ribonuclease A.

7.2.3 Experimental Overview

Figure 7.1 outlines the experimental and analytical procedures used for the first chromatography stage.

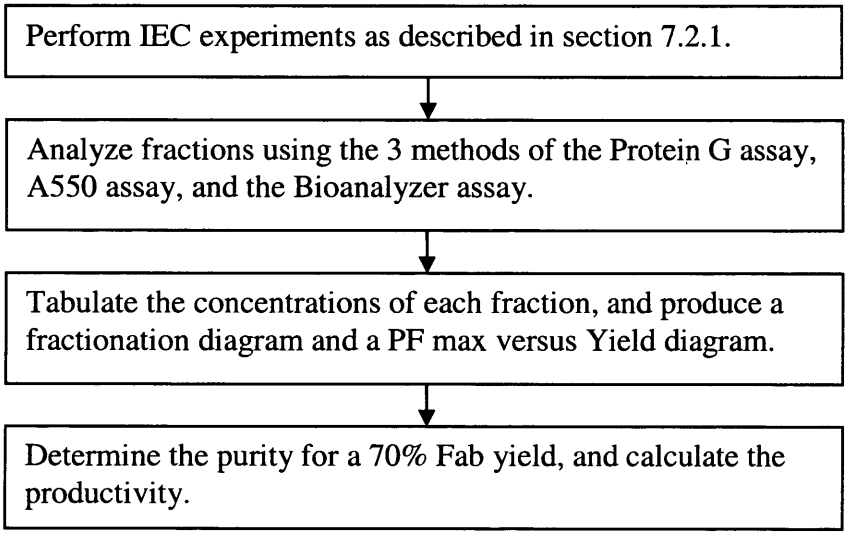

Figure 7.1 Experimental Steps for IEC

Once all nine runs in the experimental set were performed and analyzed, a Window of Operation was produced showing how purity and productivity were affected when flow rate and load volume were altered. Table 7.1 outlines the specifications required for both first and second stage operations to make the Windows of Operation.

Table 7.1 Constraints for the Construction of Windows of Operation

Constraint	First Chromatographic Stage	Second Chromatographic Stage	Combined Sequence Specification
Purity (%)	≥50	≥96	≥96
Yield (%)	≥70	≥99	≥69.3
Productivity (g protein h^{-1} L of matrix^{-1})	≥1	≥4.5	≥2.75

When the first stage Window of Operation was produced, the investigation into the placement of a tie-line separating the sequence-feasible zone and the sequence-infeasible zone commenced. The procedure outline in Figure 5.2 was used in order to locate the tie-line. For each point tested on the first stage Window of Operation, the procedure in Figure 7.2 was employed.

Once all nine runs in the experimental set were performed and analyzed, a Window for the second chromatographic stage was produced showing how purity and productivity were affected when flow rate and load volume were altered. The area of the feasible region was also calculated. This was repeated for ten points in the second stage Window of Operation.

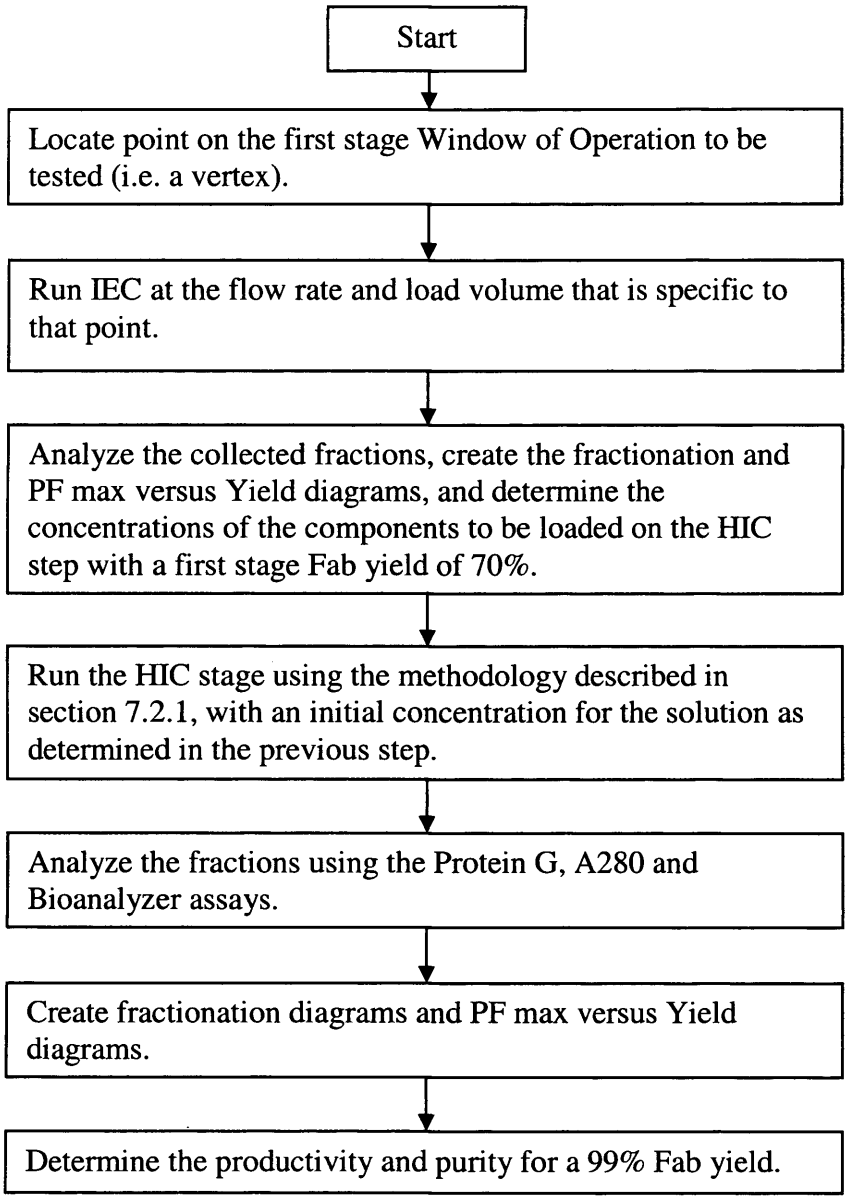

Figure 7.2 Experimental Steps Sequencing IEC and HIC

Results

The Window of Operation for the first chromatographic stage, ion exchange chromatography, is shown in Figure 7.3. Example calculations outlining how to derive information for the Windows of Operation from the raw experimental data (i.e. the chromatogram and the results of the protein concentration determining assays) are shown in Appendix F.

The contour lines presented in Figure 7.3 and the other Windows of Operation for experimental data are jagged in comparison to the smoother contours presented for the simulated data (as seen in Chapters 4 and 5). This is due to the number of data points used to create the Window of Operation. Each experimental Window of Operation was created using nine combinations of flow rate and load volume, whereas each simulated Window of Operation was created using 25 combinations of flow rate and breakthrough %. The number of experimental combinations was limited due to time and cost. However, nine experimental runs per Window of Operation provided enough information to create viable Windows from which the tie-lie methodology could be verified.

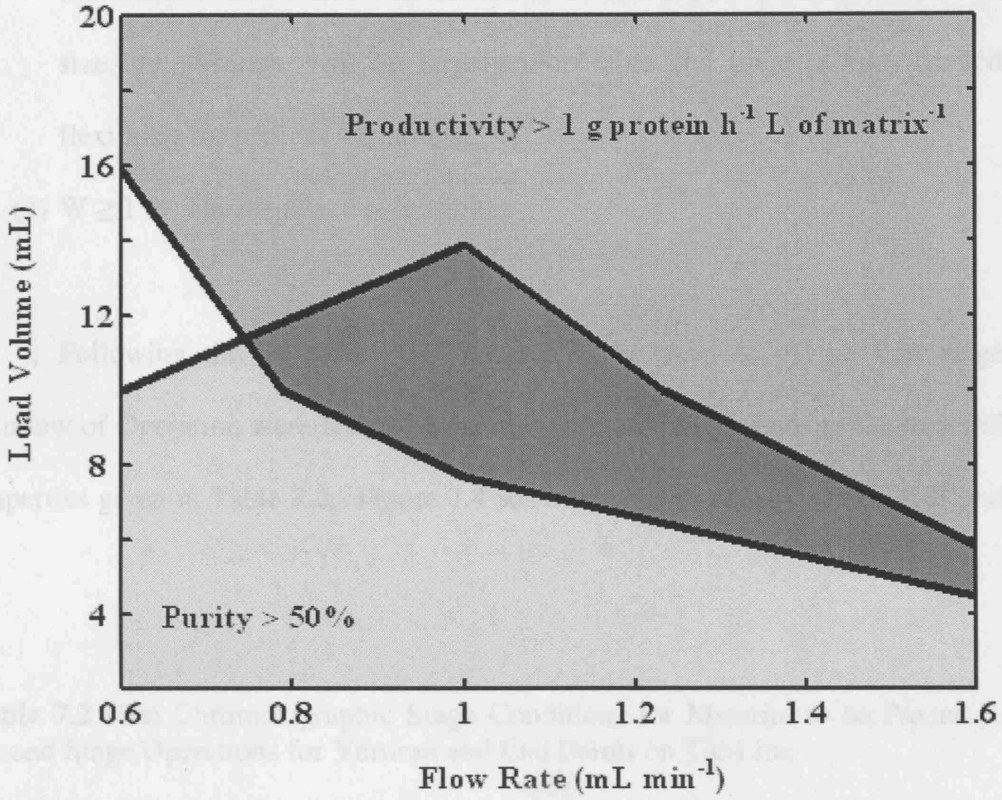

Figure 7.3 First Chromatographic Stage Window of Operation (IEC)

- Purity > 50%, Productivity < 1 g protein h^{-1} L of $matrix^{-1}$
- Productivity > 1 g protein h^{-1} L of $matrix^{-1}$, Purity < 50%
- Purity > 50% and Productivity > 1 g protein h^{-1} L of $matrix^{-1}$
- Purity < 50% and Productivity < 1 g protein h^{-1} L of $matrix^{-1}$

The following conditions were used in order to determine the position of the tie-line. In the following, W represents the Window of Operation area for the second chromatographic stage.

(1) W = 0. There are no conditions where the product specifications can be met.

(2) 0 < W < 1.8. The feasible region is less than 10% of the available Window area. In Figure 7.3, there is a range of 1 unit across the x-axis and a range of 18 units along the y-axis. Therefore, the maximum available Window space was calculated to be 18 units. Thus, the

minimum Window size was desired to be less than 1.8 units. Below this size, the Window will be largely inoperable and there is very limited flexibility for process variations.

(3) $W \geq 1.8$. The sequence is feasible.

Following the procedure in Figure 5.2, the vertices of the first stage Window of Operation were tested. Operating at these points leads to the material properties given in Table 7.2. Figure 7.4 shows the placement of points A, B and C.

Table 7.2 First Chromatographic Stage Conditions for Material to be Passed to Second Stage Operations for Vertices and End Points on Tie-Line

Stage 1 Conditions				**Composition of Material Produced from Stage 1 Operation**		
Point on 1st Stage Window	**Yield (%)**	**Load Volume (mL)**	**Flow Rate (mL min^{-1})**	**Ribonuclease A (mg mL^{-1})**	**Fab (mg mL^{-1})**	**Cytochrome C (mg mL^{-1})**
A	70	11.4	0.8	0.284	0.384	0.223
B	70	6.0	1.6	0.148	0.210	0.121
C	70	4.4	1.6	0.094	0.138	0.061
D	70	10.8	1.2	0.391	0.442	0.274

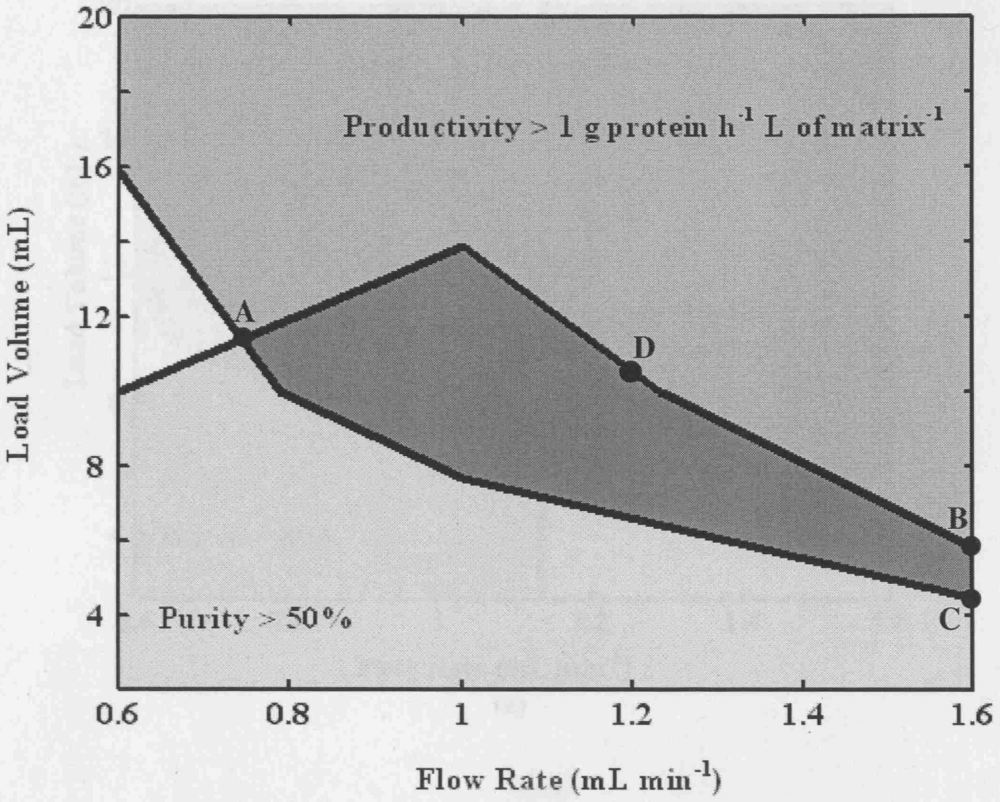

Figure 7.4 Positions of Tested Points on First Chromatographic Stage Window of Operation (IEC)

- Purity > 50%, Productivity < 1 g protein h^{-1} L of $matrix^{-1}$
- Productivity > 1 g protein h^{-1} L of $matrix^{-1}$, Purity < 50%
- Purity > 50% and Productivity > 1 g protein h^{-1} L of $matrix^{-1}$
- Purity < 50% and Productivity < 1 g protein h^{-1} L of $matrix^{-1}$

Point A gave rise to a successful Window of Operation as seen in Figure 7.5 a, with an area of 7.4 arbitrary units. Point B did not yield a second stage Window, as seen in Figure 7.5 b. However, point C gave rise to a successful second stage Window of Operation, seen in Figure 7.5 c. The area of this Window is 1.2 arbitrary units, which falls within the conditions outlined for the transition region between sequence-feasible and sequence-infeasible. Thus, point C is a point on the tie-line.

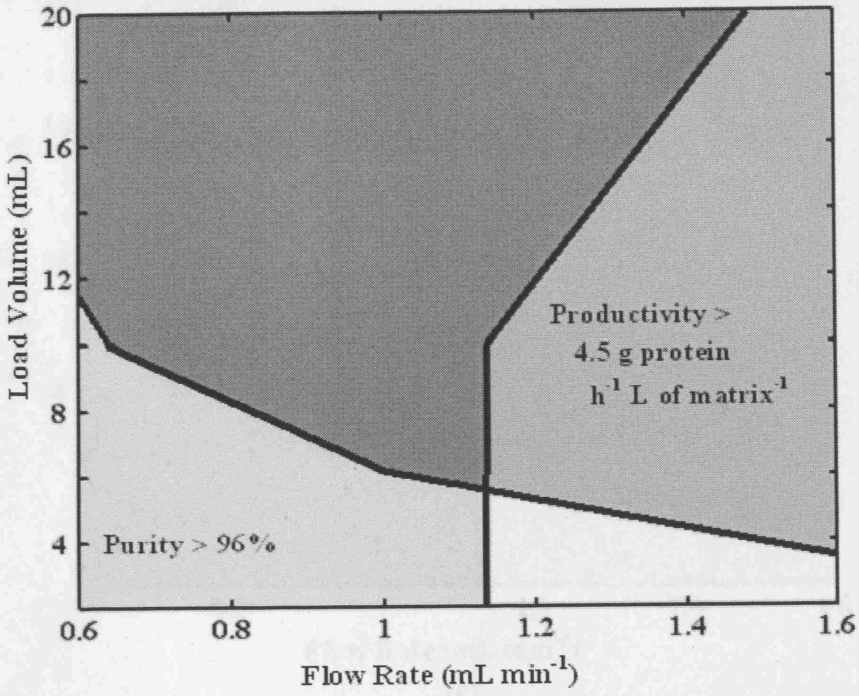
20
16
12
8
4
Load Volume (mL)
Productivity >
4.5 g protein
h-1 L of matrix-1
Purity > 96%
0.6
0.8
1
1.2
1.4
1.6
Flow Rate (mL min-1)

(a)

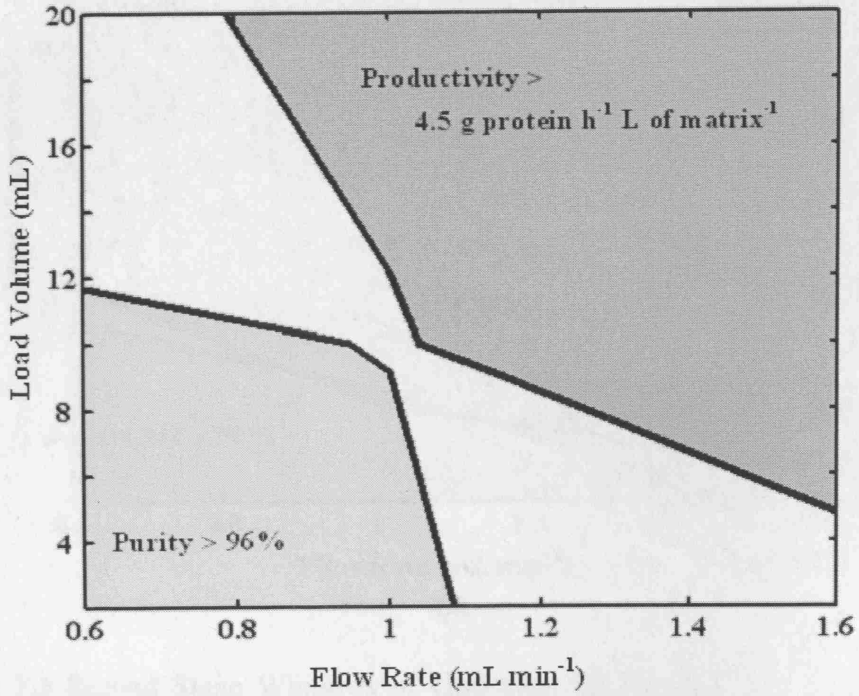
20
16
12
8
4
Load Volume (mL)
Productivity >
4.5 g protein h-1 L of matrix-1
Purity > 96%
0.6
0.8
1
1.2
1.4
1.6
Flow Rate (mL min-1)

(b)

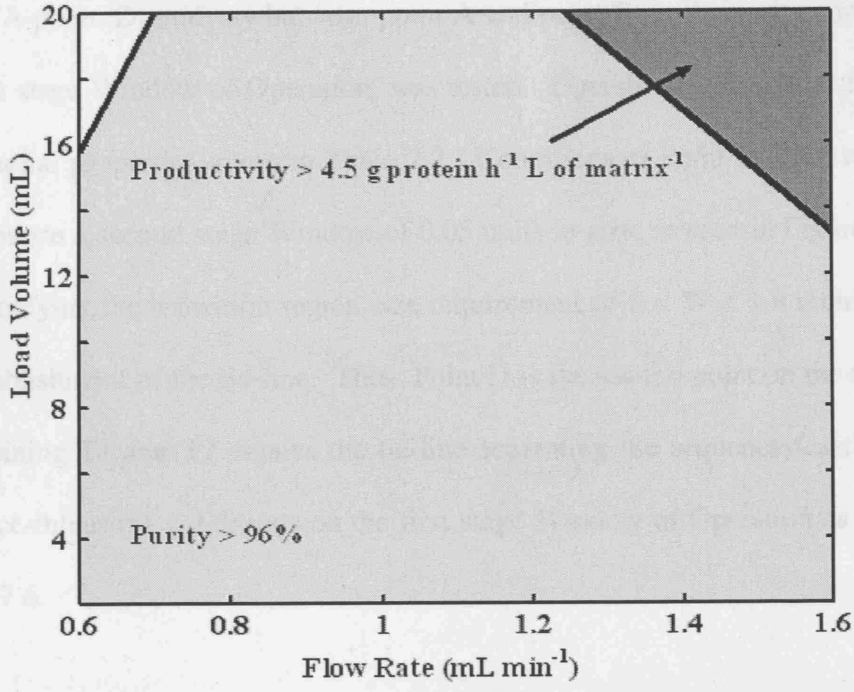

(c)

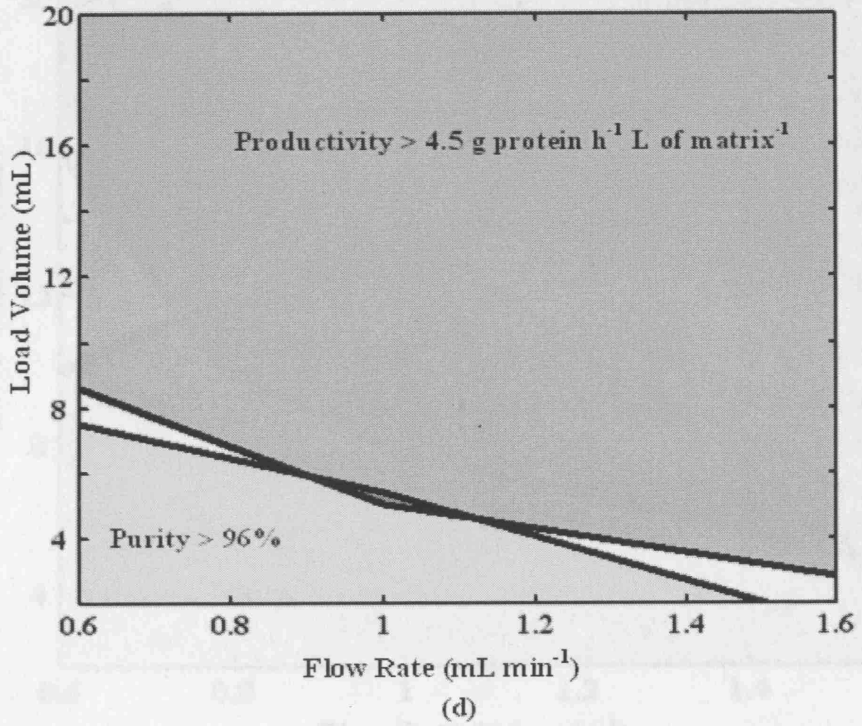

(d)

Figure 7.5 Second Stage Windows of Operation. (a) Point A, (b) Point B, (c) Point C, (d) Point D

- Purity > 96%, Productivity < 4.5 g protein h^{-1} L of $matrix^{-1}$
- Productivity > 4.5 g protein h^{-1} L of $matrix^{-1}$, Purity < 96%
- Purity > 96% and Productivity > 4.5 g protein h^{-1} L of $matrix^{-1}$
- Purity < 96% and Productivity < 4.5 g protein h^{-1} L of $matrix^{-1}$

A point, D, midway between point A and point B on the purity contour of the first stage Window of Operation, was tested. Operating at this point leads to the material properties given in Table 7.2. Conditions at Point D yield material that produce a second stage Window of 0.05 units in size, as seen in Figure 7.5 d, thus satisfying the transition region size requirement of $0 < W < 1.8$ required for the establishment of the tie-line. Thus, Point D is the second point on the tie-line, T2. Joining T1 and T2 creates the tie-line separating the sequence-feasible and sequence-infeasible conditions on the first stage Window of Operation as seen in Figure 7.6.

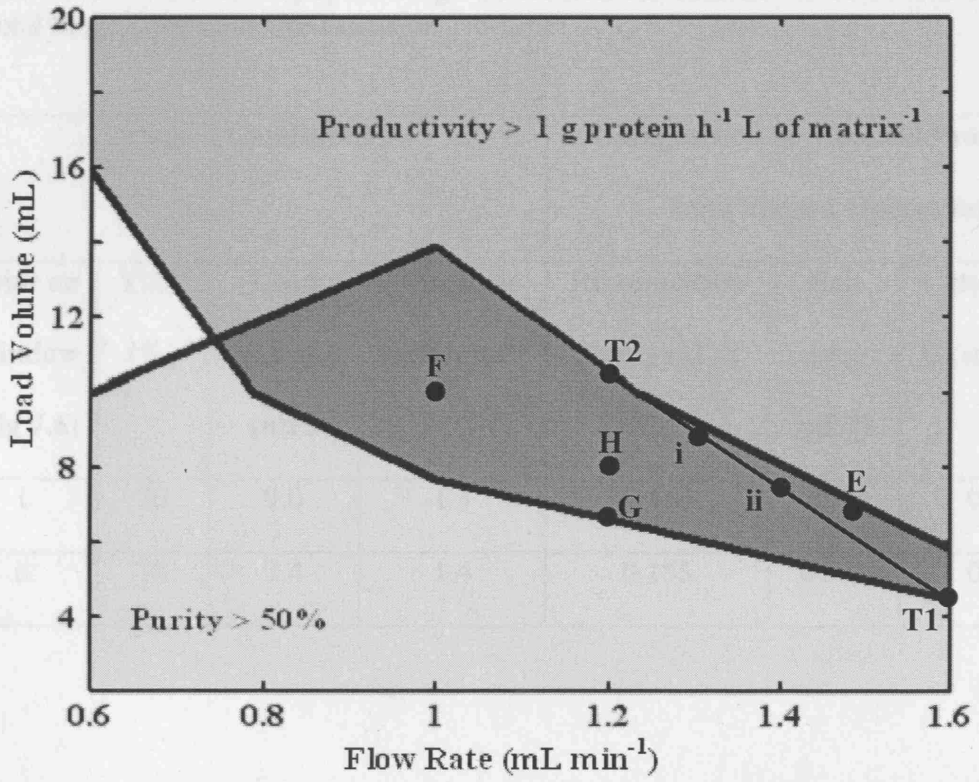

Figure 7.6 Positions of Tie-Line and Points Proving its Validity on the First Chromatographic Stage Window of Operation (IEC)

- Purity > 50%, Productivity < 1 g protein h^{-1} L of $matrix^{-1}$
- Productivity > 1 g protein h^{-1} L of $matrix^{-1}$, Purity < 50%
- Purity > 50% and Productivity > 1 g protein h^{-1} L of $matrix^{-1}$
- Purity < 50% and Productivity < 1 g protein h^{-1} L of $matrix^{-1}$

Two points were tested along the established tie-line, and are labelled as i and ii on Figure 7.6. These points were tested to verify that material they produce during ion exchange chromatography could be successfully purified using hydrophobic interaction chromatography to produce a second stage Window of Operation that satisfies the condition, $0 < W < 1.8$. The materials produced in the first chromatographic stage by the conditions described by these points are detailed in Table 7.3, and the resulting second stage Windows are shown in Figures 7.7 a and b.

Table 7.3 First Chromatographic Stage Conditions for Material to be Passed to Second Stage Operations for Points on Tie-Line

Stage 1 Conditions				**Composition of Material Produced from Stage 1 Operation**		
Point on Window (Fig 7.6)	**Yield (%)**	**Load Volume (mL)**	**Flow Rate (mL min^{-1})**	**Ribonuclease A (mg mL^{-1})**	**Fab (mg mL^{-1})**	**Cytochrome C (mg mL^{-1})**
i	70	9.0	1.3	0.140	0.319	0.069
ii	70	7.4	1.4	0.155	0.302	0.033

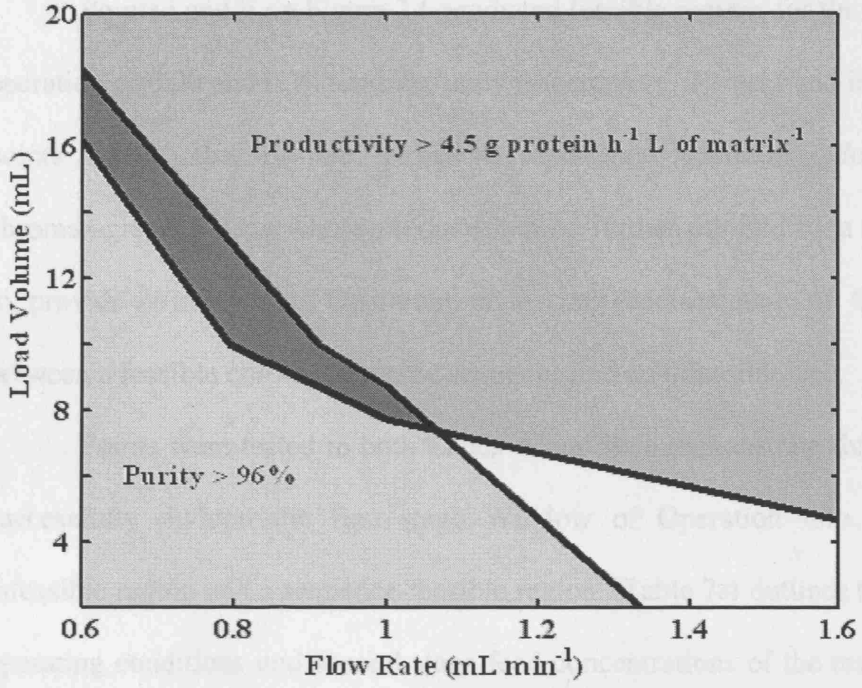

(a)

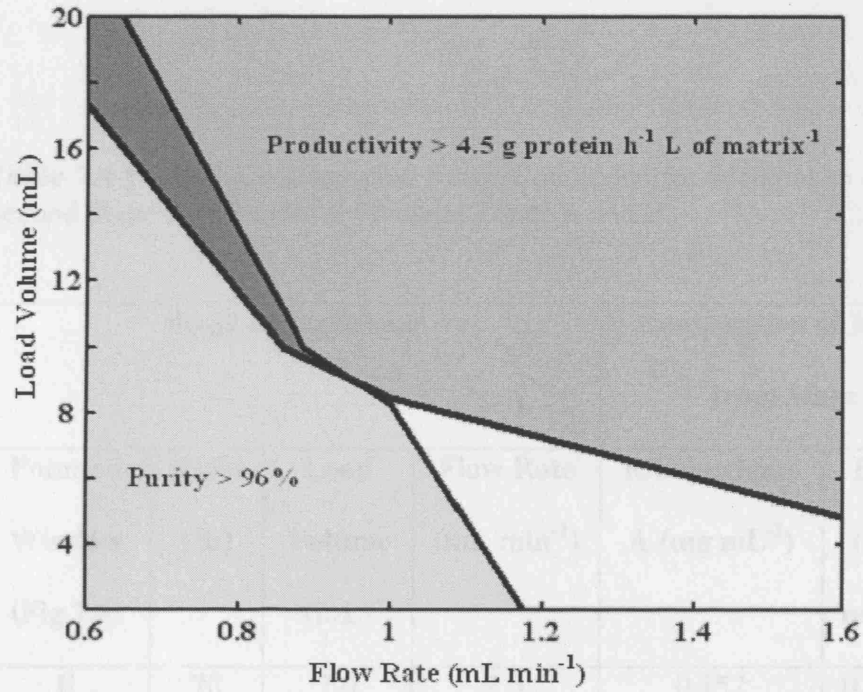

(b)

Figure 7.7 Second Stage Windows of Operation for Points on Tie-Line in Figure 7.6 (a) i, (b) ii

- Purity > 96%, Productivity < 4.5 g protein h^{-1} L of $matrix^{-1}$
- Productivity > 4.5 g protein h^{-1} L of $matrix^{-1}$, Purity < 96%
- Purity > 96% and Productivity > 4.5 g protein h^{-1} L of $matrix^{-1}$
- Purity < 96% and Productivity < 4.5 g protein h^{-1} L of $matrix^{-1}$

Points i and ii on Figure 7.6 produced feasible regions for the second stage operation of 0.90 and 0.70 arbitrary units respectively. Points i and ii confirm that points along the tie-line represent operating conditions for the first chromatographic stage whose products can be further purified by a second stage to provide Windows of Operation of a size representative of the transition between a feasible chromatographic sequence and an infeasible one.

Points were tested in both Zones A and B to demonstrate that the tie-line successfully divided the first stage Window of Operation into a sequence-infeasible region and a sequence-feasible region. Table 7.4 outlines the first stage operating conditions and second stage feed concentrations of the tested points in both zones.

Table 7.4 First Chromatographic Stage Conditions for Material to be Passed to Second Stage Operations for Points in Zones A and B

Stage 1 Conditions				**Composition of Material Produced from Stage 1 Operation**		
Point on Window (Fig 7.6)	**Yield (%)**	**Load Volume (mL)**	**Flow Rate (mL min^{-1})**	**Ribonuclease A (mg mL^{-1})**	**Fab (mg mL^{-1})**	**Cytochrome C (mg mL^{-1})**
E	70	7.0	1.5	0.152	0.281	0.044
F	70	10.0	1.0	0.323	0.367	0.023
G	70	6.5	1.2	0.211	0.252	0.079
H	70	8.0	1.2	0.189	0.332	0.050

One point, E, was tested in the infeasible region of the first stage Window of Operation. Only one point was tested due to the small size of the infeasible region, and the fact that the AKTA Prime can only run at flow rates to an accuracy of one decimal point, i.e. 1.5 mL min^{-1}, but not 1.55 mL min^{-1}. Figure 7.8 shows the resultant second stage Window for Point E. The Window has an area of 1.1 arbitrary units, placing it in the transition region represented by the tie-line. This is an acceptable result as the point is located in close proximity to the tie-line. Furthermore, since the tie-line represents a 2-dimensional region, it in reality most probably displays a degree of curvature. If the Window had an area greater than 1.8 units, then the point would not have been successful in proving the division between the sequence-feasible and sequence-infeasible regions. Figure 7.9 provides an example of how the tie-line represents such a 2-D region.

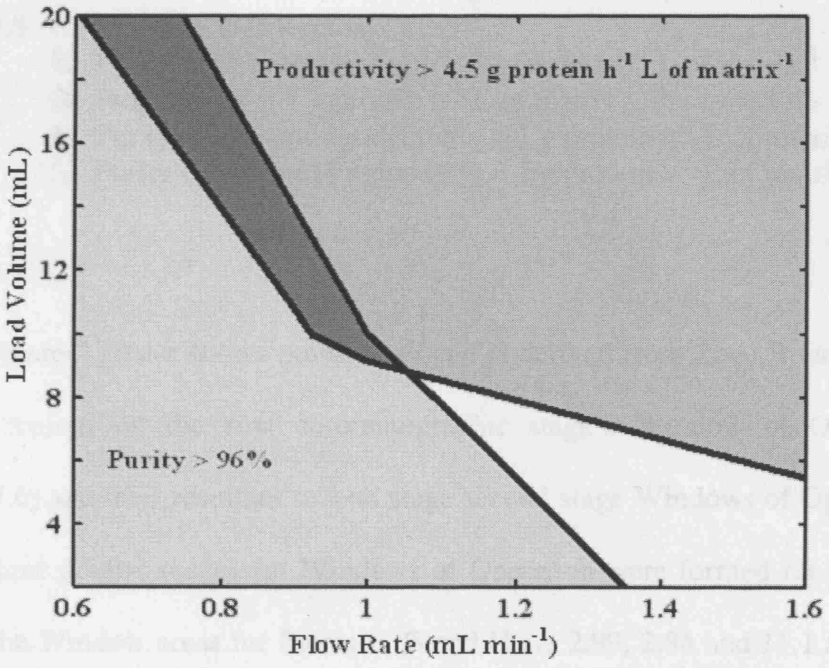

Figure 7.8 Second Stage Windows of Operation for Point E in Figure 7.6
- Purity > 96%, Productivity < 4.5 g protein h^{-1} L of $matrix^{-1}$
- Productivity > 4.5 g protein h^{-1} L of $matrix^{-1}$, Purity < 96%
- Purity > 96% and Productivity > 4.5 g protein h^{-1} L of $matrix^{-1}$
- Purity < 96% and Productivity < 4.5 g protein h^{-1} L of $matrix^{-1}$

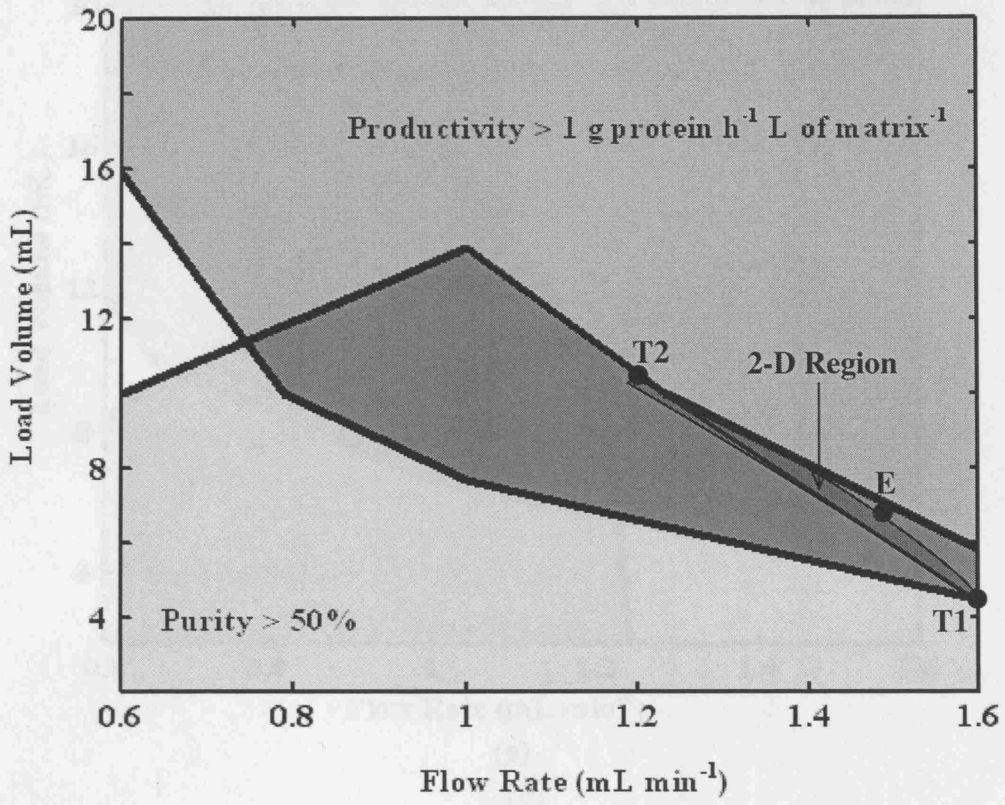

Figure 7.9 Tie-Line as a 2-D Region
- Purity > 50%, Productivity < 1 g protein h^{-1} L of $matrix^{-1}$
- Productivity > 1 g protein h^{-1} L of $matrix^{-1}$, Purity < 50%
- Purity > 50% and Productivity > 1 g protein h^{-1} L of $matrix^{-1}$
- Purity < 50% and Productivity < 1 g protein h^{-1} L of $matrix^{-1}$

Figure 7.10 a-c shows points F, G and H derived from Zone B (sequence-feasible region) on the first chromatographic stage's Window of Operation (Figure 7.6) and their resultant second stage second stage Windows of Operation. For all three points, successful Windows of Operation were formed for the HIC stage. The Window areas for Points F, G and H are 2.99, 2.84 and 11.1 arbitrary units respectively. These all comply with the third requirement of W > 1.8, thus proving the first stage's operating conditions are within the sequence-feasible zone.

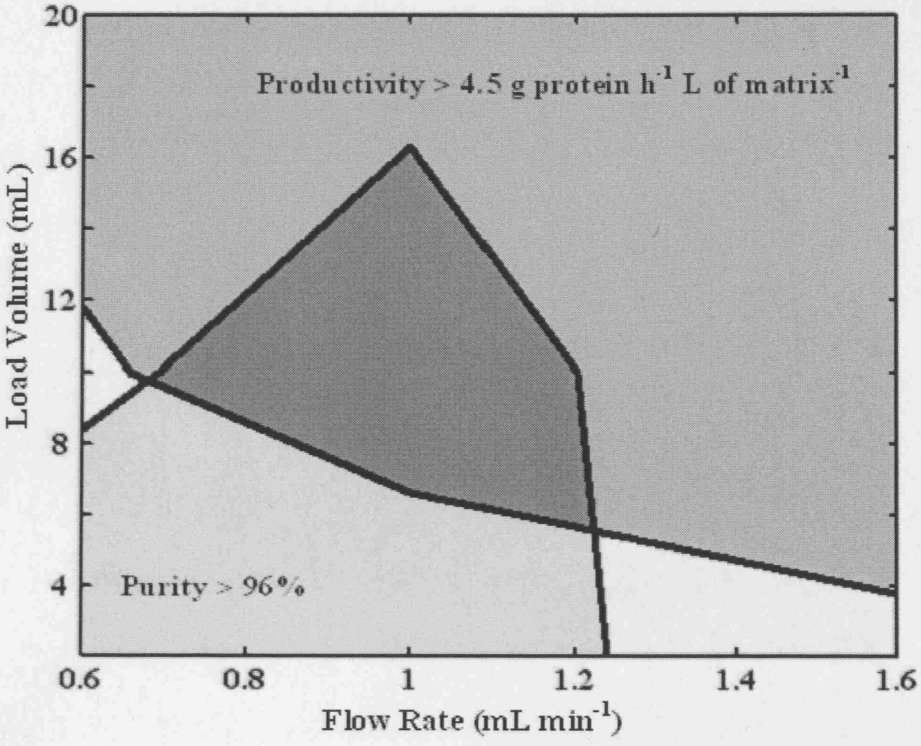
Productivity > 4.5 g protein h-1 L of matrix-1
Purity > 96%
Load Volume (mL)
Flow Rate (mL min-1)
20
16
12
8
4
0.6
0.8
1
1.2
1.4
1.6

(a)

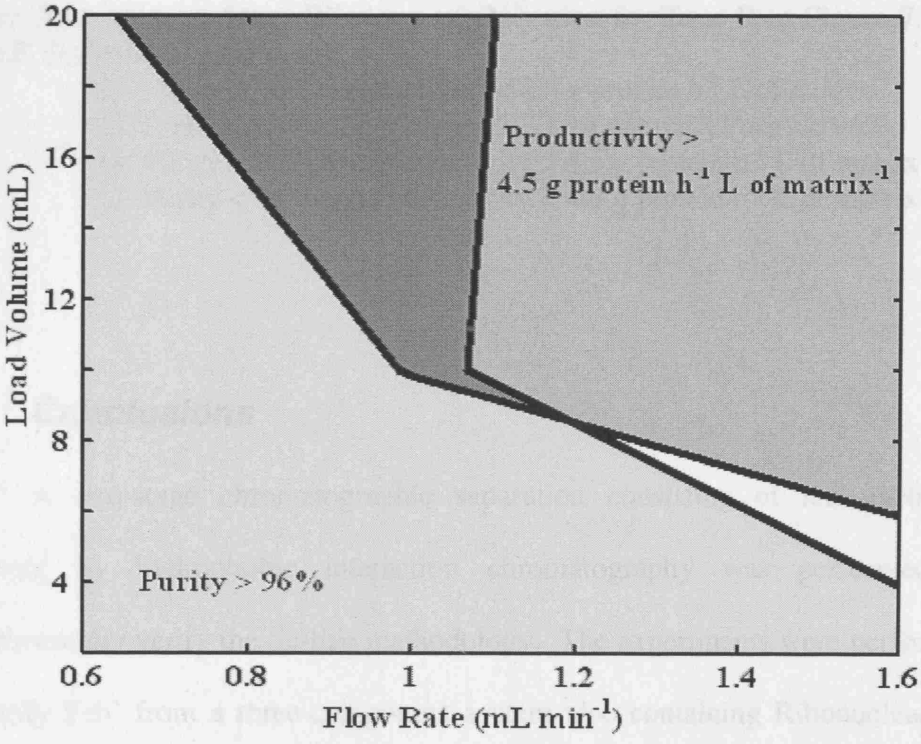
Productivity >
4.5 g protein h-1 L of matrix-1
Purity > 96%
Load Volume (mL)
Flow Rate (mL min-1)
20
16
12
8
4
0.6
0.8
1
1.2
1.4
1.6

(b)

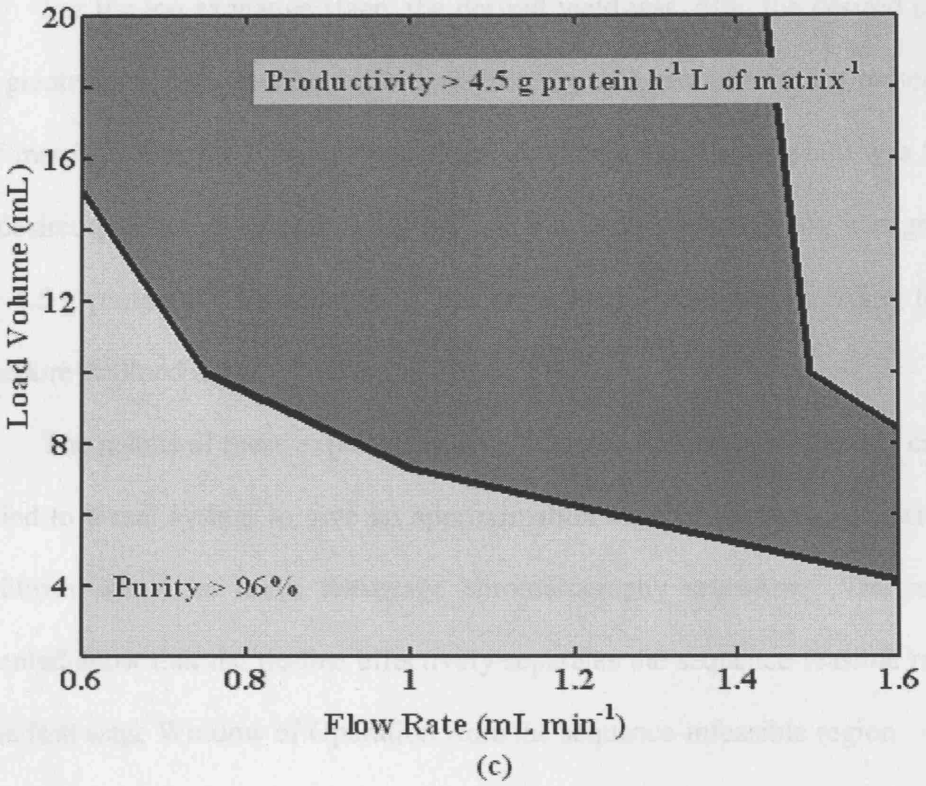

Figure 7.10 Second Stage Windows of Operation for Zone B in Figure 7.6 (a) Point F, (b) Point G, (c) Point H

- Purity > 96%, Productivity < 4.5 g protein h^{-1} L of $matrix^{-1}$
- Productivity > 4.5 g protein h^{-1} L of $matrix^{-1}$, Purity < 96%
- Purity > 96% and Productivity > 4.5 g protein h^{-1} L of $matrix^{-1}$
- Purity < 96% and Productivity < 4.5 g protein h^{-1} L of $matrix^{-1}$

7.4 Conclusions

A two-stage chromatographic separation consisting of ion exchange followed by hydrophobic interaction chromatography was performed to experimentally verify the tie-line methodology. The experiments were performed to purify Fab' from a three-component system also containing Ribonuclease A and Cytochrome C.

For the ion exchange stage, the desired yield was 70%, the desired purity was greater than 50% and the desired productivity was greater than 1 g protein h^{-1} L of $matrix^{-1}$. For the hydrophobic interaction stage the desired yield was 99%, the desired purity was greater than 96% and the desired productivity was greater than 4.5 g protein h^{-1} L of $matrix^{-1}$. The experiments were run according to the procedure outlined in the flowchart in Figure 7.2.

The results of these experiments show that the tie-line methodology can be applied to a real system to give an approximation to what the optimal operating conditions would be for a two-stage chromatography sequence. The results presented show that the tie-line effectively separates the sequence-feasible region of the first stage Window of Operation from the sequence-infeasible region.

The next chapter provides a discussion of the presented work and recommendations for future work.

8. Discussion and Recommendations for Future Work

The aims of this project were the following:

1. To use chromatography simulation to examine the operation of chromatography sequences and the impact the operation of the first chromatographic stage has on the outcome of the second purification stage.
2. To analyze the simulated data in order to develop a graphical methodology that would enable the selection of operating conditions for chromatography sequences.
3. To validate the methodology using experimental data. This also included obtaining adsorption isotherm values for the experimental protein components so that the experimental results could be compared to simulated results.

A tie-line methodology was developed that enables the fast graphical selection of operating conditions for chromatography sequences.

Both the simulated and experimental case studies confirmed that the tie-line separated the first chromatographic stage's Window of Operation into a sequence-feasible zone and a sequence-infeasible zone. It was also demonstrated that the methodology has a degree of flexibility. The methodology can be successfully applied when either load volume or breakthrough % are used to describe the amount of material loaded onto the column. The tie-line methodology is also successfully applied when both purity and productivity

contours are used to make the Window of Operation at a fixed yield, and when yield and productivity contours are used to make the Window of Operation at a fixed purity. For the experimental system under study, the linkage between the simulations and the experiments proved unsuccessful, most likely due to the limitations of the simulation programme which requires competitive Langmuir type behaviour. In reality the biological feeds are more complex and highly non-linear relationships are observed.

The number of experiments required to find the position of the tie-line is dependent upon the protein system and the size of the first chromatographic stage's Window of Operation. The system may be favourable, and it may only require five experiments to determine the position of the tie-line, i.e. test each vertex of the first stage Window, find each end of the tie-line to be the mid-point of each contour determining the boundaries of the Window, and test one point on the tie-line to verify its position. However, for a first stage Window of Operation that has a large area, more experiments may be required to find the position of the tie-line end points. Obtaining accurate adsorption isotherm data for the experimental system would greatly speed up the process of finding the tie-line for an experimental system since simulations could be used to narrow down the area on the experimental Window that should be searched for the tie-line end points.

8.1 Isotherm Recommendations

It is recommended in future, different isotherm models should be incorporated into simulation models. This would allow for the purification of a larger range of proteins to be simulated accurately. Simulations could then be

performed to generate the bulk of the data and experiments would only need to be performed to verify the simulated results in a 'spot check' manner. This would speed up the design of the process while lowering the cost of design.

8.2 Simple versus Complex Systems

Both the simulated and experimental models were performed using simple three-component mixtures. In industry, it would be rare to be purifying such a simple process stream. Thus, it would be beneficial to verify the tie-line methodology using a complex process stream such as a clarified lysate or homogenate. The complex system would however be much more difficult to simulate due to the high number of components in the process stream. The following is a proposal for future work, using the example of purifying Fab' lysate.

The first step would be to simplify the composition of the process stream in order that the simulation could be carried out. Preliminary first-stage chromatography experiments could be performed, collecting fractions at regular intervals during elution. An A280 analysis and a Protein G analysis could be done on each fraction to determine whether Fab' and other proteins were present in the sample. A Bioanalyzer assay on the fractions would also be beneficial in helping to determine how many different proteins are in each fraction, their approximate molecular weights and concentrations. The goal of all this analysis would be to try and approximate the first stage chromatogram into three peaks; one that contains materials that elute before Fab', the Fab' itself, and one that contains materials that elute after Fab' (the product and its nearest neighbours).

The next step would be to determine parameters that could be used in simulating the lysate purification. The main concern is the isotherm parameters. Material that elutes pre-Fab' could be pooled together and batch adsorption isotherm experiments could be then performed to determine isotherm parameters as if the pooled material was a single component; a pseudo component. The same could be done for Fab' and the post-Fab' elution material. Bioanalyzer results could be used to estimate average molecular weights of the pre and post-Fab' elution material. By doing this, a complex system would be simplified into a three-component system that would be much easier to simulate, hence speeding up the design of the chromatography steps.

8.3 Extension to a Three-Stage Separation

The tie-line method proposed in this thesis was based on a two-stage chromatographic separation. It would be beneficial to look into how the method could be adapted in order to select operating conditions for a three-stage chromatography sequence. In a two-stage chromatographic separation, only the first stage's feasible region was searched to find the tie-line. The three-stage separation would be more complex, as a number of second stage feasible regions would have to be searched. Because of this, it would be beneficial to create a computer programme that automatically produces Windows of Operation from chromatogram data, and also has the capability to perform feasible region searches in which second and ultimately thirds stage Windows of Operation can be produced.

8.4 The Use of More than Two Constraints to Produce Windows of Operation

In this thesis, Windows of Operation were produced using two constraints; purity and productivity. However, Windows of Operation can be produced with two or more constraints. Another proposal for future work would be to see how the tie-line method is affected by the introduction of a third constraint to the Window of Operation, e.g. cost of production. It is hypothesized that the tie-line method would function in the same way; only the size of the feasible region would decrease due to the addition of the third constraint. However, it would be beneficial to verify this.

The tie-line method is a user-friendly method of selecting operation conditions for a chromatography sequence. By the addition of the above suggestions for future work, the tie-line method would be proven to be more complete, proving capable of dealing with complex process streams and a wider range of process specifications and sequence steps.

9. References

[1] Marshall, S.A., Lazar, G.A., Chirino, A.J., Desjarlais, J.R., Rational Design and Engineering of Therapeutic Proteins. *Drug Discovery Today*, 8(5): 212-221 (2003)

[2] Harrison, R.G., Todd, P., Rudge, S.R., Petrides, D.P., Bioseparation Science and Engineering, Oxford University Press, Oxford, 2003; pp. 191-242

[3] Deyl, Z., Macek, K., Janak, J., Liquid Column Chromatography: A Survey of Modern Techniques and Applications, Elsevier Scientific Publishing Company, Oxford, 1975, p. 1-6, 31-37

[4] Wheelwright, S.M., Protein Purification and Scale Up of Downstream Processing, John Wiley and Sons Inc., New York, 1991; pp. 127-150, 205-212

[5] Lyndersen, B.K., D'Elia, N.A., Nelson, K.L., Bioprocess Engineering: Systems, Equipment and Facilities, John Wiley and Sons Inc., New York, 1994, p.159-186

[6] Ngiam, S.H., Graphical Frameworks for Facilitating the Study of Chromatographic Separations, University College of London Thesis, May 2002

[7] Simpson, J.M., Harakas, N.K., edited by Harrison, R.G., Protein Purification Process Engineering, Marcel Dekker Inc., New York, 1994, p.209-317

[8] *http://www. Biotech.vt.edu/classes/bion_4784/9-Protein Purification*, Protein Purification, October 13, 2003

[9] Guerrier, L., Flayeux, I., Boschetti, E., A dual-mode approach to the selective separation of antibodies and their fragments. *Journal of Chromatography B*, 755: 37-46 (2001)

[10] Amersham Pharmacia Biotech, Affinity Chromatography – Principles and Methods, Sweden 2001

[11] Lightfoot, E.N., The invention and development of process chromatography: Interaction of mass transfer and fluid mechanics. *American Laboratory*, June 1999, pp. 13-23

[12] Lopez, K.Z., Tejeda, A., Montesinos, R.M., Magana, I., Guzman, R., Modeling column regeneration effects on ion-exchange chromatography. *Journal of Chromatography A*, 791: 99-107 (1997)

[13] Natarajan, V., Bequette, B.W., Cramer, S.M., Optimization of ion-exchange displacement separations I. Validation of an iterative scheme and its use as a methods development tool. *Journal of Chromatography A,* 876: 51-62 (2000)

[14] Amersham Parmacia Biotech, Protein Purification – Handbook, Sweden 2001

[15] Amersham Biosciences, HiTrap – Convenient Protein Purification, 2002

[16] Pharmacia Bioprocess Technology, Hydrophobic Interaction Chromatography – Principles and Methods, Sweden 1993

[17] Amersham Biosciences, Gel Filtration – Principles and Methods, Sweden 2002

[18] Garcia, A.A., Bonen, M.R., Ramirez-Vick, J., Sadaka, M., Vuppu, A., Bioseparation Process Science, Blackwell Science Inc., London, 1999, p. 11-13, 178-229, 358

[19] Cramer, S.M., Brooks, C.A., Frenz, J., edited by Horvath, C., Ettre, L.S., Chromatography in Biotechnology, American Chemical Society, Washington, 1993, p. 1-12, 27-42

[20] Gu, T., Tsai, G.-J., Tsao, G.T., Modeling of Nonlinear Multicomponent Chromatography. *Advances in Biochemical Engineering Biotechnology*, 49: 45-71 (1993)

[21] Lode, F.G., Rosenfeld, A., Yuan, Q.S., Root, T.W., Lightfoot, E.N., Refining the scale-up of chromatographic separations. *Journal of Chromatography A*, 796: 3-14 (1998)

[22] Kučera, E., Contribution to the theory of chromatography: Linear non-equilibrium elution chromatography. *Journal of Chromatography*, 19: 237-247 (1965)

[23] Hearle, D.C., An Investigation into Process Related Fouling of Chromatographic Supports, University College of London Thesis, March 1997

[24] Gu, T., Tsai, G.J., Tsao, G.T., New approach to a general nonlinear multicomponent chromatographic model. *AICHE Journal*, 36 (5): 784-788 (1990)

[25] Klatt, K-U., Hanisch, F., Dunnebier, G., Engell, S., Model-based optimization and control of chromatographic processes. *Computers and Chemical Engineering* 24:1119-1126 (2000)

[26] Doran, P.M., Bioprocess Engineering Principles, Academic Press Limited, London, 1995, pp. 235-237

[27] Zola, H., Monoclonal Antibodies: The Second Generation, Information Press Ltd., Oxford, 1995, pp. 70-85, 122

[28] Ngiam, S.H., Zhou, Y.H., Turner, M.K., Titchener-Hooker, N.J., Graphical method for the calculation of chromatographic performance in representing the trade-off between purity and recovery. *Journal of Chromatography A*, 937: 1-11 (2001)

[29] Dooley, H., Grant, S.D., Harris, W.J., Porter, A.J., Stabilization of Antibody Fragments in Adverse Environment. *Biotechnology and Applied Biochemistry,* 28: 77-83 (1998)

[30] Reff, M.E., Heard, C., A Review of Modifications to Recombinant Antibodies: Attempt to Increase Efficacy in Oncology Applications. *Critical Reviews in Oncology/Hematology,* 40: 25-35 (2001)

[31] Chapman, A.P., Antoniw, P., Spitali, M., West, S., Stephens, S., King, D.J., Therapeutic antibody fragments with prolonged in vivo half-lives. *Nature Biotechnology*, 17: 780-783 (1999)

[32] Groep ME, Gregory ME, Kershenbaum LS and Bogle IDL, Modeling and simulation of biochemical process sequences with interacting unit operations. *Biotechnol. Bioeng.* 67:300-311 (2000)

[33] Mao QM and Hearn MTW, Optimization of affinity and ion-exchange chromatographic processes for the purification of proteins. *Biotechnol. Bioeng.* 52:204-222 (1996)

[34] Felinger A and Guiochon G, Comparing the optimum performance of the different modes of preparative liquid chromatography. *J. Chromatogr. A* 796:59-74 (1998)

[35] Woodley JM and Titchener-Hooker NJ, The use of windows of operation as a bioprocess design tool. *Bioprocess and Biosystems Eng.* 14:263-268 (1996)

[36] Zhou YH, Holwill ILJ and Titchener-Hooker NJ, A study of the use of computer simulations for the design of integrated downstream processes. *Bioprocess Eng.* 16:367-374 (1997)

[37] Sofer G and Hagel L, Handbook of Process Chromatography: A Guide to Optimization, Scale-Up and Validation. Academic Press Ltd., London (1997)

[38] Ngiam S-H, Bracewell DG, Zhou Y and Titchener-Hooker NJ, Quantifying process tradeoffs in the operation of chromatographic sequences. *Biotechnol. Prog.* 19:1315-1322 (2003)

[39] Mao Q-M, Prince IG and Hearn MTW, High-performance liquid chromatography of amino acids, peptides and proteins CXXXIX. Impact of operating parameters in large-scale chromatography of proteins. *J. Chromatogr. A* 691:273-283 (1995)

[40] Wiblin DJ, Roe SD and Myhill RG, Computer aided desk-top scale-up and optimization of chromatographic processes. *J. Chromatogr. A* 702:81-87 (1995)

[41] Li Z, Gu Y and Gu T, Mathematical modeling and scale-up of size-exclusion chromatography. *Biochemical Engineering Journal* 2:145-155 (1998)

[42] Kempe H, Axelsson A, Nilsson B and Zacchi G, Simulation of chromatographic processes applied to separation of proteins. *J. Chromatogr. A* 846:1-12 (1999)

[43] Hoang TH, Cuerrier D, McClintock S and DiMaso M, Computer-assisted method development and optimization in high-performance liquid chromatography. *J. Chromatogr. A* 991:281-287 (2003)

[44] Karlsson D, Jakobsson N, Brink KJ, Axelsson A and Nilsson B, Methodologies for model calibration to assist the design of a preparative ion-exchange step for antibody purification. *J. Chromatogr. A* 1033:71-82 (2004)

[45] Jakobsson N, Karlsson D, Axelsson JP, Zacchi G and Nilsson B, Using computer simulation to assist in the robustness analysis of an ion-exchange chromatography step. *J. Chromatogr. A* 1063:99-109 (2005)

[46] Guiochon G, Preparative liquid chromatography. *J. Chromatogr. A* 965:129-161 (2002)

[47] Chromulator, Version 2.0, Gu T, Department of Chemical Engineering, Ohio University, Athens, Ohio, USA (2000)

[48] Richardson P, Hoare M and Dunhill P, A new biochemical engineering approach to the fractional precipitation of proteins. *Biotechnol. Bioeng.* 36:354-366 (1990)

[49] Matlab, Version 6, Release 13, The Mathworks Inc., Natick, MA, USA (2003)

[50] Gu T, Hsu K-H, Syu M-J, Scale-up of affinity chromatography for purification of enzymes and other proteins. *Enzyme and Microbial Technology* 33:430-437 (2003)

[51] Gu T, Zheng Y, A study of scale-up of reversed-phase liquid chromatography. *Separation and Purification Technology* 15:41-58 (1999)

[52] *http://www.assaydesigns.com/products/catalog/immuno_assay/product_protein_G.htm*, August 20, 2006.

[53] *http://www4.amershambiosciences.com*, August 20, 2006

[54] Bailey, J.E., Ollis, D.F., Biochemical Engineering Fundamentals, McGraw Hill, New York, 1986, pp.753-764

[55] Ljunglof, A., Lacki, K.M., Mueller, J., Harinarayan, C., van Reis, R., Fahrner, R., Van Alstine, J.M., Ion exchange chromatography of antibody fragments. *Biotechnology Bioengineering,* 96: 515-524 (2007)

[56] Jozwik, M., Kaczmarski, K., Freitag, R., Evaluation of the Langmuir formalism for modelling the adsorption isotherms of proteins and polyelectrolytes in simulations of ion exchange chromatography. *Chemical Engineering Technology* 28: 1346-1359 (2005)

[57] Perry, R.H., Green, D.W., Perry's Chemical Engineers' Handbook, McGraw Hill, New York, 1999, pp.16-13

[58] GE Healthcare, Hydrophobic Interaction and Reversed Phase Chromatography Principles and Methods, Handbook # 11-0012-69 AA, p.65

[59] Woodley, J, Titchener-Hooker, N, The use of windows of operation as a bioprocess design tool. *Bioprocess Engineering* 14: 263-268 (1996)

[60] Saite, H, King, J, Baganz, F, Hoare, M, Titchener-Hooker, N, A methodology for centrifuge selection for the separation of high solids density cell broths by visualisation of performance using windows of operation. *Biotechnology and Bioengineering* 95 (6): 1218-1227 (2006)

[61] Collins, A, Woodley, J, Liddell, J, Determination of reactor operation for the microbial hydroxylation of toluene in a 2-phase process. *Journal of Industrial Microbiology* 14 (5): 382-388 (1995)

Appendix A - Data for Breakthrough Curve

This section provides the raw data for the breakthrough curve for a chromatography simulation performed with a linear velocity of 150 cm h^{-1} from Section 3.3.

	Dimensionless Concentration					Concentration (g/L)			Area Under Peak Segment			
Dimensionless Time	Impurity 1	Product	Impurity 2	Time (s)	Volume (mL)	Impurity 1	Product	Impurity 2	Impurity 1 Curve	Product Curve	Impurity 2 Curve	Product Breakthrough
0.10	0.00E+00	0.00E+00	0.00E+00	1.92E+01	6.28E+01	0.00E+00	0.00E+00	0.00E+00	0.00E+00	0.00E+00	0.00E+00	0.00E+00
1.30	1.63E-01	1.00E-05	0.00E+00	2.50E+02	8.17E+02	1.22E+00	4.00E-05	0.00E+00	3.21E+01	6.28E-04	0.00E+00	7.18E-08
1.35	2.20E-01	3.00E-05	0.00E+00	2.60E+02	8.48E+02	1.65E+00	1.20E-04	0.00E+00	4.51E+01	2.51E-03	0.00E+00	3.59E-07
1.40	2.80E-01	6.00E-05	0.00E+00	2.69E+02	8.80E+02	2.10E+00	2.40E-04	0.00E+00	5.89E+01	5.65E-03	0.00E+00	1.00E-06
1.45	3.39E-01	1.30E-04	0.00E+00	2.79E+02	9.11E+02	2.54E+00	5.20E-04	0.00E+00	7.28E+01	1.19E-02	0.00E+00	2.37E-06
1.50	3.96E-01	2.70E-04	0.00E+00	2.89E+02	9.42E+02	2.97E+00	1.08E-03	0.00E+00	8.66E+01	2.51E-02	0.00E+00	5.24E-06
1.55	4.52E-01	5.10E-04	0.00E+00	2.98E+02	9.74E+02	3.39E+00	2.04E-03	0.00E+00	9.99E+01	4.90E-02	0.00E+00	1.08E-05
1.60	5.04E-01	9.10E-04	0.00E+00	3.08E+02	1.01E+03	3.78E+00	3.64E-03	0.00E+00	1.13E+02	8.92E-02	0.00E+00	2.10E-05
1.65	5.54E-01	1.52E-03	0.00E+00	3.17E+02	1.04E+03	4.15E+00	6.08E-03	0.00E+00	1.25E+02	1.53E-01	0.00E+00	3.85E-05
1.70	6.00E-01	2.39E-03	0.00E+00	3.27E+02	1.07E+03	4.50E+00	9.56E-03	0.00E+00	1.36E+02	2.46E-01	0.00E+00	6.65E-05
1.75	6.43E-01	3.60E-03	0.00E+00	3.37E+02	1.10E+03	4.82E+00	1.44E-02	0.00E+00	1.46E+02	3.76E-01	0.00E+00	1.09E-04
1.80	6.82E-01	5.19E-03	0.00E+00	3.46E+02	1.13E+03	5.11E+00	2.08E-02	0.00E+00	1.56E+02	5.52E-01	0.00E+00	1.73E-04
1.85	7.18E-01	7.23E-03	0.00E+00	3.56E+02	1.16E+03	5.38E+00	2.89E-02	0.00E+00	1.65E+02	7.80E-01	0.00E+00	2.62E-04
1.90	7.50E-01	9.77E-03	0.00E+00	3.65E+02	1.19E+03	5.63E+00	3.91E-02	0.00E+00	1.73E+02	1.07E+00	0.00E+00	3.84E-04
1.95	7.80E-01	1.29E-02	0.00E+00	3.75E+02	1.23E+03	5.85E+00	5.14E-02	0.00E+00	1.80E+02	1.42E+00	0.00E+00	5.46E-04
2.00	8.06E-01	1.65E-02	0.00E+00	3.85E+02	1.26E+03	6.05E+00	6.60E-02	0.00E+00	1.87E+02	1.84E+00	0.00E+00	7.57E-04
2.05	8.30E-01	2.08E-02	0.00E+00	3.94E+02	1.29E+03	6.23E+00	8.31E-02	0.00E+00	1.93E+02	2.34E+00	0.00E+00	1.02E-03
2.10	8.51E-01	2.57E-02	0.00E+00	4.04E+02	1.32E+03	6.38E+00	1.03E-01	0.00E+00	1.98E+02	2.92E+00	0.00E+00	1.36E-03
2.15	8.70E-01	3.13E-02	0.00E+00	4.14E+02	1.35E+03	6.52E+00	1.25E-01	0.00E+00	2.03E+02	3.58E+00	0.00E+00	1.77E-03
2.20	8.87E-01	3.75E-02	0.00E+00	4.23E+02	1.38E+03	6.65E+00	1.50E-01	0.00E+00	2.07E+02	4.32E+00	0.00E+00	2.26E-03
2.25	9.02E-01	4.44E-02	0.00E+00	4.33E+02	1.41E+03	6.76E+00	1.78E-01	0.00E+00	2.11E+02	5.14E+00	0.00E+00	2.85E-03
2.30	9.15E-01	5.20E-02	0.00E+00	4.42E+02	1.45E+03	6.86E+00	2.08E-01	0.00E+00	2.14E+02	6.05E+00	0.00E+00	3.54E-03
2.35	9.26E-01	6.02E-02	0.00E+00	4.52E+02	1.48E+03	6.95E+00	2.41E-01	0.00E+00	2.17E+02	7.05E+00	0.00E+00	4.34E-03
2.40	9.36E-01	6.91E-02	0.00E+00	4.62E+02	1.51E+03	7.02E+00	2.76E-01	0.00E+00	2.19E+02	8.12E+00	0.00E+00	5.27E-03
2.45	9.45E-01	7.86E-02	0.00E+00	4.71E+02	1.54E+03	7.09E+00	3.15E-01	0.00E+00	2.22E+02	9.28E+00	0.00E+00	6.33E-03
2.50	9.53E-01	8.88E-02	0.00E+00	4.81E+02	1.57E+03	7.14E+00	3.55E-01	0.00E+00	2.24E+02	1.05E+01	0.00E+00	7.53E-03

	Dimensionless Concentration					Concentration (g/L)			Area Under Peak Segment			
Dimensionless Time	Impurity 1	Product	Impurity 2	Time (s)	Volume (mL)	Impurity 1	Product	Impurity 2	Impurity 1 Curve	Product Curve	Impurity 2 Curve	Product Breakthrough
2.55	9.59E-01	9.96E-02	0.00E+00	4.90E+02	1.60E+03	7.20E+00	3.98E-01	0.00E+00	2.25E+02	1.18E+01	0.00E+00	8.88E-03
2.60	9.65E-01	1.11E-01	0.00E+00	5.00E+02	1.63E+03	7.24E+00	4.44E-01	0.00E+00	2.27E+02	1.32E+01	0.00E+00	1.04E-02
2.65	9.69E-01	1.23E-01	0.00E+00	5.10E+02	1.67E+03	7.27E+00	4.91E-01	0.00E+00	2.28E+02	1.47E+01	0.00E+00	1.21E-02
2.70	9.74E-01	1.35E-01	0.00E+00	5.19E+02	1.70E+03	7.31E+00	5.41E-01	0.00E+00	2.29E+02	1.62E+01	0.00E+00	1.39E-02
2.75	9.78E-01	1.48E-01	0.00E+00	5.29E+02	1.73E+03	7.34E+00	5.93E-01	0.00E+00	2.30E+02	1.78E+01	0.00E+00	1.60E-02
2.80	9.82E-01	1.62E-01	0.00E+00	5.39E+02	1.76E+03	7.36E+00	6.47E-01	0.00E+00	2.31E+02	1.95E+01	0.00E+00	1.82E-02
2.85	9.84E-01	1.76E-01	0.00E+00	5.48E+02	1.79E+03	7.38E+00	7.02E-01	0.00E+00	2.32E+02	2.12E+01	0.00E+00	2.06E-02
2.90	9.85E-01	1.90E-01	0.00E+00	5.58E+02	1.82E+03	7.39E+00	7.59E-01	0.00E+00	2.32E+02	2.30E+01	0.00E+00	2.32E-02
2.95	9.88E-01	2.04E-01	0.00E+00	5.67E+02	1.85E+03	7.41E+00	8.18E-01	0.00E+00	2.33E+02	2.48E+01	0.00E+00	2.61E-02
3.00	9.91E-01	2.19E-01	0.00E+00	5.77E+02	1.88E+03	7.43E+00	8.77E-01	0.00E+00	2.33E+02	2.66E+01	0.00E+00	2.91E-02
3.05	9.92E-01	2.35E-01	0.00E+00	5.87E+02	1.92E+03	7.44E+00	9.39E-01	0.00E+00	2.34E+02	2.85E+01	0.00E+00	3.23E-02
3.10	9.92E-01	2.50E-01	0.00E+00	5.96E+02	1.95E+03	7.44E+00	1.00E+00	0.00E+00	2.34E+02	3.05E+01	0.00E+00	3.58E-02
3.15	9.94E-01	2.66E-01	1.00E-05	6.06E+02	1.98E+03	7.46E+00	1.06E+00	7.50E-06	2.34E+02	3.24E+01	1.18E-04	3.95E-02
3.20	9.97E-01	2.82E-01	1.00E-05	6.16E+02	2.01E+03	7.47E+00	1.13E+00	7.50E-06	2.35E+02	3.44E+01	2.36E-04	4.35E-02
3.25	9.95E-01	2.98E-01	1.00E-05	6.25E+02	2.04E+03	7.46E+00	1.19E+00	7.50E-06	2.35E+02	3.64E+01	2.36E-04	4.76E-02
3.30	9.96E-01	3.14E-01	1.00E-05	6.35E+02	2.07E+03	7.47E+00	1.26E+00	7.50E-06	2.34E+02	3.85E+01	2.36E-04	5.2019E-02
3.35	9.99E-01	3.31E-01	2.00E-05	6.44E+02	2.10E+03	7.50E+00	1.32E+00	1.50E-05	2.35E+02	4.05E+01	3.53E-04	5.66E-02
3.40	9.96E-01	3.47E-01	2.00E-05	6.54E+02	2.14E+03	7.47E+00	1.39E+00	1.50E-05	2.35E+02	4.26E+01	4.71E-04	6.15E-02
3.45	9.97E-01	3.64E-01	2.00E-05	6.64E+02	2.17E+03	7.48E+00	1.45E+00	1.50E-05	2.35E+02	4.47E+01	4.71E-04	6.66E-02
3.50	1.00E+00	3.80E-01	3.00E-05	6.73E+02	2.20E+03	7.50E+00	1.52E+00	2.25E-05	2.35E+02	4.67E+01	5.89E-04	7.20E-02
3.55	9.97E-01	3.97E-01	4.00E-05	6.83E+02	2.23E+03	7.47E+00	1.59E+00	3.00E-05	2.35E+02	4.88E+01	8.25E-04	7.75E-02
3.60	1.00E+00	4.13E-01	5.00E-05	6.92E+02	2.26E+03	7.50E+00	1.65E+00	3.75E-05	2.35E+02	5.09E+01	1.06E-03	8.33E-02
3.65	9.99E-01	4.30E-01	6.00E-05	7.02E+02	2.29E+03	7.49E+00	1.72E+00	4.50E-05	2.36E+02	5.30E+01	1.30E-03	8.94E-02
3.70	9.98E-01	4.46E-01	7.00E-05	7.12E+02	2.32E+03	7.49E+00	1.78E+00	5.25E-05	2.35E+02	5.50E+01	1.53E-03	9.57E-02
3.75	1.00E+00	4.62E-01	8.00E-05	7.21E+02	2.36E+03	7.51E+00	1.85E+00	6.00E-05	2.36E+02	5.71E+01	1.77E-03	1.02E-01

Appendix B – Data for Chromulator Simulation of First Chromatographic Stage

This section provides the raw data determined by the Chromulator Simulation for a first stage chromatography step operated at a Linear Velocity of 150 cm h^{-1} and a loading breakthrough of 5% as described in Section 3.3.

	Dimensionless Concentration						Concentration (g/L)			Area Under Peak Segment			Fractionation	
Dimensionless Time	Impurity 1	Product	Impurity 2	Displacer	Time (s)	Volume (mL)	Impurity 1	Product	Impurity 2	Impurity 1 Curve	Product Curve	Impurity 2 Curve	X	Y
0.05	0.00E+00	0.00E+00	0.00E+00	0.00E+00	9.62E+00	3.14E+01	0.00E+00	0.00E+00	0.00E+00					
0.10	0.00E+00	0.00E+00	0.00E+00	0.00E+00	1.92E+01	6.28E+01	0.00E+00	0.00E+00	0.00E+00	0.00E+00	0.00E+00	0.00E+00	0.00E+00	0.00E+00
1.30	1.65E-01	1.00E-05	0.00E+00	0.00E+00	2.50E+02	8.17E+02	1.24E+00	4.00E-05	0.00E+00	3.25E+01	6.28E-04	0.00E+00	2.85E-03	7.69E-08
1.35	2.23E-01	3.00E-05	0.00E+00	0.00E+00	2.60E+02	8.48E+02	1.67E+00	1.20E-04	0.00E+00	4.56E+01	2.51E-03	0.00E+00	4.68E-03	3.85E-07
1.50	3.98E-01	2.90E-04	0.00E+00	0.00E+00	2.89E+02	9.42E+02	2.99E+00	1.16E-03	0.00E+00	8.70E+01	2.70E-02	0.00E+00	1.35E-02	5.92E-06
1.65	5.55E-01	1.60E-03	0.00E+00	0.00E+00	3.17E+02	1.04E+03	4.16E+00	6.40E-03	0.00E+00	1.25E+02	1.61E-01	0.00E+00	2.70E-02	4.37E-05
1.90	7.50E-01	1.01E-02	0.00E+00	0.00E+00	3.65E+02	1.19E+03	5.62E+00	4.05E-02	0.00E+00	1.73E+02	1.11E+00	0.00E+00	5.81E-02	4.29E-04
2.35	9.25E-01	6.14E-02	0.00E+00	0.00E+00	4.52E+02	1.48E+03	6.94E+00	2.45E-01	0.00E+00	2.17E+02	7.19E+00	0.00E+00	1.32E-01	4.78E-03
2.55	9.58E-01	1.01E-01	0.00E+00	0.00E+00	4.90E+02	1.60E+03	7.19E+00	4.04E-01	0.00E+00	2.25E+02	1.20E+01	0.00E+00	1.69E-01	9.73E-03
2.95	9.89E-01	2.06E-01	0.00E+00	0.00E+00	5.67E+02	1.85E+03	7.42E+00	8.25E-01	0.00E+00	2.33E+02	2.50E+01	0.00E+00	2.49E-01	2.83E-02
3.00	9.89E-01	2.21E-01	0.00E+00	0.00E+00	5.77E+02	1.88E+03	7.42E+00	8.84E-01	0.00E+00	2.33E+02	2.68E+01	0.00E+00	2.59E-01	3.16E-02
3.05	9.90E-01	2.36E-01	0.00E+00	0.00E+00	5.87E+02	1.92E+03	7.43E+00	9.45E-01	0.00E+00	2.33E+02	2.87E+01	0.00E+00	2.69E-01	3.51E-02
3.10	9.95E-01	2.52E-01	0.00E+00	0.00E+00	5.96E+02	1.95E+03	7.46E+00	1.01E+00	0.00E+00	2.34E+02	3.07E+01	0.00E+00	2.80E-01	3.89E-02
3.15	9.94E-01	2.68E-01	1.00E-05	0.00E+00	6.06E+02	1.98E+03	7.45E+00	1.07E+00	7.50E-06	2.34E+02	3.26E+01	1.18E-04	2.91E-01	4.29E-02
3.20	9.93E-01	2.84E-01	1.00E-05	0.00E+00	6.16E+02	2.01E+03	7.45E+00	1.13E+00	7.50E-06	2.34E+02	3.46E+01	2.36E-04	3.01E-01	4.71E-02
3.25	9.97E-01	3.00E-01	1.00E-05	0.00E+00	6.25E+02	2.04E+03	7.48E+00	1.20E+00	7.50E-06	2.34E+02	3.66E+01	2.36E-04	3.12E-01	5.16E-02
3.30	9.96E-01	3.16E-01	1.00E-05	0.00E+00	6.35E+02	2.07E+03	7.47E+00	1.26E+00	7.50E-06	2.35E+02	3.87E+01	2.36E-04	3.23E-01	5.63E-02
3.35	9.96E-01	3.32E-01	2.00E-05	0.00E+00	6.44E+02	2.10E+03	7.47E+00	1.33E+00	1.50E-05	2.35E+02	4.07E+01	3.53E-04	3.34E-01	6.13E-02
3.40	9.98E-01	3.49E-01	2.00E-05	0.00E+00	6.54E+02	2.14E+03	7.48E+00	1.39E+00	1.50E-05	2.35E+02	4.28E+01	4.71E-04	3.45E-01	6.66E-02
3.55	9.99E-01	3.98E-01	4.00E-05	0.00E+00	6.83E+02	2.23E+03	7.49E+00	1.59E+00	3.00E-05	2.35E+02	4.90E+01	8.25E-04	3.79E-01	8.38E-02
3.60	9.99E-01	4.14E-01	5.00E-05	0.00E+00	6.92E+02	2.26E+03	7.49E+00	1.66E+00	3.75E-05	2.35E+02	5.10E+01	1.06E-03	3.91E-01	9.00E-02
3.65	9.99E-01	4.31E-01	6.00E-05	0.00E+00	7.02E+02	2.29E+03	7.49E+00	1.72E+00	4.50E-05	2.35E+02	5.31E+01	1.30E-03	4.02E-01	9.65E-02
3.80	9.99E-01	4.79E-01	1.00E-04	0.00E+00	7.31E+02	2.39E+03	7.50E+00	1.92E+00	7.50E-05	2.35E+02	5.92E+01	2.12E-03	4.37E-01	1.18E-01
4.00	1.00E+00	5.42E-01	2.00E-04	0.00E+00	7.69E+02	2.51E+03	7.50E+00	2.17E+00	1.50E-04	2.36E+02	6.71E+01	4.36E-03	4.85E-01	1.49E-01
4.05	1.00E+00	5.57E-01	2.40E-04	0.00E+00	7.79E+02	2.54E+03	7.50E+00	2.23E+00	1.80E-04	2.36E+02	6.90E+01	5.18E-03	4.97E-01	1.57E-01
4.10	1.00E+00	5.72E-01	2.80E-04	0.00E+00	7.89E+02	2.58E+03	7.50E+00	2.29E+00	2.10E-04	2.36E+02	7.09E+01	6.13E-03	5.10E-01	1.66E-01
4.15	1.00E+00	5.86E-01	3.20E-04	0.00E+00	7.98E+02	2.61E+03	7.50E+00	2.34E+00	2.40E-04	2.36E+02	7.27E+01	7.07E-03	5.22E-01	1.75E-01
4.30	9.98E-01	6.29E-01	5.00E-04	4.00E-05	8.27E+02	2.70E+03	7.49E+00	2.52E+00	3.75E-04	2.35E+02	7.81E+01	1.10E-02	5.59E-01	2.03E-01
4.35	9.90E-01	6.42E-01	5.70E-04	3.00E-05	8.37E+02	2.73E+03	7.42E+00	2.57E+00	4.28E-04	2.34E+02	7.98E+01	1.26E-02	5.72E-01	2.13E-01
4.45	9.35E-01	6.71E-01	7.30E-04	7.00E-05	8.56E+02	2.80E+03	7.01E+00	2.69E+00	5.48E-04	2.24E+02	8.33E+01	1.61E-02	5.97E-01	2.33E-01
4.55	8.37E-01	7.11E-01	1.02E-03	1.50E-03	8.75E+02	2.86E+03	6.28E+00	2.84E+00	7.65E-04	2.03E+02	8.83E+01	2.26E-02	6.20E-01	2.54E-01
4.65	7.23E-01	8.35E-01	1.72E-03	3.18E-03	8.94E+02	2.92E+03	5.42E+00	3.34E+00	1.29E-03	1.77E+02	9.80E+01	3.11E-02	6.42E-01	2.77E-01

	Dimensionless Concentration						Concentration (g/L)			Area Under Peak Segment			Fractionation	
Dimensionless Time	Impurity 1	Product	Impurity 2	Displacer	Time (s)	Volume (mL)	Impurity 1	Product	Impurity 2	Impurity 1 Curve	Product Curve	Impurity 2 Curve	X	Y
4.70	6.65E-01	1.28E+00	3.22E-03	1.48E-02	9.04E+02	2.95E+03	4.99E+00	5.14E+00	2.42E-03	1.63E+02	1.33E+02	5.82E-02	6.54E-01	2.94E-01
4.75	6.07E-01	2.17E+00	2.56E-03	5.35E-02	9.14E+02	2.98E+03	4.56E+00	8.70E+00	1.92E-03	1.50E+02	2.17E+02	6.81E-02	6.69E-01	3.20E-01
4.80	5.52E-01	3.16E+00	9.03E-03	1.36E-01	9.23E+02	3.02E+03	4.14E+00	1.26E+01	6.77E-03	1.37E+02	3.35E+02	1.37E-01	6.88E-01	3.61E-01
4.85	4.98E-01	3.78E+00	5.81E-02	2.67E-01	9.33E+02	3.05E+03	3.74E+00	1.51E+01	4.36E-02	1.24E+02	4.36E+02	7.91E-01	7.10E-01	4.15E-01
4.90	4.48E-01	3.95E+00	1.86E-01	4.32E-01	9.42E+02	3.08E+03	3.36E+00	1.58E+01	1.39E-01	1.11E+02	4.86E+02	2.87E+00	7.34E-01	4.74E-01
4.95	4.01E-01	3.84E+00	3.91E-01	6.02E-01	9.52E+02	3.11E+03	3.01E+00	1.53E+01	2.94E-01	1.00E+02	4.89E+02	6.80E+00	7.58E-01	5.34E-01
5.00	3.58E-01	3.57E+00	6.44E-01	7.50E-01	9.62E+02	3.14E+03	2.68E+00	1.43E+01	4.83E-01	8.93E+01	4.65E+02	1.22E+01	7.81E-01	5.91E-01
5.05	3.18E-01	3.25E+00	9.06E-01	8.59E-01	9.71E+02	3.17E+03	2.38E+00	1.30E+01	6.80E-01	7.96E+01	4.29E+02	1.83E+01	8.02E-01	6.43E-01
5.10	2.82E-01	2.91E+00	1.17E+00	9.29E-01	9.81E+02	3.20E+03	2.11E+00	1.17E+01	8.74E-01	7.06E+01	3.87E+02	2.44E+01	8.21E-01	6.91E-01
5.15	2.49E-01	2.59E+00	1.41E+00	9.68E-01	9.91E+02	3.24E+03	1.87E+00	1.04E+01	1.06E+00	6.25E+01	3.46E+02	3.03E+01	8.39E-01	7.33E-01
5.20	2.19E-01	2.28E+00	1.63E+00	9.87E-01	1.00E+03	3.27E+03	1.64E+00	9.13E+00	1.22E+00	5.51E+01	3.06E+02	3.58E+01	8.54E-01	7.71E-01
5.25	1.93E-01	2.00E+00	1.83E+00	9.96E-01	1.01E+03	3.30E+03	1.44E+00	8.00E+00	1.38E+00	4.85E+01	2.69E+02	4.08E+01	8.69E-01	8.04E-01
5.30	1.69E-01	1.75E+00	2.01E+00	9.99E-01	1.02E+03	3.33E+03	1.27E+00	6.98E+00	1.51E+00	4.26E+01	2.35E+02	4.53E+01	8.82E-01	8.32E-01
5.35	1.48E-01	1.51E+00	2.17E+00	1.00E+00	1.03E+03	3.36E+03	1.11E+00	6.06E+00	1.63E+00	3.73E+01	2.05E+02	4.93E+01	8.93E-01	8.57E-01
5.40	1.29E-01	1.31E+00	2.30E+00	1.00E+00	1.04E+03	3.39E+03	9.66E-01	5.24E+00	1.73E+00	3.26E+01	1.77E+02	5.27E+01	9.04E-01	8.79E-01
5.45	1.12E-01	1.13E+00	2.40E+00	1.00E+00	1.05E+03	3.42E+03	8.41E-01	4.50E+00	1.80E+00	2.84E+01	1.53E+02	5.54E+01	9.13E-01	8.98E-01
5.50	9.74E-02	9.65E-01	2.48E+00	1.00E+00	1.06E+03	3.46E+03	7.31E-01	3.86E+00	1.86E+00	2.47E+01	1.31E+02	5.75E+01	9.22E-01	9.14E-01
5.55	8.45E-02	8.24E-01	2.53E+00	1.00E+00	1.07E+03	3.49E+03	6.33E-01	3.30E+00	1.90E+00	2.14E+01	1.12E+02	5.90E+01	9.30E-01	9.28E-01
5.60	7.31E-02	7.01E-01	2.55E+00	1.00E+00	1.08E+03	3.52E+03	5.48E-01	2.80E+00	1.91E+00	1.86E+01	9.58E+01	5.98E+01	9.37E-01	9.39E-01
5.70	5.45E-02	5.02E-01	2.52E+00	1.00E+00	1.10E+03	3.58E+03	4.08E-01	2.01E+00	1.89E+00	1.39E+01	6.89E+01	5.97E+01	9.49E-01	9.58E-01
5.80	4.03E-02	3.55E-01	2.41E+00	1.00E+00	1.12E+03	3.64E+03	3.02E-01	1.42E+00	1.81E+00	1.03E+01	4.88E+01	5.75E+01	9.58E-01	9.71E-01
5.90	2.96E-02	2.48E-01	2.24E+00	1.00E+00	1.13E+03	3.71E+03	2.22E-01	9.92E-01	1.68E+00	7.56E+00	3.43E+01	5.39E+01	9.66E-01	9.80E-01
5.95	2.54E-02	2.07E-01	2.14E+00	1.00E+00	1.14E+03	3.74E+03	1.90E-01	8.26E-01	1.61E+00	6.48E+00	2.86E+01	5.16E+01	9.70E-01	9.84E-01
6.10	1.58E-02	1.18E-01	1.80E+00	1.00E+00	1.17E+03	3.83E+03	1.18E-01	4.70E-01	1.35E+00	4.04E+00	1.63E+01	4.39E+01	9.78E-01	9.91E-01
6.20	1.14E-02	7.98E-02	1.57E+00	1.00E+00	1.19E+03	3.90E+03	8.57E-02	3.19E-01	1.18E+00	2.93E+00	1.11E+01	3.84E+01	9.83E-01	9.94E-01
6.30	8.23E-03	5.37E-02	1.34E+00	1.00E+00	1.21E+03	3.96E+03	6.17E-02	2.15E-01	1.01E+00	2.11E+00	7.49E+00	3.30E+01	9.86E-01	9.96E-01
6.50	4.22E-03	2.38E-02	9.38E-01	1.00E+00	1.25E+03	4.08E+03	3.17E-02	9.50E-02	7.04E-01	1.09E+00	3.33E+00	2.32E+01	9.92E-01	9.98E-01
6.75	1.79E-03	8.24E-03	5.56E-01	1.00E+00	1.30E+03	4.24E+03	1.34E-02	3.30E-02	4.17E-01	4.62E-01	1.16E+00	1.39E+01	9.96E-01	9.99E-01
6.80	1.51E-03	6.62E-03	4.96E-01	1.00E+00	1.31E+03	4.27E+03	1.13E-02	2.65E-02	3.72E-01	3.89E-01	9.34E-01	1.24E+01	9.96E-01	1.00E+00
7.50	1.20E-04	2.80E-04	7.89E-02	1.00E+00	1.44E+03	4.71E+03	9.00E-04	1.12E-03	5.92E-02	3.18E-02	3.96E-02	2.00E+00	1.00E+00	1.00E+00

Appendix C – Purification Factor Versus Yield Algorithm

This algorithm was provided courtesy of Simon Edwards-Parton, University College London.

The algorithm requires fractionation diagram data input as a text file, where there are two columns of data. The first column contains the mass fraction of eluted material, and the second column contains the corresponding mass fraction of eluted product. A searching-type algorithm is then run and seeks/calculates all the purification factors corresponding to each yield value (from 0-100% yield). The output is a table detailing yield and its corresponding maximum purification factor as seen in Table 3.3.

```
function [PFOut]=PFMaxVYield(Total, Target)

% [PFOut]=PFMaxVYield(Total, Target)
% function for conversion of fractionation diagram to Max_PF vs Yield
% returned array gives yield and PF_MAx values in first two
% columns, and the Ystart value in the third column

[RowX ColX]=size(Total);
[RowY ColY]=size(Total);

%check dimesions are correct and then set Row value

if RowX==1
   Total=Total';
   RowX=ColX;
end

if RowY==1
   Target=Target';
   RowX=ColX;
end

if RowX~=RowY
   error('Inputs not same dimensions');
```

```
end

%combine array

XYData=[Total Target];

%round to 3 dp

XYData=RoundDP(XYData, 3);

%remove 0s and 1s

SearchLocation=find((XYData(:,1)==1 & XYData(:,2)==1) | (XYData(:,1)==0 &
XYData(:,1)==0));
XYData(SearchLocation,:)=[];

%add back zeros and ones

XYData=[0 0; XYData; 1 1];

%sort it

XYData=sortrows(XYData, 1);

[Rows Cols]=size(XYData);

PFArray=[1 1 0];

%Obtain array of all PF values for yields

for i=1:Rows-1

  LowerYValue=XYData(1:Rows-i,2);
  UpperYValue=XYData(i+1:Rows,2);
  Yield=[UpperYValue-LowerYValue];
  DeltaX=[XYData(i+1:Rows,1)-XYData(1:Rows-i,1)];

%check and remove zero x change values to avoid division by 0

ZeroCheck=find(DeltaX<eps);

  if isempty(ZeroCheck)==0
    LowerYValue(ZeroCheck,:)=[];
    Yield(ZeroCheck,:)=[];
    DeltaX(ZeroCheck,:)=[];

  end
```

```
   PF=Yield./DeltaX;

   PFArray=[PFArray; [Yield PF LowerYValue]];

end

%round new array to 3 DP

PFArray=RoundDP(PFArray, 3);

%Sort this new array by Yield

PFArray=sortrows(PFArray,[1 2]);

PFStructure.PFArray=PFArray;

%Now have completed array of all PFValues and corresponding yields

[Rows Cols]=size(PFArray);

i=0;

%starting with the largest yield remove all yields the same or less where
%the PF factor is less

PFOut=[1 1 0];

while isempty(PFArray)==0
   %get current PF values
   Yield=PFArray(Rows,1);
   PF=PFArray(Rows,2);
   StartPoint=PFArray(Rows,3);

%find values that match yield or are less and PF or are less

LowerVals=find((PFArray(:,1)<=Yield) & (PFArray(:,2)<=PF));

%Remove these values

PFArray(LowerVals,:)=[]; %or remove those rows and re-evaluate PF Array and
values

   PFOut=[PFOut; [Yield PF StartPoint]];

   [Rows Cols]=size(PFArray);

%   plot(PFArray(:,1), PFArray(:,2))

end
```

Appendix D – Matlab Code for the Creation of Windows of Operation

This appendix provides the Matlab code used to create Windows of Operation, as detailed in Section 3.3.

```
% Step 1, 85% Yield

Q = [50 100 150 200 250]  % These are linear velocities

V = [0 1 3 5 10]  % These are loading breakthrough

T = [0.55 0.9 1.20 1.49 1.70; 0.92 1.68 2.34 2.94 3.43; 1 1.89 2.68 3.46 4.17; 1.04 1.99
    2.89 3.71 4.55; 1.12 2.21 3.22 4.22 5.38]  % These are productivity values

P = [84.6 74.3 67.8 63.5 60.3; 72.4 67.3 62.8 59.7 56.9; 66.2 60.9 57.5 54.5 52.2; 63.7
    58.4 55.0 52.5 50.2; 59.95 54.7 51.6 49.5 47.2]  % These are purity values

contour(Q,V,P,[60,60], 'k')  % This defines the limit for the purity contour

hold on

contour(Q,V,T,[2,2], 'k')  % This defines the limit for the productivity contour

xlabel('Linear Velocity')

ylabel('Breakthrough (%)')

title('Window of Operation - Step 1')
```

Appendix E - Standard Curves

The following are standard curves used for the determination of Fab', Ribonuclease A and Cytochrome C concentrations in the experimental work in Chapters 6 and 7.

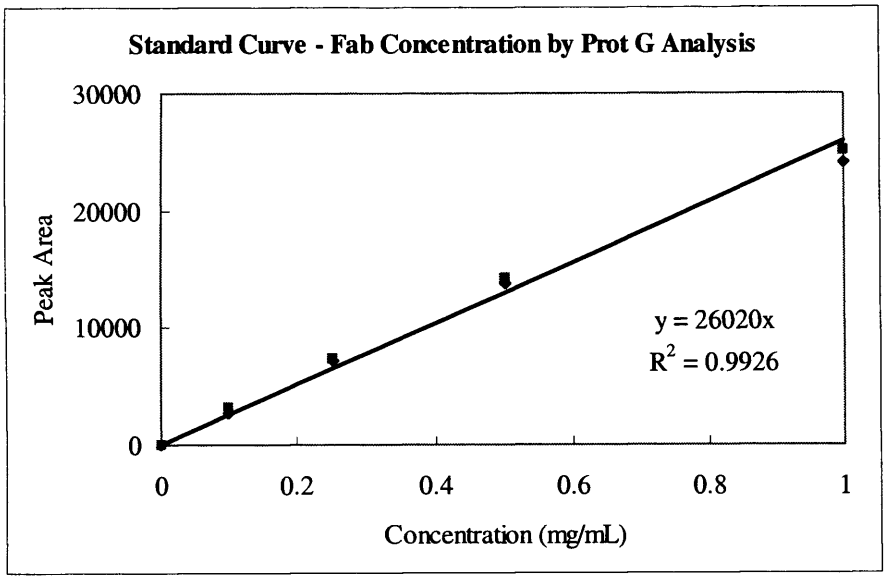

Figure E1. Standard Curve for Fab Concentration Determination by Protein G Analysis

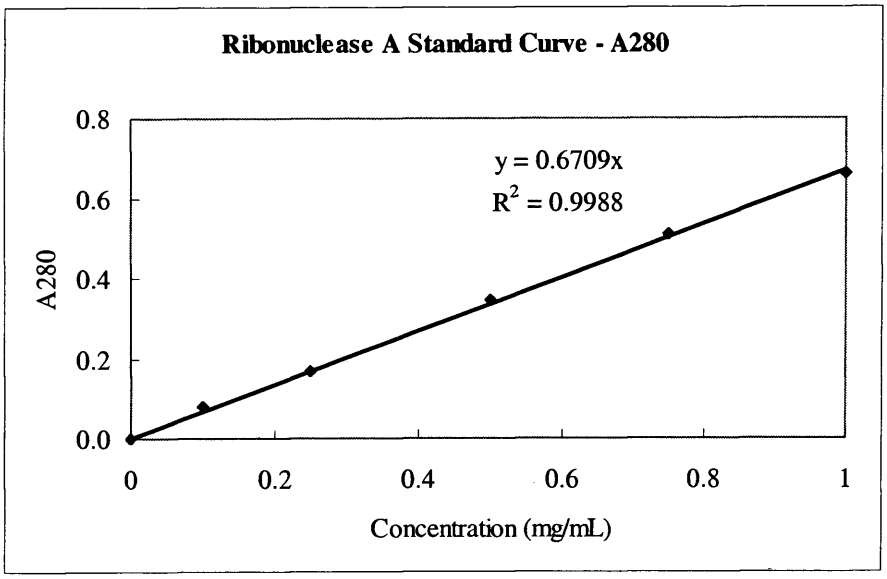

Figure E2. Standard Curve for Ribonuclease A Concentration Determination by A280 Analysis

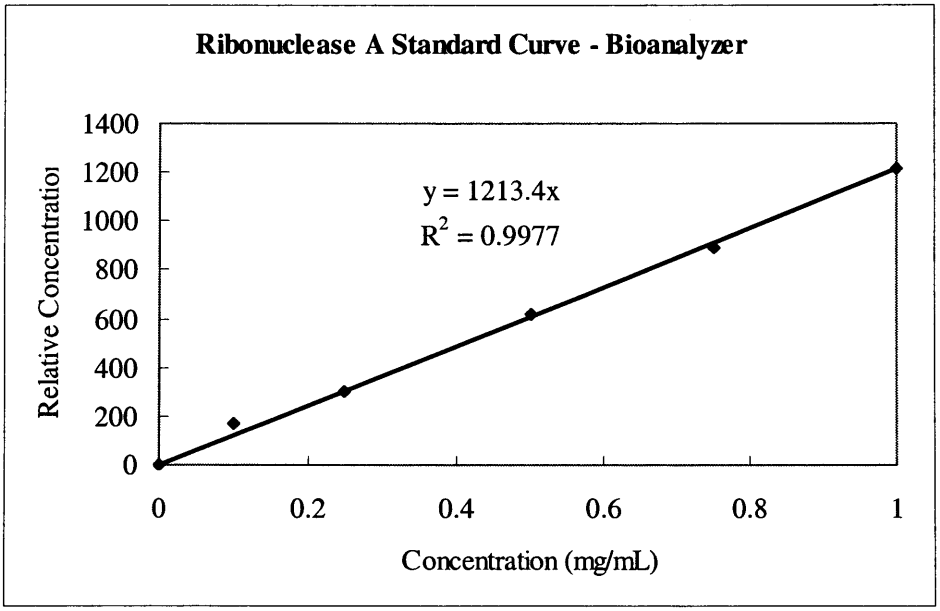

Figure E3. Standard Curve for Ribonuclease A Concentration Determination by Bioanalyzer Assay

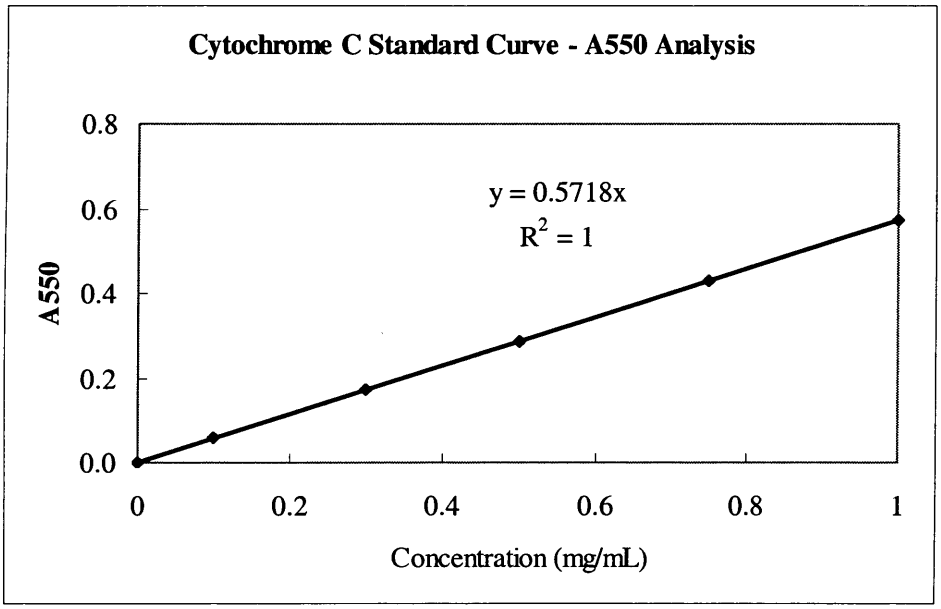

Figure E4. Standard Curve for Cytochrome C Concentration Determination by A550 Analysis

Appendix F – Experimental Calculations

The following calculations were required to treat the experimental data obtained in Chapter 7. It explains how concentration data was obtained and analyzed to produce fractionation diagrams and obtain maximum purification factors and productivity values required to generate Windows of Operation.

Concentration Calculations:

During elution, fractions of the eluted material were collected. Each fraction was then analyzed using the following methods:

- Fab concentration was calculated by comparing the peak area obtained by Protein G analysis to a standard curve (Appendix E).
- Ribonuclease A concentration was calculated by comparing the Bioanalyzer result to a standard curve (Appendix E).
- Cytochrome C concentration was calculated by comparing the A550 absorbance measurement of the sample to a standard curve (Appendix E).

From the concentration calculations, a chromatogram is produced, where:

$$Elution\ volume = \sum_{1}^{n} (Elution\ Volume) \qquad (F.1)$$

and n = elution fraction

An example of such a chromatogram is shown in Figure F1.

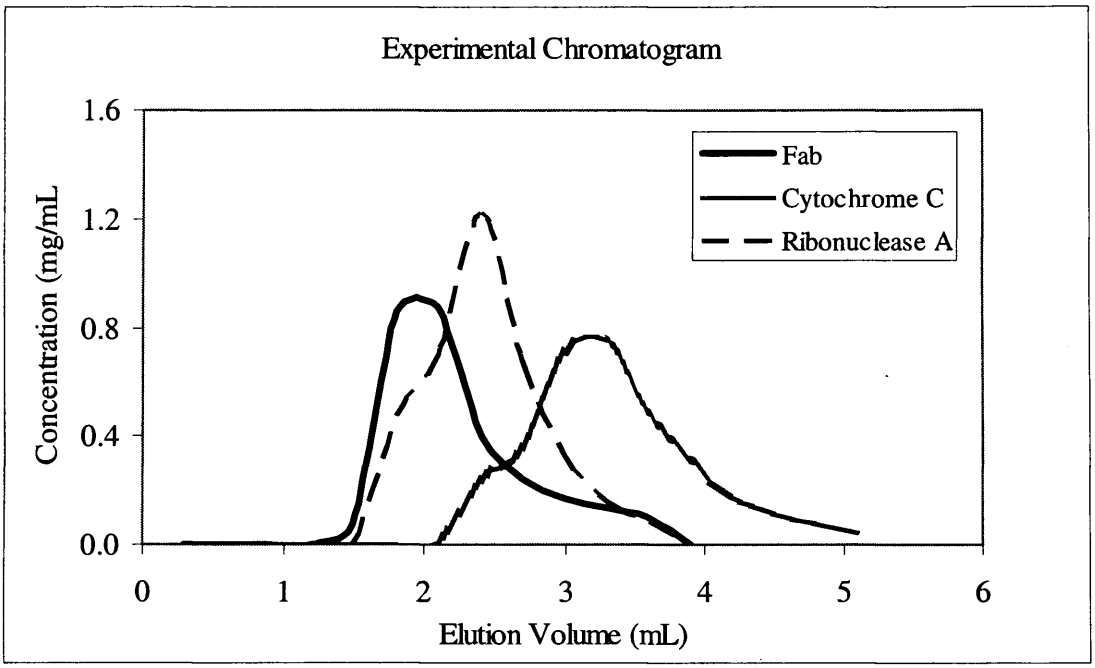

Figure F1. Chromatogram for an Experimental Run at Q = 1 mL min^{-1} and V = 10 mL

Calculations for the fractionation diagram are as follows. Note, the summations were done to n = 17 because 17 elution fractions were collected. This number varies from experiment to experiment.

$$X = \frac{\sum_{1}^{n} Fab\ Concentration + \sum_{1}^{n} Ribonuclease\ A\ Concentration + \sum_{1}^{n} Cytochrome\ C\ Concentration}{\sum_{1}^{17} Fab\ Concentration + \sum_{1}^{17} Ribonuclease\ A\ Concentration + \sum_{1}^{17} Cytochrome\ C\ Concentration} \quad \text{(F.2)}$$

$$Y = \frac{\sum_{1}^{n} Fab\ Concentration}{\sum_{1}^{17} Fab\ Concentration} \quad \text{(F.3)}$$

The fractionation diagram for this data set was the following:

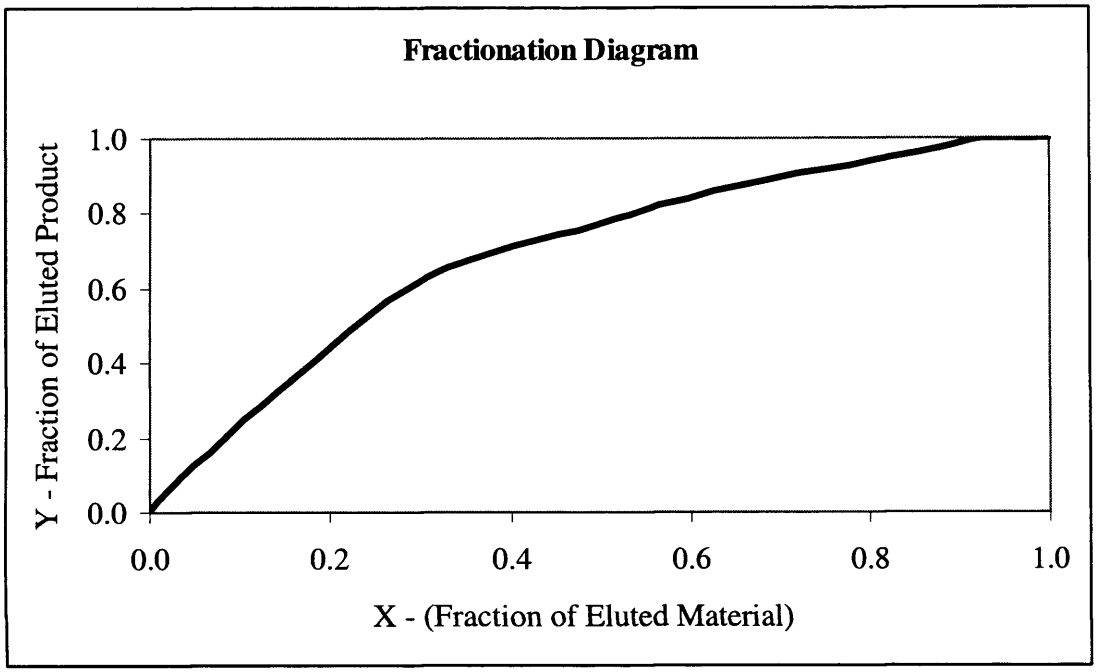

Figure F2. Fractionation Diagram for an Experimental Run at Q = 1 mL min^{-1} and V = 10 mL

The purification versus yield diagram was also produced using the computer algorithm outlined in Appendix C. The following chart summarizes the results for the example experimental run.

Table F1. Purification Factor versus Yield for Experimental Run at Q = 1 mL min^{-1} and V = 10 mL

Yield	Max PF	Start Yield	% Purity
1	1.000	0	28.6
1	1.080	0	30.9
0.965	1.126	0	32.2
0.918	1.224	0	35.0
0.857	1.369	0	39.1
0.773	1.562	0	44.6
0.633	2.069	0	59.1
0.329	2.269	0	64.8
0.327	2.271	0.002	64.9
0.03	3.333	0	95.2
0.028	3.500	0.002	100.0
0.703			51.9

For a 70% product yield, the start yield for fraction collection would be at 0% yield, thus fraction collection would stop at 70% yield. Table F2 shows the mass of each protein in the 70% product yield space (as calculated from the Experimental Data Spreadsheet), and the concentration of each component that will be passed to the second chromatographic stage.

Table F2. Concentrations of Proteins to be Passed to Second Chromatographic Stage Operation

Protein	**Mass in 70% Product Yield Space (mg)**	**Elution Volume (mL)**	**Concentration (mg mL^{-1})**
Fab	0.605	1.65	0.367
Ribonuclease A	0.038	1.65	0.023
Cytochrome C	0.533	1.65	0.323

Although it appears in the Experimental Data Spreadsheet that the elution volume is 2.25 mL for a 70% product yield, no product was eluted in the first 0.6 mL. Therefore, 1.65 mL (2.25 mL-0.6 mL) was determined to be the elution volume.

For the productivity calculation, load time, wash time, regeneration time, and overall elution time were calculated.

Load time = V/Q = (10 mL)/(1 mL min^{-1}) = 10 min

Wash time = 5 min (5 column volumes (CV) at 1 mL min^{-1} where 1 CV is 1 mL)

Regeneration time = 10 min (10 CV at 1 mL min^{-1})

Overall elution time = 8 min (8 CV at 1 mL min^{-1})

Therefore, the total chromatographic cycle time is 33 min (0.55 h).

Productivity is calculated as:

$$Productivity = \frac{Amount\ of\ Fab'}{Chromatographic\ Cycle\ Time \times Volume\ of\ Matrix} \quad \text{(F.4)}$$

$$Productivity = \frac{0.605\ mg}{0.55\ h \times 1\ mL} \quad \text{(F.5)}$$

$$Productivity = 1.10\ g\ h^{-1}\ L^{-1} \quad \text{(F.6)}$$

Appendix G - Publications